

INVESTIGATING THE HOMO-DIMERIZATION OF ADGRD1/GPR133 AND
ADGRG5/GPR114 VIA RESONANCE ENERGY TRANSFER TECHNIQUES

A THESIS SUBMITTED TO
THE GRADUATE SCHOOL OF NATURAL AND APPLIED SCIENCES
OF
MIDDLE EAST TECHNICAL UNIVERSITY

BY

BERKAY DEMİRBAŞ

IN PARTIAL FULFILLMENT OF THE REQUIREMENTS
FOR
THE DEGREE OF MASTER OF SCIENCE
IN
BIOLOGY

JUNE 2023

Approval of the thesis:

**INVESTIGATING THE HOMO-DIMERIZATION OF ADGRD1/GPR133
AND ADGRG5/GPR114 VIA RESONANCE ENERGY TRANSFER
TECHNIQUES**

submitted by **BERKAY DEMİRBAŞ** in partial fulfillment of the requirements for
the degree of **Master of Science in Biology, Middle East Technical University** by,

Prof. Dr. Halil Kalıpçılar
Dean, Graduate School of **Natural and Applied Sciences**

Prof. Dr. Ayşe Gül Gözen
Head of the Department, **Biology**

Assoc. Prof. Dr. Çağdaş Devrim Son
Supervisor, **Biology, METU**

Dr. Orkun Cevheroğlu
Co-Supervisor, **Stem Cell Institute, Ankara University**

Examining Committee Members:

Prof. Dr. Sreeparna Banerjee
Biology, METU

Assoc. Prof. Dr. Çağdaş Devrim Son
Biology, METU

Assoc. Prof. Dr. Tülin Yanık
Biology, METU

Assoc. Prof. Dr. Erkan Kiriş
Biology., METU

Assoc. Prof. Dr. Pınar Baydın
Stem Cell Institute, Ankara University

Date: 01.06.2023

I hereby declare that all information in this document has been obtained and presented in accordance with academic rules and ethical conduct. I also declare that, as required by these rules and conduct, I have fully cited and referenced all material and results that are not original to this work.

Name Last name : Berkay Demirbaş

Signature :

ABSTRACT

INVESTIGATING THE HOMO-DIMERIZATION OF ADGRD1/GPR133 AND ADGRG5/GPR114 VIA RESONANCE ENERGY TRANSFER TECHNIQUES

Demirbař, Berkay
Master of Science, Biology
Supervisor: Assoc. Prof. Dr. aędař Devrim Son
Co-Supervisor: Dr. Orkun Cevheroęlu

June 2023, 98 pages

G protein-coupled receptors (GPCRs) are the largest plasma membrane protein family in mammals. Through extracellular ligand binding, they go through a conformational change and a signaling cascade begins. Extracellular ligands that act on GPCRs can be hormones, neurotransmitters, ions, light, and even mechanical forces. In living cells, GPCRs are known to form homo- and/or hetero- oligomeric complexes. These complexes have impacts on receptor maturation, trafficking, and signaling. Adhesion G protein-coupled receptors (aGPCRs) constitute the second largest sub-family of GPCRs in mammals and they are known to interact with the extracellular matrix proteins and various other ligands on the cell surface and modulate the tissue and organ development. Adhesion GPCRs are amongst the least studied cell surface receptors hence their oligomeric structures are not yet fully understood, unlike other GPCR families. In the current study, two members of the aGPCRs, ADGRD1/GPR133 and ADGRG5/GPR114 were tagged with fluorescent and bioluminescent proteins, and their homo-oligomerization was studied using BRET and FRET in live cells. ADGRD1 is known to be upregulated in glioblastoma and ADGRG5 has significant roles in the immune cells. Therefore, understanding

the receptor oligomerization and its consequences is crucial for these intriguing receptors which have important physiological and pathological roles. Our findings, for the very first time, suggest that ADGRD1 and ADGRG5 form oligomeric complexes, and the methods reported in this study will open the path for investigating the physiology of this receptor oligomerization.

Keywords: Adhesion GPCR, ADGRD1, ADGRG5, Dimerization, RET

ÖZ

REZONANS ENERJİ TRANSFER TEKNİKLERİYLE ADGRD1/GPR133 VE ADGRG5/GPR114'ÜN HOMO-DİMERİZASYONUNU ARAŞTIRMAK

Demirbaş, Berkay
Yüksek Lisans, Biyoloji
Tez Yöneticisi: Doç. Dr. Çağdaş Devrim Son
Ortak Tez Yöneticisi: Dr. Orkun Cevheroğlu

Haziran 2023, 98 sayfa

G protein kenetli reseptörler (GPKR'ler), memelilerdeki en büyük plazma zarı protein ailesidir. Hücre dışı ligand bağlanması yoluyla konformasyonel bir değişiklik meydana gelir ve sinyal iletimi başlar. GPKR'ler üzerinde etki eden hücre dışı ligandlar; hormonlar, nörotransmitterler, iyonlar, ışık ve hatta mekanik kuvvetler olabilir. Canlı hücrelerde, GPKR'lerin homo- ve/veya hetero-oligomerik kompleksler oluşturduğu bilinmektedir. Bu komplekslerin reseptör olgunlaşması, hareketi ve sinyal iletimi üzerinde etkileri vardır. Adhezyon G protein kenetli reseptörler (aGPKR'ler), memelilerde bulunan GPKR'ler arasında ikinci en büyük ailedir ve hücre yüzeyindeki hücre dışı hücrel matris proteinleri ve çeşitli ligandlarla etkileşime girdikleri, ayrıca doku ve organ gelişimini module ettikleri bilinmektedir. Adhezyon GPKR'leri, en az çalışılan hücre yüzeyi reseptörleri arasındadır. Bu nedenle, oligomeric yapıları, diğer GPKR ailelerinin aksine henüz tam olarak bilinmemektedir. Mevcut çalışmada, aGPKR'lerin iki üyesi olan, ADGRD1/GPR133 ve ADGRG5/GPR114 reseptörleri, floresan veya biyoluminesan proteinler ile işaretlenip, canlı hücrelerde BRET ve FRET teknikleri kullanılarak homo-oligomerizasyonları incelendi. ADGRD1'in glioblastomada upregülasyonu

düzenlediđi bilinmektedir. ADGRG5'in bađışıklık hücrelerinde önemli rolü vardır. Bu nedenle, reseptör oligomerizasyonunu ve bunun sonuçlarını anlamak, önemli fizyolojik ve patolojik rollere sahip olan bu merak uyandıran reseptörler için çok önemlidir. Bulgular, ilk kez ADGRD1 ve ADGRG5'in oligomerik kompleksler oluşturduđunu ve bu çalışmada bildirilen yöntemlerin bu reseptör oligomerizasyonlarının fizyolojisinin araştırılmasına yol açacağını düşündürmektedir.

Anahtar Kelimeler: Adezyon GPKR, ADGRD1, ADGRG5, Dimerizasyon, RET

To my beloved my grandmother Şirin Cömert

ACKNOWLEDGMENTS

First of all, I would like to show my gratitude to my supervisor Assoc. Prof. Dr. Çağdaş Devrim Son for his patience and guidance. He was always there when I needed him, and his sense of humor and great spirit was always making me relax when I'm buried in anxious thoughts. He always lifts me up. I, also, would like to express my special regards to my co-supervisor Dr. Orkun Cevheroğlu. Thanks to his determination and knowledge, my thesis was finalized. He is the one who opened the door of adhesion GPCRs to me and guide me through in my first step of academia. I will be forever grateful to both of them for giving me a chance.

I would like to thank Dr. Ines Liebscher and Dr. Caroline Wilde for their guidance and for the plasmids I need. They have giving me a new perspective about science and their friendly attitude made me feel I am in the right path.

My special thanks go to my colleagues in Son Lab and aGPCR team, especially to Dilara Öğütçü, Nil Demir, Merve Aydoğan, Bengü İrem Çakır, and Zeynep Eda Karaboğa. Each of them gave me an assistance over the years. Their support and wisdom are one of the key points behind of this research.

I am indebted for my friends who helped me grow and be there whenever I needed. Many thanks to my beloved best friends, Buğra Kaan Eminoğlu, İnci Topçuoğlu, Hazan Özçelik, Merve Telli, Nevzat Can Yerlikaya, Funda Ardıç, Işıl Erol, Doğa Harmancı, Özgür Gür and Yasemin Karakaş.

Most importantly, my thanks go to my parents, especially to my beautiful mother Gülsen Demirbaş, my father Halit Demirbaş. Moreover, I will always be indebted to the most beautiful and caring aunts, Güler Cömert and Gülten Cömert.

This work is partially funded by Scientific and Technological Research Council of Turkey under grant number TUBİTAK 121Z907 and TUBİTAK 118Z590.

TABLE OF CONTENTS

ABSTRACT.....	v
ÖZ.....	vii
ACKNOWLEDGMENTS.....	x
TABLE OF CONTENTS.....	xi
LIST OF TABLES.....	xiv
LIST OF FIGURES.....	xv
LIST OF ABBREVIATIONS.....	xix
CHAPTERS	
1 INTRODUCTION.....	1
1.1 G protein-coupled receptors.....	1
1.2 Adhesion G Protein-Coupled Receptor.....	3
1.2.1 Classification of adhesion G protein-coupled receptors.....	3
1.2.2 Structure of adhesion G protein-coupled receptors.....	5
1.2.3 Activation mechanism of adhesion G protein-coupled receptors.....	6
1.2.4 NTF cleavage in adhesion G protein-coupled receptors.....	8
1.2.5 Overview of ADGRD1/GPR133.....	9
1.2.6 Overview of ADGRG5/GPR114.....	13
1.3 G protein-coupled receptor oligomerization.....	14
1.4 Bioluminescence resonance energy transfer (BRET).....	15
1.4.1 BRET saturation assay.....	18
1.4.2 BRET competition assay.....	20
1.5 Förster resonance energy transfer (FRET).....	21

1.6	Aim of the thesis	23
2	MATERIAL AND METHOD.....	25
2.1	Construction of fluorescent or bioluminescent-tagged ADGRD1 and ADGRG5	25
2.2	Cell culture.....	34
2.2.1	HEK 293 maintenance, passage, seeding into culture vessels	34
2.2.2	Transient plasmid transfection of HEK 293 cells.....	36
2.3	Western blotting.....	37
2.3.1	Sample preparation and protein harvesting	37
2.3.2	Cell loading and SDS-PAGE.....	37
2.3.3	Protein Transfer	38
2.3.4	Antibody probing.....	38
2.4	Confocal microscopy	39
2.5	BRET assay.....	39
2.5.1	BRET saturation assay	40
2.5.2	BRET competition assay	40
2.6	FRET assay	41
3	RESULTS	43
3.1	Construction of bioluminescent and fluorescent tagged receptors	43
3.2	Laser scanning confocal microscopy imaging.....	46
3.3	Western Blot	48
3.4	BRET	51
3.4.1	NanoBRET	51
3.4.2	Saturation assay	53

3.4.3	Competition assay	54
3.5	FRET	55
4	DISCUSSION	59
4.1	Construction of bioluminescent and fluorescent-tagged receptors	59
4.2	Western Blot.....	59
4.3	Laser Scanning Confocal Microscopy	60
4.4	BRET.....	60
4.5	Saturation BRET	61
4.6	Competition BRET.....	61
4.7	FRET	62
5	CONCLUSION.....	63
	REFERENCES	65
APPENDICES		
A.	Coding constructs of ADGRD1 and ADGRG5 constructs	79
B.	Bacterial medium preparation	95
C.	Western blot and cell culture solutions and buffers	96

LIST OF TABLES

TABLES

Table 2.1 Primers used for the mEGFP and NLuc amplification with GSSG linker. Primers are extended in a 5' to 3' direction.....	28
Table 2.2 First PCR conditions and component concentration for the mEGFP and NLuc amplification.....	29
Table 2.3 Integration PCR conditions and component concentrations to attach first PCR products into ADGRD1 and ADGRG5 cDNA in pcDNA3.1(+). Molar ratio for receptor to amplified mEGFP and NLuc is set to 1:50.....	30
Table 2.4 Digestion with DpnI components.....	30
Table 2.5 Primers used for the colony PCR. Primers are extended in a 5' to 3' direction.....	32
Table 2.6 Colony PCR conditions and component concentrations.....	33
Table 2.7 Control digestion with restriction enzymes for the conformation of the positive inserts.....	34
Table 2.8 Seeding densities of HEK 293 cells into vessels.....	36
Table 2.9 Transient transfection reagents for the vessels.....	36
Table 3.1 BRET ₅₀ value comparison from saturation BRET assay for ADGRD1, ADGRG5 and negative control. Respectively, ADGRD1-L-EGFP and ADGRD1-L-NLuc; ADGRG5-L-EGFP and ADGRG5-L-NLuc; EGFP and ADGRG5-L-NLuc. $p < 0.05$. $n = 9$	54
Table B.1 Luria-Bertani (LB) broth preparation.....	95
Table B.2 Super Optimum Broth with catabolite repression (SOC) preparation....	95
Table C.3 5X radioimmunoprecipitation assay (RIPA) buffer preparation.....	96
Table C.4 1X RIPA buffer with protease inhibitor preparation.....	96
Table C.5 Laemmli buffer preparation.....	97
Table C.6 Running buffer amounts.....	97
Table C.7 TBS preparation amounts.....	97
Table C.8 HBSS preparation.....	98

LIST OF FIGURES

FIGURES

Figure 1.1. Illustration of the phylogenetic relationships of aGPCR family with the new nomenclature and old and their NTF structure. Adapted from (Hamann et al., 2015)). Calx, calnexin; CUB, Cs1 and Csr/Uegf/BMP1; EGF_CA, calcium binding EGF; EPTP, epitempin; HRM, hormone receptor motif; I-set, immunoglobulin I-set domain; LRR, Leucine-rich repeat; PTX, pentraxin; RBL, rhamnose-binding lectin; SEA, sperm protein, enterokinase, agrin module; TSP, thrombospondin.	4
Figure 1.2 NTF-CTF disassociation. Adapted from (Vizurraga <i>et al.</i> , 2020).....	7
Figure 1.3 Structural illustration of the Stachel. His-Leu/Thr (GPS) tripeptide sequence for the ADGRL1. Adapted from (Vizurraga <i>et al.</i> , 2020).....	8
Figure 1.4 Illustration of bioluminescence energy transfer in tagged GPCRs. Luciferase catalyzes the substrate and emits light and transfer its energy to the fluorescent protein if they are in close proximity. (Created using BioRender.com.)	16
Figure 1.5 Theoretical saturation curves. BRET ₅₀ , a ratio of the receptor concentration where the curve reaches half-maximum, while the maximum value is called BRET _{max} . [A] is acceptor tagged receptor, [D] is donor-tagged receptor. Taken from (Drinovec <i>et al.</i> , 2012).	20
Figure 1.6 Theoretical competition curves. [A] is acceptor tagged receptor, [D] is donor-tagged receptor, and [C] is untagged receptor. Taken from (Drinovec <i>et al.</i> , 2012).	21
Figure 1.7 Illustration of Förster resonance energy transfer in tagged GPCRs. Donor fluorescent protein is excited with a certain laser and emits light and transfer its energy to the acceptor fluorescent protein if they are in close proximity. (Created using BioRender.com.)	22
Figure 2.1 The plasmid carrying full-length ADGRD1/GPR133 receptor with HA and FLAG tag.	26

Figure 2.2 The plasmid carrying full-length ADGRG5/GPR114 receptor with HA and FLAG tag. 27

Figure 3.1 Agarose gel electrophoresis image of colony PCR for ADGRD1 cDNAs tagged with EGFP carrying linker (3378 bp) or NLuc carrying linker (3174 bp) in the C-tail. Red boxes indicate the plasmid and insert with the correct size. Primers used are seqp31-1f and seqp31-1r. DNA ladder is Invitrogen™ 1 kb Plus DNA Ladder. 43

Figure 3.2 Agarose gel electrophoresis image of colony PCR for ADGRG5 cDNAs tagged with EGFP carrying linker (2316 bp) or NLuc carrying linker (2109 bp) in the C-tail. Red boxes indicate the plasmid and insert with the correct size. Primers used are seqp31-1f and seqp31-1r. DNA ladder is Invitrogen™ 1 kb Plus DNA Ladder. 44

Figure 3.3 Agarose gel electrophoresis image of colony PCR for ADGRD1 cDNAs tagged with mCherry carrying linker (3369 bp) or ADGRG5 cDNAs tagged with mCherry carrying linker (2307 bp) in the C-tail. Red boxes indicate the plasmid and insert with the correct size. Primers used are Seqd1-2358F, Seqg5-1453F and seqCherry412r. DNA ladder is Invitrogen™ 1 kb Plus DNA Ladder. 44

Figure 3.4 Agarose gel image of insertional PCR products after restriction enzyme (NheI-EcoRV) digestion to control the size of the EGFP and NLuc tagged ADGRD1 on C-terminus. The size of EGFP tagged ADGRD1 cDNAs is 3378 bp and NLuc tagged ADGRD1 cDNAs is 3174 bp. Red boxes indicate the plasmid and insert with the correct size. DNA ladder is Invitrogen™ 1 kb Plus DNA Ladder. 45

Figure 3.5 Agarose gel image of insertional PCR products after restriction enzyme (NheI-NotI) digestion to control the size of the EGFP and NLuc tagged ADGRG5 on C-terminus. The size of EGFP tagged ADGRG5 cDNAs is 2316 bp and NLuc tagged ADGRG5 cDNAs is 2109 bp. Red boxes indicate the plasmid and insert with the correct size. DNA ladder is Invitrogen™ 1 kb Plus DNA Ladder. 45

Figure 3.6 Agarose gel image of insertional PCR products after restriction enzyme (NheI-EcoRV&NheI-NotI) digestion to control the size of the EGFP and NLuc

tagged ADGRG5 on C-terminus. The size of mCherry tagged ADGRD1 cDNAs is 3369 bp and mCherry tagged ADGRG5 cDNAs is 2307 bp. Red boxes indicate the plasmid and insert with the correct size. DNA ladder is Invitrogen™ 1 kb Plus DNA Ladder.....	46
Figure 3.7 Laser scanning confocal microscopy images of ADGRD1-L-EGFP with Seq61b-mApple (A) and with GAP43-mCherry (B). Scale bar corresponds to 5 μm	47
Figure 3.8 Laser scanning confocal microscopy images of ADGRG5-L-EGFP with Seq61b-mApple (A) and with GAP43-mCherry (B). Scale bar corresponds to 5 μm	48
Figure 3.9 The immunoblot image of ADGRD1 constructs. Bands were detected with Anti-HA antibody. Protein marker is Precision Plus Protein™ All Blue Prestained Protein Standards #1610373 (Bio-Rad).	49
Figure 3.10 The immunoblot image of ADGRG5 constructs. Bands were detected with Anti-HA antibody. Protein marker is Precision Plus Protein™ All Blue Prestained Protein Standards #1610373 (Bio-Rad).	50
Figure 3.11 The Net BRET ratios of ADGRD1, ADGRG5 and negative control. Respectively, ADGRD1-L-EGFP and ADGRD1-L-NLuc; ADGRG5-L-EGFP and ADGRG5-L-NLuc; EGFP and ADGRG5-L-NLuc. $p < 0.05$. $n = 9$	52
Figure 3.12 Spectral scanning data of ADGRD1, ADGRG5 and NLuc. Respectively, ADGRD1-L-EGFP and ADGRD1-L-NLuc; ADGRG5-L-EGFP and ADGRG5-L-NLuc; NLuc. Black arrow indicated the shift. $n = 6$	53
Figure 3.13 Saturation BRET assay for ADGRD1, ADGRG5 and negative control. Respectively, ADGRD1-L-EGFP and ADGRD1-L-NLuc; ADGRG5-L-EGFP and ADGRG5-L-NLuc; EGFP and ADGRG5-L-NLuc. A: acceptor, D: donor. $n = 9$...	54
Figure 3.14 Competition BRET assay for ADGRD1 and ADGRG5. Respectively, ADGRD1-L-EGFP and ADGRD1-L-NLuc; ADGRG5-L-EGFP and ADGRG5-L-NLuc. C: competitor, A: acceptor. $n = 6$	55

Figure 3.15 FRET parameters gathered from Zeiss LSM880 Laser Scanning Confocal Microscope Zeiss Zen Modul FRET plus Macro using the Xia <i>et.al.</i> method settings for donor bleed-through and direct acceptor excitation.	56
Figure 3.16 Laser scanning confocal microscopy images of ADGRD1 homo-oligomerization. Each column shows the FRET efficiencies, EGFP channel, mCherry channel, FRET channel and T-PMT and FRET channel merged images in order. Scale bar corresponds to 5 μ m.	56
Figure 3.17 Laser scanning confocal microscopy images of ADGRG5 homo-oligomerization. Each column shows the FRET efficiencies, EGFP channel, mCherry channel, FRET channel and T-PMT and FRET channel merged images in order. Scale bar corresponds to 5 μ m.	57
Figure 3.18 N_{FRET} results for ADGRD1, ADGRG5, positive and negative control. Respectively, ADGRD1-L-EGFP and ADGRD1-L-mCherry; ADGRG5-L-EGFP and ADGRG5-L-mCherry; GAP43-EGFP-LVPR-mCherry; GAP43-EGFP and GAP43-mCherry. $p < 0.05$. $n = 25$	57
Figure C.1 The β -Actin control immunoblot image of ADGRG5 and ADGRD1 transfected cells. Bands were detected with Anti- β -Actin antibody. Protein marker is Precision Plus Protein™ All Blue Prestained Protein Standards #1610373 (Bio-Rad)	98

LIST OF ABBREVIATIONS

ABBREVIATIONS

7-TM: 7-transmembrane

ADGRD1: Adhesion G protein-coupled Receptor, D subfamily, 1

ADGRG5: Adhesion G protein-coupled Receptor, G subfamily, 5

aGPCR: Adhesion G protein-coupled receptor

CTF: C-terminal fragment

ECD: Extracellular domain

G protein: Guanine nucleotide-binding protein

GAIN: GPCR autoproteolysis-inducing

GBM: Glioblastoma

GPCR: G protein-coupled Receptor

GPS: GPCR proteolysis site

mEGFP: Monomeric enhanced green fluorescent protein

NLuc: Nanoluciferase

NTF: N-terminal fragment

WT: Wild-type

CHAPTER 1

INTRODUCTION

1.1 G protein-coupled receptors

G protein-coupled receptors (GPCR) are the largest plasma membrane protein family found in many species from unicellular organisms to mammals (Venter *et al.*, 2001). GPCRs have a distinct structural feature composed of seven transmembrane domains (7-TM) which spans the plasma membrane. Each transmembrane domain is composed of an alpha-helical structure that penetrates through the plasma membrane (Henderson & Unwin, 1975). As the name indicates they couple to membrane-anchored heterotrimeric guanine nucleotide-binding proteins called G proteins. Through extracellular ligand binding, GPCRs go through conformational changes and G proteins couple to the receptors and signal transduction begins. There is a wide variety of extracellular ligands that act on GPCRS such as hormones, neurotransmitters, ions, light, and even mechanical forces (Gurevich & Gurevich, 2008; Wilde *et al.*, 2016). Activation of GPCRs results in lots of physiological reactions like taste, vision, smell, secretion, neurotransmission, metabolic activities, growth, and immune-related actions (Latek *et al.*, 2012; Schonenbach *et al.*, 2015). Furthermore, many diseases such as cancer, diabetes, hypertension, and drug addiction are related to the GPCR functionality (Hauser *et al.*, 2018). Almost 40% of the prescribed drugs target GPCRs (Hauser *et al.*, 2018). Henceforth, the importance of the GPCR in medicine is undeniable. Moreover, in 2012, the Nobel prize in chemistry went to Robert J. Lefkowitz and Brian K. Kobilka for their “studies of G Protein-Coupled Receptors (GPCRs)”.

Activation of the GPCRs, results in the binding of a specific G protein, and the alpha subunit of the G protein releases GDP (Duc *et al.*, 2015). The cascade of intracellular reactions results in the signal transduction. The α and $\beta\gamma$ subunits of G proteins trigger effector proteins. The activation of GPCRs ceases after the receptor is phosphorylated by protein kinase A (PKA) and protein kinase C (PKC) or G protein-coupled receptor kinases (GRK) (Pierce *et al.*, 2002), and arrestin binding functions as negative feedback (Latek *et al.*, 2012). The binding of arrestins inhibits the interaction of GPCRs with G proteins and promotes receptor internalization from the plasma membrane through endocytosis. After that, these receptors might go to lysosomes for degradation or be dephosphorylated and recycled back to the plasma membrane (Tan *et al.*, 2004).

G Protein Coupled Receptors are categorized based on their sequence and function (Alexander *et al.*, 2017). The Nomenclature Committee of the International Union of Basic and Clinical Pharmacology (NC-IUPHAR) groups GPCRs into six classes:

- Class A – Rhodopsin-like receptors
- Class B – Secretin family
- Class C – Metabotropic glutamate receptors
- Class D – Fungal mating pheromone receptors
- Class E – cAMP receptors
- Class F – Frizzled (FZD) and smoothed (SMO) receptors.

More recently, GPCRs were also classified through phylogenetic studies as well (Lagerström & Schiöth, 2008). Upon phylogenetic criteria, GPCRs are divided into five families:

- Glutamate
- Rhodopsin
- Adhesion

- Frizzled/Taste2
- Secretin.

This classification is called GRAFS through families' acronyms (Lagerström & Schiöth, 2008).

1.2 Adhesion G Protein-Coupled Receptor

In human proteome, adhesion GPCRs (aGPCRs) with 33 members, are the second largest GPCR family (Kovacs & Schöneberg, 2016). Adhesion GPCRs are further divided into nine subcategories with phylogenetic analysis based on the similarity of their large N-termini and conserved 7-TM domains (Bjarnadóttir *et al.*, 2004; Langenhan *et al.*, 2013).

1.2.1 Classification of adhesion G protein-coupled receptors

Before the current phylogenetic GPCR classification, aGPCRs subfamilies have been described with known aGPCR genes and named on their functions such as brain angiogenesis inhibitor 1 (BAI1). After the human genome project, newly identified GPCR genes were given names that start with GPR# (e.g., GPR133). The expansion of aGPCRs research resulted in a need for a new nomenclature. According to the new nomenclature, each aGPCR name starts with the prefix ADGR and every subfamily is categorized with a letter, like B in BAI followed by a number (Figure 1.1) (Hamann *et al.*, 2015; Krishnan *et al.*, 2016).

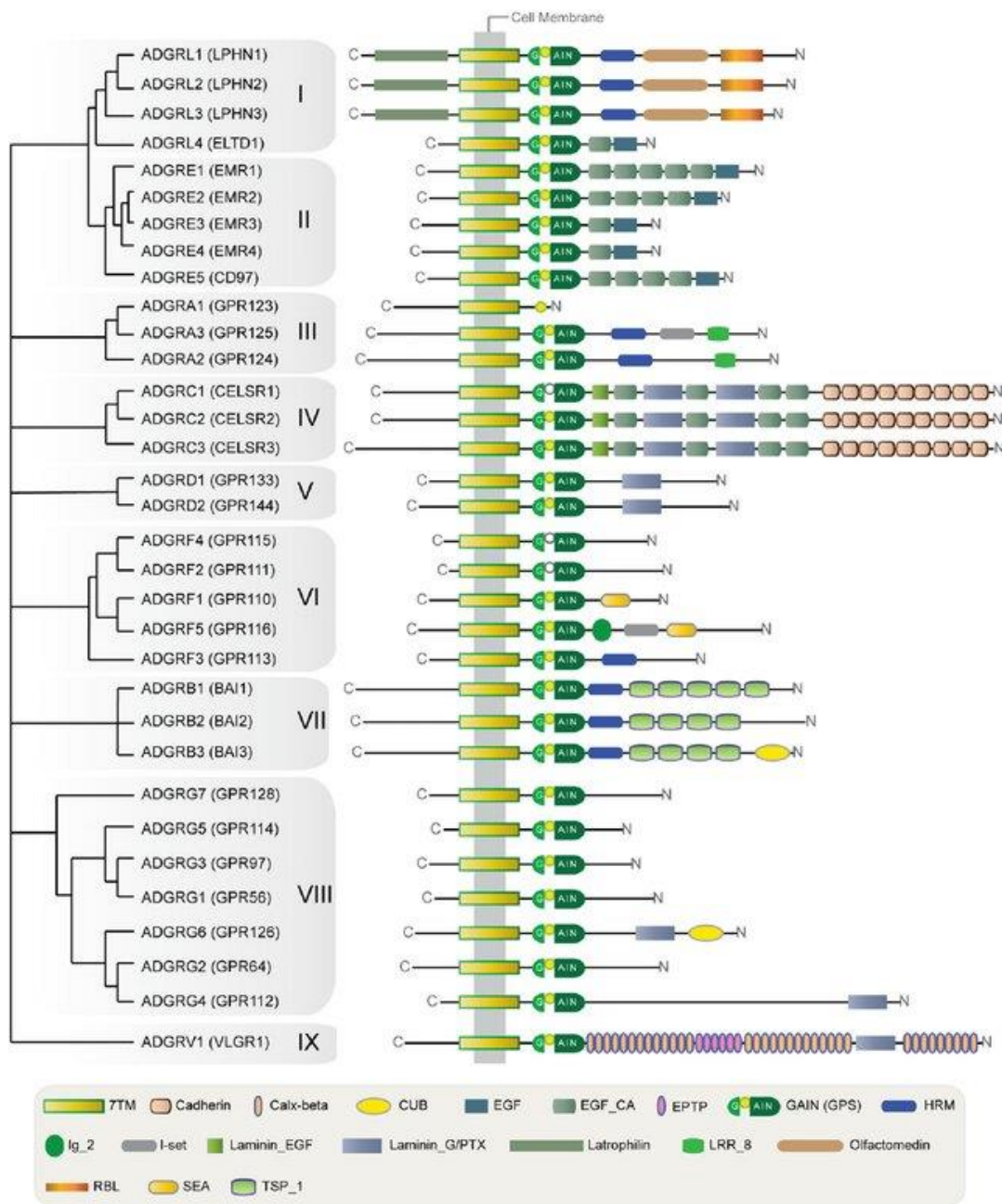


Figure 1.1. Illustration of the phylogenetic relationships of aGPCR family with the new nomenclature and old and their NTF structure. Adapted from (Hamann et al., 2015)). Calx, calnexin; CUB, Cs1 and Csr/Uegf/BMP1; EGF_CA, calcium binding EGF; EPTP, epitempin; HRM, hormone receptor motif; I-set, immunoglobulin I-set domain; LRR, Leucine-rich repeat; PTX, pentraxin; RBL, rhamnose-binding lectin; SEA, sperm protein, enterokinase, agrin module; TSP, thrombospondin.

1.2.2 Structure of adhesion G protein-coupled receptors

Unlike other GPCRs, aGPCRs have a huge N-terminus fragment (NTF), which carries a GPCR autoproteolysis inducing (GAIN) domain and GPCR proteolytic site (GPS) motif (Araç *et al.*, 2012; Hamann *et al.*, 2015). In addition, aGPCRs have a 7-TM region in their carboxy-terminal fragment (CTF) as it is the common structure in all GPCRs. GAIN domain and GPS motif is known to be very critical for the function and maturation of these receptors (Yona *et al.*, 2008).

N-termini of the aGPCRs can be up to 5000 amino acid residues and contains many adhesive domains which vary in each receptor. All human aGPCRs, except ADGRA1 have GAIN domain in their NTF region. GPS motif is the most conserved region of the GAIN domain (Araç *et al.*, 2016). There are also various other domains on the NTF region of aGPCRs such as cadherin, epidermal growth factor (EGF), thrombospondin, leucine-rich repeat (LRR), pentraxin (PTX), lectin and many more (Araç & Leon, 2020). Some of these domains can exist as multiple repeats, for example, one of the isoforms of ADGRV1/VLGR1 has 35 repeats of Calx- β motif (McMillan & White, 2010), ADGRE2/EMR2 has 5 repeats of EGF-like domain (Stacey *et al.*, 2003), and ADGRC1/CELSR1 receptor contains 9 atypical cadherin repeats and 6 EGF-like domains (Wang *et al.*, 2014). These various domains and motifs can be crucial for these receptors to be function in many different cell types/organs and they can have important roles in receptor functionality.

The GAIN domain architecture consists of two sub-domains. In domain A, 6 alpha helices, and in domain B, a beta-sandwich with 2 alpha-helices and 13 beta-strands form the GAIN structure, as confirmed by the X-ray crystal structure of this domain (Araç *et al.*, 2012; Prömel *et al.*, 2013).

Stachel or stalk in the aGPCRs is known to be hydrophobic β strand found in the very C-terminal end of the GAIN domain and located in the N-terminus of the 7-TM region. The receptor NTF restricts the *Stachel* and when the NTF separates from the

CTF, or the receptor is activated through ligand binding on the NTF, *Stachel* peptide becomes exposed to the CTF. This highly hydrophobic peptide interacts with the TM region and activates the receptor (Demberg *et al.*, 2015; Liebscher *et al.*, 2014; Nazarko *et al.*, 2018; Stoveken *et al.*, 2015). Through the GPS motif found within the GAIN domain most aGPCRs are autoproteolytically cleaved yielding a CTF-NTF heterodimeric receptor (Frenster *et al.*, 2021; Huang *et al.*, 2012). The GPS is located around the 14-25 residues of the N-terminal of the CTF region which is embedded in the GAIN domain (Vizurraga *et al.*, 2020).

Autoproteolysis in the GPS, cleaves the receptor into two parts: NTF and CTF. This autoproteolytic cleavage is known to occur as a result of the nucleophilic attack during the receptor maturation in the Endoplasmic reticulum. However, after the autoproteolysis, NTF and CTF remains noncovalently bonded to each other due to the web of hydrogen bonds and goes to the membrane as a heterodimer (Lin *et al.*, 2004).

1.2.3 Activation mechanism of adhesion G protein-coupled receptors

One of the first studies about the signaling of aGPCRs showed that truncation of NTF, after the first residue of autoproteolysis site, significantly increased the signaling activity of these receptors (Paavola *et al.*, 2011). Therefore, it gives a clue about the huge impact of the NTF on the signaling. Later, it is made clear that these receptors are activated by an anchored peptide which is also called *Stachel*, stalk, or the tethered agonist (Liebscher *et al.*, 2014; Stoveken *et al.*, 2015). It is understood that the *Stachel* peptide acts as a tethered agonist which activates the receptor by adding synthesized *Stachel* to aGPCRs (Liebscher *et al.*, 2014). Ligand binding to the NTF causes conformational changes in the receptor, exposing the *Stachel* peptide and ripping the NTF from CTF which is called *NTF shedding*. Moreover, truncation of the NTF domain of auto proteolytically cleavable aGPCR also activates the

receptor (Bhudia *et al.*, 2020; Salzman *et al.*, 2016; Stoveken *et al.*, 2015). Due to its highly hydrophobic nature, *Stachel* peptide interacts with the transmembrane domain and activates the receptor (Figure 1.2) (Demberg *et al.*, 2015; Kishore *et al.*, 2016; Liebscher *et al.*, 2014). This activation type is called *Stachel*-dependent activation of aGPCRs.

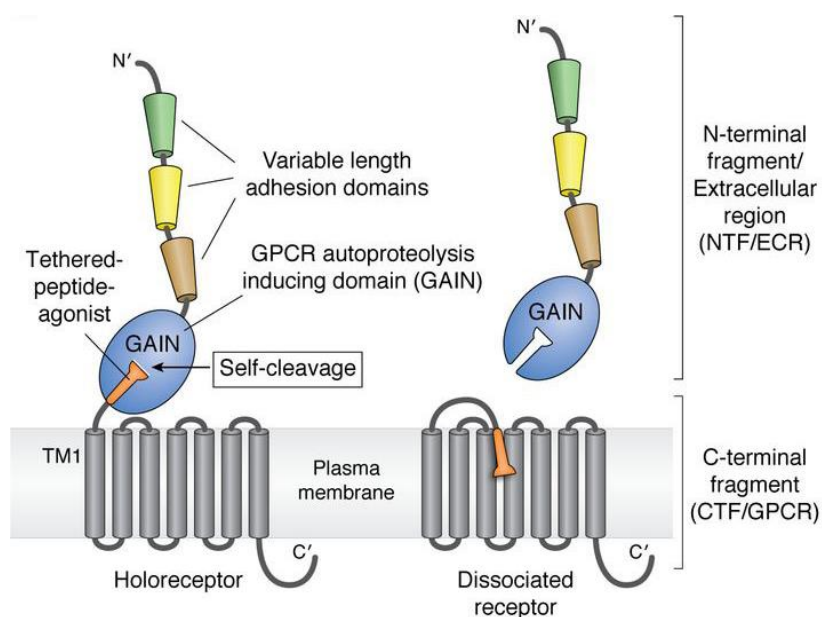


Figure 1.2 NTF-CTF disassociation. Adapted from (Vizurraga *et al.*, 2020).

Another activation mechanism is called the *Stachel*-independent activation. There are several aGPCRs that lack the critical residues for autoproteolysis (Araç *et al.*, 2012; Wilde *et al.*, 2016). ADGRG1 is found to be highly important in the skeletal muscle cell (White *et al.*, 2014), however; it is shown that in the skeletal muscle, it remains uncleaved (Iguchi *et al.*, 2008). A study, by Salzman *et al.* targeting the extracellular region (ECR) of ADGRG1 by nanobodies on autoproteolysis deficient receptors also modulates signaling (Salzman *et al.*, 2017). The direct effect of the extracellular region (ECR) on the transmembrane is also another point in the activation of some aGPCRs. This phenomenon occurs through ligand binding or conformational change (Araç & Leon, 2020; Kishore *et al.*, 2016; Langenhan *et al.*, 2013; Paavola *et al.*, 2011).

1.2.4 NTF cleavage in adhesion G protein-coupled receptors

One of the distinguishing factors in the aGPCRs from other receptor families is their highly conserved G protein-coupled receptor Proteolysis Site (GPS). Except for ADGRA1, every member of the aGPCR family has a GPS motif. The core of GPS is a tripeptide sequence His-Leu/Ile-^{*}-Ser/Thr (Figure 1.3) (Lin *et al.*, 2010). GPS is part of a larger GPCR-Autoproteolysis Inducing (GAIN) domain, which gives GPS a suitable environment for cleavage reaction to occur (Araç *et al.*, 2012). After the GPS, *Stachel* sequence is found which acts as a tethered-agonist (Liebscher *et al.*, 2014). Cleavage of NTF from CTF probably occurs after the receptor is synthesis on the ER. In a study, DPAGT1 inhibitor, tunicamycin treated cells inhibits the cleavage of PC1 receptor (Wei *et al.*, 2007). It can be said that N-glycosylation event might be a crucial factor for cleavage to occur since tunicamycin is an inhibitor for N-glycosylation.

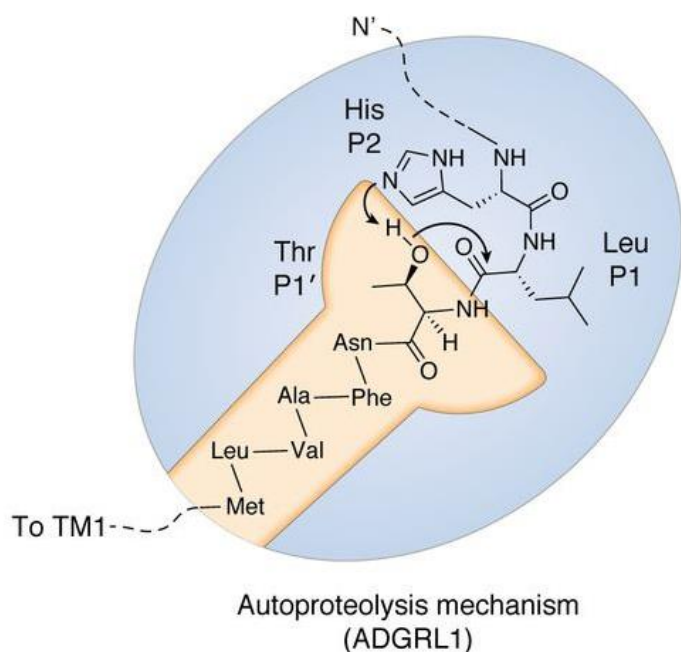


Figure 1.3 Structural illustration of the Stachel. His-Leu/Thr (GPS) tripeptide sequence for the ADGRL1. Adapted from (Vizurraga *et al.*, 2020).

Even though the GPS motif is a global feature in almost all aGPCRs, some receptors are partially cleaved while some of them are not cleaved at all (Kurbegovic *et al.*, 2014; Wilde *et al.*, 2016). ADGRG1 is known to be fully cleaved in the developing brain tissue while it remains uncleaved in the adult tissue (Iguchi *et al.*, 2008). In the ADGRE5/CD97, it seems the receptor autoproteolytic cleavage is concentration dependent (Yang *et al.*, 2017). This might provide clues about the function of oligomerization on the receptor activation and that the higher oligomerization states might help this cleavage process.

1.2.5 Overview of ADGRD1/GPR133

ADGRD1/GPR133 is a member of the aGPCR family. It belongs to class B in NC-IUPHAR and the adhesion subfamily in the GPCR family in the GRAFS classification. In the adhesion GPCRs, it belongs to the D group along with ADGRD2/GPR144. Genomic location of ADGRD1 is in 12q24.33. It couples with G_s protein and activates the adenylyl cyclase pathway (Bohnkamp & Schöneberg, 2011). Like most of the aGPCRs, ADGRD1 also has a large NTF region. In the NTF of the ADGRD1, signal peptide and 111 amino acids long pentraxin-like (PTX) domain is found along with the GAIN domain and the GPS motif (Fischer *et al.*, 2016). In the CTF region, there is a classical 7-TM domain as a GPCR hallmark structure. After protein synthesis in the ER, ADGRD1 undergoes an autoproteolytic cleavage through its GPS motif. NTF was shown to be immaturely glycosylated in ER and maturely glycosylate in the Golgi (Frenster *et al.*, 2021). Nevertheless, the NTF and the CTF regions remain noncovalently bound to each other and traffic to the plasma membrane, where they dissociate from each other. Due to GPS deficient ADGRD1 was shown to also localize in the plasma membrane and this uncleaved mutant does not show any defect while trafficking to the membrane it can be said that cleavage of the NTF was shown not to be required for the plasma membrane localization. (Frenster *et al.*, 2021). On the other hand, NTF truncation of the receptor showed little to no trafficking to the plasma membrane 10% of the truncated receptor

were shown to be located on the plasma membrane according to cell surface ELISA experiments (Liebscher *et al.*, 2014). However, Fischer and colleagues showed that CTF truncation of the receptor in the first transmembrane helix as a naturally occurring Q600Stop mutant traffics to the plasma membrane (Fischer *et al.*, 2016). Altogether it shows that NTF is a crucial part for ADGRD1 transport to the plasma membrane.

According to structural studies, extracellular parts of the transmembrane domain are open like a “V” shape in between second - fifth helices, and first – fourth - seventh helices, so the *Stachel* at the N-terminus can fit in this helical bundle. The extracellular ends of the first, sixth and seventh helices turn clockwise in extracellular view, which makes a large gap so the tip of the *Stachel* can accommodate that cleft. In the intracellular region of the sixth helix, a conserved motif P^{6.47b}xxG^{6.50b} acts as a shaft. This feature is shared in the class B1 secretin GPCRs and in ADGRG3 “P” in this motif becomes “S”. This difference shows that there is diversity in the transmembrane domains of the aGPCRs, and activation modes differ. Moreover, after the NTF shedding, in the *Stachel*, highly conserved F⁵³, L⁵⁶, and M⁵⁷ residues locates downwards to the bottom of the gap and their side chains perform hydrophobic contacts with all the helices except forth and extracellular loop 2 (ECL2) (Ping *et al.*, 2022; Qu *et al.*, 2022).

Similar to other aGPCRs, ADGRD1 has up to 33 low-frequency splice variants, that have been identified in high-depth RNA-seq datasets (Knierim *et al.*, 2019). Nonetheless, the greater part of these splice variants are inactive or only occur very seldom, with 80% of the isoforms constituting less than 1% of the whole ADGRD1 transcript (Knierim *et al.*, 2019).

ADGRD1 as a member of GPCRs, couples to G protein, specifically to the G α_s . Through activation with its tethered agonist, ADGRD1 couples to G α_s and switches on the adenylyl cyclase pathway (Bohnekamp & Schöneberg, 2011; Fischer *et al.*, 2016). Functional studies which involve the truncation of NTF from T⁵⁴⁵ in ADGRD1 showed an increased cAMP activity. Truncation of all the GPS motifs

does not lead to an increase in cAMP accumulation. Nevertheless, when a peptide derived from the *Stachel* is added to the NTF truncated receptor, and a GPS-deficient mutant receptor, it increases the cAMP accumulation. Altogether, these findings show that the disassociation of NTF from the CTF activates the receptor via setting the *Stachel* free, and *in vitro* analysis of ADGRD1 was shown to be activated in a *Stachel*-mediated manner. In ADGRD1, systematic deletion of *Stachel* also displayed that *Stachel* is composed of 13 amino acids in length and one-by-one deletion of these amino acids reduced the agonistic activity (Liebscher *et al.*, 2014). Another study to investigate the activation of ADGRD1 is through antibody-mediated activation. Monoclonal antibody against the PTX domain of ADGRD1 was shown to increase the cAMP accumulation. Anti-HA antibody also been shown to activate the HA-epitope introduced ADGRD1 (Stephan *et al.*, 2022). However, when applied to the autoproteolysis-deficient receptor, antibody-treatment did not yield a cAMP-based receptor activation. These results show that antibodies targeting the NTF region might mediate the NTF dissociation or give rise to a conformational change, therefore activating the receptor.

When looking at the expression of the ADGRD1, it can be seen that it is expressed in glioblastoma (GBM). Glioblastoma is an incurable brain cancer (Stupp *et al.*, 2005). GBM is a cell population that uses cell-intrinsic and microenvironment-mediated pathways to maintain the tumor progression and makes it resistance to conventional therapy (Bayin *et al.*, 2014; Singh *et al.*, 2004). Among those microenvironmental elements that support GBM phenotypes, intratumoral hypoxia which is a naturally occurring effect of arterial thrombosis is promoted (Li *et al.*, 2009). The relationship between hypoxia and ADGRD1 is another study that shows the relation via transcriptional activation of Hif and co-localization of ADGRD1 receptor and Hif (Bayin *et al.*, 2016). Moreover, reducing the ADGRD1 expression and knockdown experiments resulted in a decrease in tumor formation both *in vivo* and *in vitro* (Bayin *et al.*, 2016). In addition, *ADGRD1* gene is shown to be the direct transcriptional target of Hif1a and it is not expressed in the normal cerebral hemisphere tissue (Frenster *et al.*, 2017). In another study, it was shown that

ADGRD1 is not expressed in the neurons, oligodendrocytes, or astrocytes, while in microglia and pericytes it was shown to be expressed in low levels (Frenster *et al.*, 2020). The role of ADGRD1 in glioblastoma progression is undeniable and might be a therapeutic target in the future.

One of the most crucial public health is lung cancer and lung adenocarcinoma (LUAD) is the most prevalent one (Cheng *et al.*, 2016). ADGRD1 as one of the crucial regulators of signal transduction has been known to be connected with cancer and expression of the receptor is related to the shorter survival rate in myeloid leukemia patients (Yang *et al.*, 2019). ADGRD1 downregulation is correlated with the prognosis of Non-Small Cell Lung Cancer (NSCLC) (Lv *et al.*, 2022). Furthermore, ADGRD1 expression decreases in LUAD samples and increased expression of ADGRD1 in LUAD patients was shown to limit tumor development and cell proliferation (Zhu *et al.*, 2022). This makes ADGRD1 a potential biomarker for NSCLC. In the gastric cancer, according to TCGA data, long non-coding RNAs is said to change the ADGRD1 expression, and the receptor is differentially expressed (Zhou *et al.*, 2019).

ADGRD1 also influences the length of the electrocardiographic RR interval and heart rate. A study within the three groups of European genetically isolated populations shows that the *ADGRD1* gene contributes to heart rate and electrocardiographic RR interval (Marroni *et al.*, 2009). More studies indicate that the *ADGRD1* gene is related to height (Kim *et al.*, 2013; Tönjes *et al.*, 2009). The most obvious variation in the frequency between tall and short people was chromosomal position 12q24.33 deletion, which is close to the *ADGRD1* gene. Compared to the short controls, taller people exhibited a deletion frequency at this location was around two times greater (Kim *et al.*, 2013).

1.2.6 Overview of ADGRG5/GPR114

ADGRG5/GPR114 is a member of aGPCRs (Schiöth *et al.*, 2010), which is in class B and the adhesion subfamily of the GPCR family. In the aGPCR subfamily, it belongs to the G group along with ADGRG1/GPR56, ADGRG2/GPR64, ADGRG3/GPR97, ADGRG4/GPR112, ADGRG6/GPR126, and ADGRG7/GPR128. ADGRG5 is located in the 16q21. This receptor has the shortest NTF in the aGPCR family with 520 amino acids in total length. ADGRG5 has the key structural elements like other aGPCRs, such as GAIN domain and GPS motif. Even though ADGRG5 has the GPS motif, it is not autoproteolytically cleaved. Therefore, showing the activation of the receptor with NTF removal is not suitable. ADGRG5 as a G protein-coupled receptor, couples to $G\alpha_s$ protein, and activates the cAMP pathway by increasing the intracellular cAMP levels (Gupte *et al.*, 2012). ADGRG5 seems to be activated through *Stachel* peptide and 3- α -DOG (Wilde *et al.*, 2016) (Stoveken *et al.*, 2018).

In humans, ADGRG5 has no splice variant, yet in mice, it has two splice variants. The first isoform is the full-length ADGRG5 (Q230), while the other one lacks the 230th amino acid which is glutamine (Δ Q230). Glutamine in the 230th position of the ADGRG5 corresponds to position 8 of the *Stachel* sequence. This gives an idea about the *Stachel* activity of the receptor. It was shown that the Q230 has higher basal activity than Δ Q230, however, both isoforms have the same surface expression levels (Wilde *et al.*, 2016). The same study suggests that the Q230 in the *Stachel* region is not required for the activation of the receptor, but is responsible for the orientation of the *Stachel* toward the 7-TM region (Wilde *et al.*, 2016).

The structural studies showed that *Stachel* is parallel to the plasma membrane and the N terminus of the *Stachel* sequence forms a helical turn and this turn is buried into the transmembrane domain. Just like ADGRD1, *Stachel* sequence of ADGRG5 has F^{ss-03}, L^{ss-06}, M^{ss-07} in the helical turn were buried deep in the transmembrane domain where forms a hydrophobic interaction with ECL2, specifically with W470^{6.53} (Ping *et al.*, 2022).

Shaking the ADGRG5 as a mechanical activation Q230 transfected cells increased the basal activity, while Δ Q230 did not, even without the ligand (Wilde *et al.*, 2016). These results suggest that the correct positioning of *Stachel* is crucial for receptor activation. Moreover, it has been proven that ADGRG5 can be activated by a mechanical force.

ADGRG5 is expressed in the colon, leukocytes, spleen, and thymus (Bjarnadóttir *et al.*, 2007). Specifically, ADGRG5 is found primarily on granulocytes and eosinophils (Peng *et al.*, 2011) with the information that ADGRG5 is upregulated in the *Mycobacterium tuberculosis* or *Trichuris muris* infected mice (Foth *et al.*, 2014; Marquis *et al.*, 2009). Therefore, it is feasible to suggest that this receptor might be a crucial receptor in the immune system.

1.3 G protein-coupled receptor oligomerization

G protein-coupled receptors can form homo-and/or hetero-oligomers by associating with themselves and/or other receptors. This phenomenon is shown to be quite important for receptors to mature, traffic, signal, and internalize (Ng *et al.*, 2012). For a long time, GPCRs were thought to work as a monomer, but a growing number of studies have shown that GPCRs can make interactions with others to form dimeric or even higher oligomeric states (Ng *et al.*, 2012). Resonance Energy Transfer (RET) techniques with their increasing popularity, have been one of the best strategies to directly study GPCR interactions. The fundament of these techniques relies on non-radiative energy transfer from the excited donor to the acceptor (Wu & Brand, 1994). For example, β 2-adrenergic receptor (β 2AR) as confirmed by fluorescence resonance energy transfer (FRET) method, can act both as a monomer and as in a higher oligomeric state (Ferré *et al.*, 2014; Whorton *et al.*, 2007). Moreover, the secretin receptor (SCTR) was also shown to form oligomers using bioluminescence resonance energy transfer (BRET) (Ding *et al.*, 2002).

In class C GPCRs, such as GABA_B and metabotropic glutamate (mGlu) receptors, acts constitutively as dimers, and in GABA_B heterodimerization is by the receptor C-termini (Kammerer *et al.*, 1999). mGlu receptors were shown to be strict dimers, which are covalently bonded to each other by the disulfide bridge (Maurel *et al.*, 2008). However, studies on class A receptor indicates that oligomerization is formed by non-covalent bonds (González-Maeso, 2011). Co-immunoprecipitation and FRET experiments on the α_{1b} -adrenergic receptor showed that TM1 and TM4 are involved in the dimeric complexes (Carrillo *et al.*, 2004).

Another point in the oligomerization is the GPCR signaling effect. μ -Opioid receptor and α_{2a} -adrenergic receptor heterodimerization is known and both receptors are involved in depression and opioid addiction (Gabilondo *et al.*, 1994) (Vilardaga *et al.*, 2008). Both μ -Opioid and α_{2a} -adrenergic receptors activate the ERK pathway, yet when the heterocomplex is formed and these receptors are activated, the signal activation decreases (Vilardaga *et al.*, 2008). Furthermore, 5-HT_{2A} receptor couples to the G_{q/11} while mGlu2 receptor couples to the G_{i/o}. 5-HT_{2A} receptor and mGlu2 receptor form heteromeric complexes and when the agonist of 5-HT_{2A} receptor is added, both G_{q/11} and G_{i/o} pathways are activated through a head-twitch response (Moreno *et al.*, 2011).

In the aGPCR oligomerization, only ADGRE2/EMR2 has been shown to oligomerize so far via FRET and co-IP analysis. It has been suggested that the oligomerization is mediated by the 7-TM region. Moreover, it has also been proposed that the ADGRE2 hetero-oligomerize with ADGRE5/CD97 (Davies *et al.*, 2007).

1.4 Bioluminescence resonance energy transfer (BRET)

Measuring the protein-protein interactions is a critical step for understanding how signal transduction occurs. For studying the protein-protein interactions, there are many methods where Resonance energy transfer (RET) method is one of the most often used one of them. RET methods for protein oligomerization detection are rising

over the years. Most RET techniques are founded on the same idea. Non-radiative energy is transferred from a “donor” molecule to an “acceptor” molecule (Wu & Brand, 1994). For resonance energy to be transmitted effectively there needs to be some overlap between the emission spectra of the donor and the excitation spectrum of the acceptor. Moreover, the distance and angle of the donor and acceptor are important for energy transfer efficiency (Mo & Fu, 2016; Sekar & Periasamy, 2003).

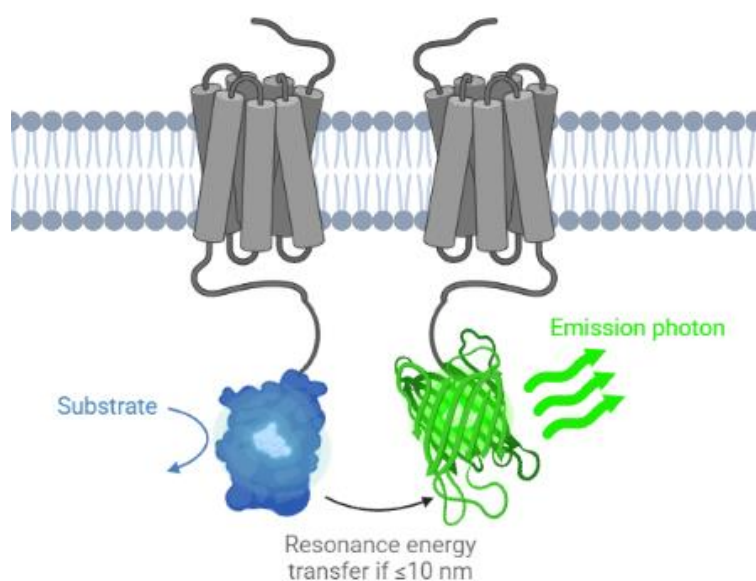


Figure 1.4 Illustration of bioluminescence energy transfer in tagged GPCRs. Luciferase catalyzes the substrate and emits light and transfer its energy to the fluorescent protein if they are in close proximity. (Created using BioRender.com.)

Bioluminescence resonance energy transfer (BRET) and fluorescence resonance energy transfer (FRET) techniques rely on the same principle. However, in BRET, the donor does not need to be excited by an external light source. In contrast to FRET, BRET might obtain a higher signal-to-noise ratio (low background). BRET is also a ratio-metric approach, allowing interferences from experimental conditions to be minimized.

Renilla luciferases (RLuc) are frequently selected as donors in artificial BRET systems. Coelenterazine, a hydrophobic and cell-permeable compound, was oxidized by RLuc, producing a light emission peak at 480 nm, and has a brief lifespan (Wu &

Brand, 1994). Firefly luciferase (FLuc), a different bioluminescent protein, has been employed in BRET systems as a donor as well. FLuc oxidizes D-luciferin, causing an emission maximum at 565 nm (Baldwin, 1996). Lower cellular autofluorescence is obtained in this BRET system, although the signal is faint (Wu & Brand, 1994). NanoLuc Luciferase (NLuc) has a narrower emission spectrum and higher stability, making it significantly brighter than RLuc and FLuc (Hall *et al.*, 2012). NLuc oxidizes the coelenterazine analog furimazine to produce light emission at 460 nm. NLuc also has the benefit of being smaller than other luciferases, which is better for fusing with the target protein (Dale *et al.*, 2019).

In BRET experiments, as an acceptor, green fluorescent protein (GFP) and its derivatives are widely used. Wild-type GFP possesses a long maturation time, two excitation peaks, and a low fluorescent signal, thus to overcome these disadvantages eGFP is engineered with two mutations F64L and S65T (Arpino *et al.*, 2012; Pakhomov & Martynov, 2008).

In BRET method, it involves the oxidation of ligands by bioluminescent enzymes, which release energy as bioluminescence emission. The reaction energy changes the electron state of the donor enzyme from the ground state to the excited state. The electrons in the excited state return to the ground state by vibrational energy or the energy is released as a photon. If the bioluminescence spectrum of the donor overlaps the excitation wavelength of the acceptor fluorophore, the energy of the excited state electrons may also be transferred as RET to the acceptor fluorophore. With a certain likelihood, excited electrons interact with the acceptor's electron cloud resulting in an excitation of the acceptor. When the donor and the acceptor are placed within the Förster distance, which is the distance at which the excitation energy has transferred to the acceptor, and 50% of the energy is transferred, it can be said that BRET is highly efficient (Pfleger & Eidne, 2006).

BRET is interpreted as ratio of transferred T over not-transferred energy Q (Drinovec *et al.*, 2012):

$$BRET = \frac{T}{Q}$$

The energy transfer efficiency E determines the likelihood that excitation is transmitted from donor to acceptor in a single BRET pair and Q_0 is the total energy (Drinovec *et al.*, 2012):

$$T = E \times Q_0$$

According to the Förster equation, the energy transfer efficiency is inversely proportional to the sixth power of the distance R between the donor and the acceptor, where the Förster radius R_0 relies on the dipole orientation and spectral overlap (Drinovec *et al.*, 2012):

$$E = \frac{R_0^6}{R_0^6 + R^6}$$

The magnitude of the energy transfer efficiency E can be determined for the dimers from the maximum BRET where all the donors' accompanied by acceptors (Drinovec *et al.*, 2012):

$$E = \frac{BRET_{\max}}{BRET_{\max} + 1}$$

All the calculations are generally simplified by assuming the E is small enough, therefore, this formula can be used (Drinovec *et al.*, 2012):

$$BRET_{E \ll 1} = \frac{T}{Q_0}$$

1.4.1 BRET saturation assay

In the saturation assay, an increasing amount of acceptor-tagged receptor is expressed while keeping the expression of donor-tagged receptor constant. The BRET signal ought to increase theoretically as acceptor concentrations rise until all donor molecules are interacting with acceptor molecules. Hence, a saturation level

“BRET_{max}” is reached at which adding more acceptors has no further effect on the BRET signal (Achour *et al.*, 2011; Ayoub & Pflieger, 2010; Hamdan *et al.*, 2006; Mercier *et al.*, 2002). In order to approximate small energy transfer efficiency, the Veatch and Stryer model BRET saturation curve is used:

$$\frac{BRET}{BRET_{\max}} = 1 - \frac{1}{\left(1 + \frac{[A]}{[D]}\right)^N}$$

N=1 for dimer, N=2 is for trimer and N=3 is for tetramer (James *et al.*, 2006). In saturation curves, BRET indicates quicker saturation for higher oligomers. A quasi-linear saturation curve resembling that of the dimers can be produced by random collisions at very high receptor concentrations (Figure 1.5). The monomer BRET signal associated with random collisions is shown for comparison. The hypothetical BRET curve for dimers and the quasi-linear curve from non-specific interactions, for which large BRET_{max} values can be produced in the event of high receptor concentrations, can be compared. Whereas, on the other hand, the overall receptor concentration has no effect on the dimer curve. The leftward shift of the saturation curve for greater oligomers makes it possible to identify the oligomerization state (Breit *et al.*, 2004; Goin & Nathanson, 2006; Mercier *et al.*, 2002; Vrecl *et al.*, 2006).

The saturation curve’s half maximum value, or BRET₅₀, is the receptor concentration ratio. One is hypothesized homodimer BRET₅₀ value. The BRET₅₀ values can be determined for the relative affinity of forming homo- or heterodimers. The saturation curve is pushed to the right and the BRET₅₀ value increases if the affinity production is reduced (Breit *et al.*, 2004; Goin & Nathanson, 2006; Mercier *et al.*, 2002; Terrillon *et al.*, 2003).

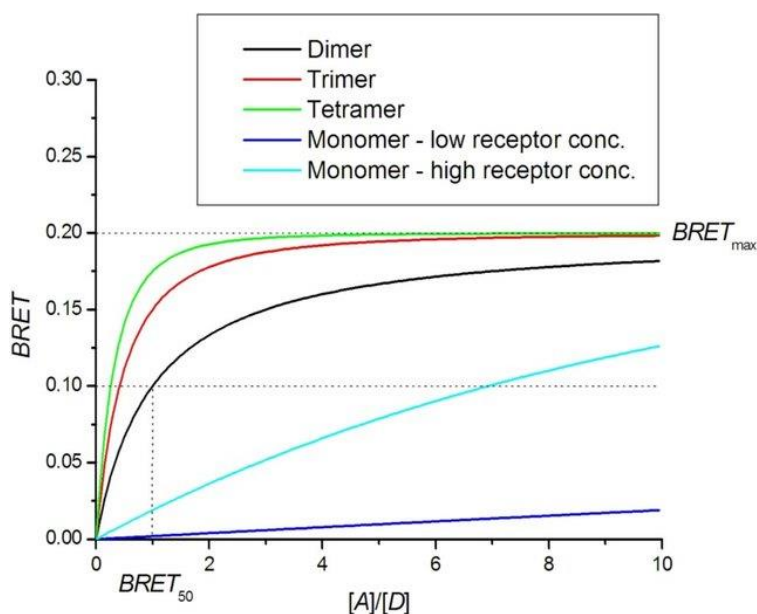


Figure 1.5 Theoretical saturation curves. $BRET_{50}$, a ratio of the receptor concentration where the curve reaches half-maximum, while the maximum value is called $BRET_{max}$. $[A]$ is acceptor tagged receptor, $[D]$ is donor-tagged receptor. Taken from (Drinovec *et al.*, 2012).

1.4.2 BRET competition assay

A competition assay can be used to further validate the existence of oligomeric complexes. In this assay, the concentration of the untagged receptors is increased while the concentration of tagged receptors remains constant (Achour *et al.*, 2011; Ayoub *et al.*, 2002; Drinovec *et al.*, 2012; Vrecl *et al.*, 2006). If the untagged receptors compete with tagged receptors for binding in complexes, the BRET signal is predicted to diminish. In BRET competition assay, a high acceptor-to-donor ratio is frequently used because fluctuations in this ratio have less of an impact on the BRET signal than when the ratio is equal to 1. The decrease is often brought on by the interaction with untagged receptors. A hyperbolic curve is formed by the signal (Figure 1.6). Although the presence of oligomerization can be determined, it is challenging to determine the precise oligomerization state since the curves for dimers and higher oligomers are too similar (Drinovec *et al.*, 2012).

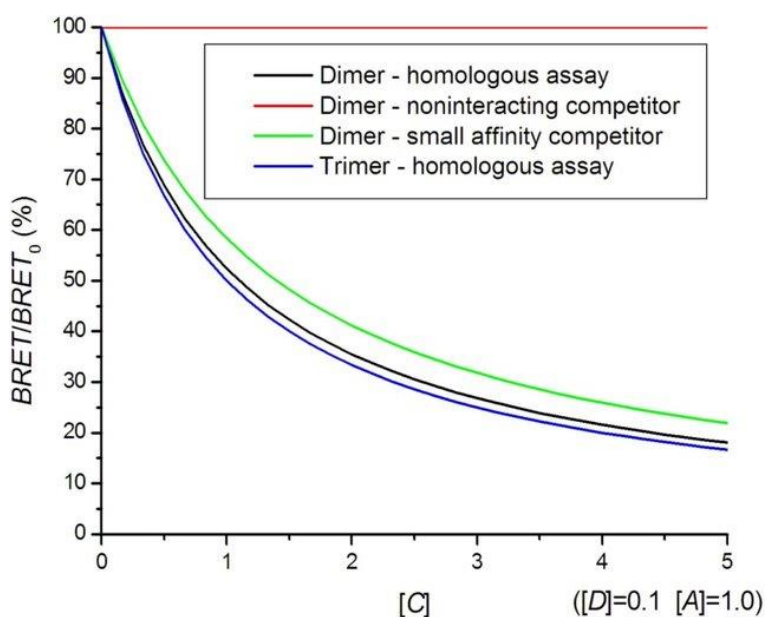


Figure 1.6 Theoretical competition curves. [A] is acceptor tagged receptor, [D] is donor-tagged receptor, and [C] is untagged receptor. Taken from (Drinovec *et al.*, 2012).

1.5 Förster resonance energy transfer (FRET)

Detection of oligomerization is widely used with Förster resonance energy transfer (FRET) technique. The technique relies on non-radiative energy transfer from an excited fluorophore (FRET donor) to a close ground-state acceptor fluorophore (FRET acceptor) with a dipole-dipole coupling (Skruzny *et al.*, 2019). The separation distance between two fluorophores determines the efficiency of energy (E_{FRET}) transfer between FRET donor and FRET acceptor. The sixth power of separation distance (r) over Förster radius (R_0^6) is inversely proportional to the E_{FRET} . If the distance between FRET donor and FRET acceptor is less than 10 nm, effective energy transfer occurs. E_{FRET} also depends on the quantum yield of the donor (Φ_0), orientation of donor and acceptor dipole moments (κ^2), extinction coefficient of the acceptor (ϵ_A) and the overlap integral between donor emission and acceptor excitation spectra (J) (Skruzny *et al.*, 2019):

$$E_{\text{FRET}} = \frac{R_0^6}{r^6 + R_0^6}$$

$$R_0^6 = 0.021 \times J \times \kappa^2 \times \Phi_0 \times n^{-4}$$

$$J = \int \Gamma^D \times \epsilon_A \times \lambda^4 \times d\lambda$$

Where Γ^D is normalized donor emission intensity, n is the refractive index of the medium, and the λ is the wavelength.

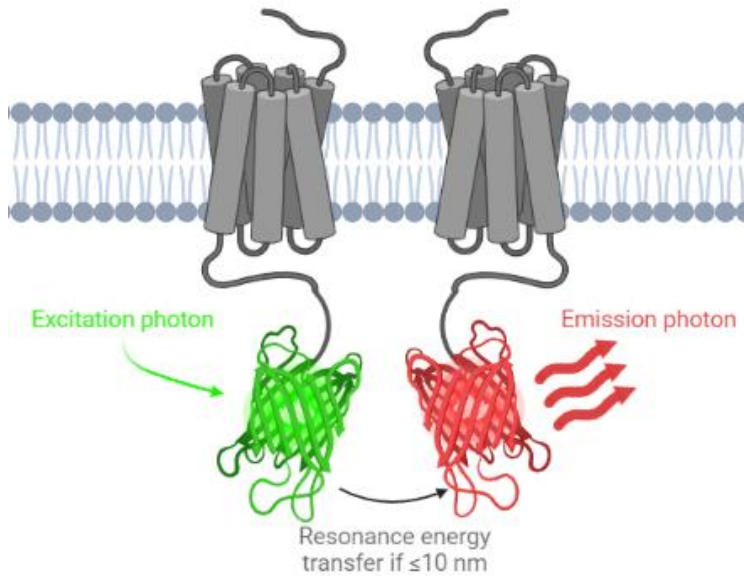


Figure 1.7 Illustration of Förster resonance energy transfer in tagged GPCRs. Donor fluorescent protein is excited with a certain laser and emits light and transfer its energy to the acceptor fluorescent protein if they are in close proximity. (Created using BioRender.com.)

Fluorescent proteins, when expressed both endogenously or exogenously do not have a toxic effect and they rarely interfere with the function of the proteins. In live-cell experiments, FRET-based methods are generally used for many assays such as calcium and cAMP response (Brzostowski *et al.*, 2009). In addition to the use of FRET as an intracellular response method, it can also be used for the detection of GPCR oligomerization. Oligomerization of class A receptors in *Drosophila*, Chemokine receptors, Ste2p in yeasts, mGluR2, β_2 AR, 5-HT_{1A}, and many more GPCR oligomerization has been detected with the FRET technique (Angers *et al.*,

2000; Asher *et al.*, 2021; Cevheroğlu *et al.*, 2021; Martínez-Muñoz *et al.*, 2016; Paila *et al.*, 2011; Rizzo & Johnson, 2020).

To measure the FRET efficiency many methods can be used: fluorescence lifetime imaging microscopy (FLIM), donor photobleaching, acceptor photobleaching, spectral imaging, 3-cube methods. In the 3-cube method FRET signals are collected by exciting the donor and measuring the acceptor emission, and it is corrected by donor and acceptor bleed-throughs (Padilla-Parra & Tramier, 2012). For the correction of these bleed-through, several formulas can be utilized. The technique developed by Xia and Liu is one of the best suitable methods for *in vivo* imaging, where proteins are frequently produced in living cells and exact control over expression levels is challenging. In this method, fluorophore levels are also taken into consideration (Xia & Liu, 2001).

1.6 Aim of the thesis

Since ADGRD1 has a crucial role in glioblastoma and ADGRG5 has a role in immune system, the outcome of this study is important for unraveling these receptors' structures and signaling mechanisms. This thesis aims to investigate the ADGRD1 and ADGRG5 receptor homo-oligomerization by using BRET and FRET methods in live cells. To achieve this, receptor constructs were tagged with NLuc, mEGFP, and mCherry with a linker (GSSG) from the end of the C-tails of the receptors. Mammalian cell line HEK 293 cells, which does not endogenously express ADGRD1 and ADGRG5, were transfected with constructs of interest and their BRET and FRET values were measured to find out the receptor dimerization.

CHAPTER 2

MATERIAL AND METHOD

2.1 Construction of fluorescent or bioluminescent-tagged ADGRD1 and ADGRG5

NLuc and mEGFP “cassettes” with linker (GSSG) constructed in pcDNA3.1(+) from pNL-1 and pEGFP-N2. These cassettes were used to tag the human ADGRD1 and ADGRG5 receptors using integration polymerase chain reaction (PCR) method. The human ADGRD1 (Figure 2.1) and ADGRG5 (Figure 2.2) receptors with HA tag were a kind gift from Dr. Ines Liebscher (University of Leipzig). After these, the receptor including plasmids, amplified, and both cDNA of the receptors has been transferred to the pcDNA3.1(+) vector by introducing NheI and NotI cut sites.

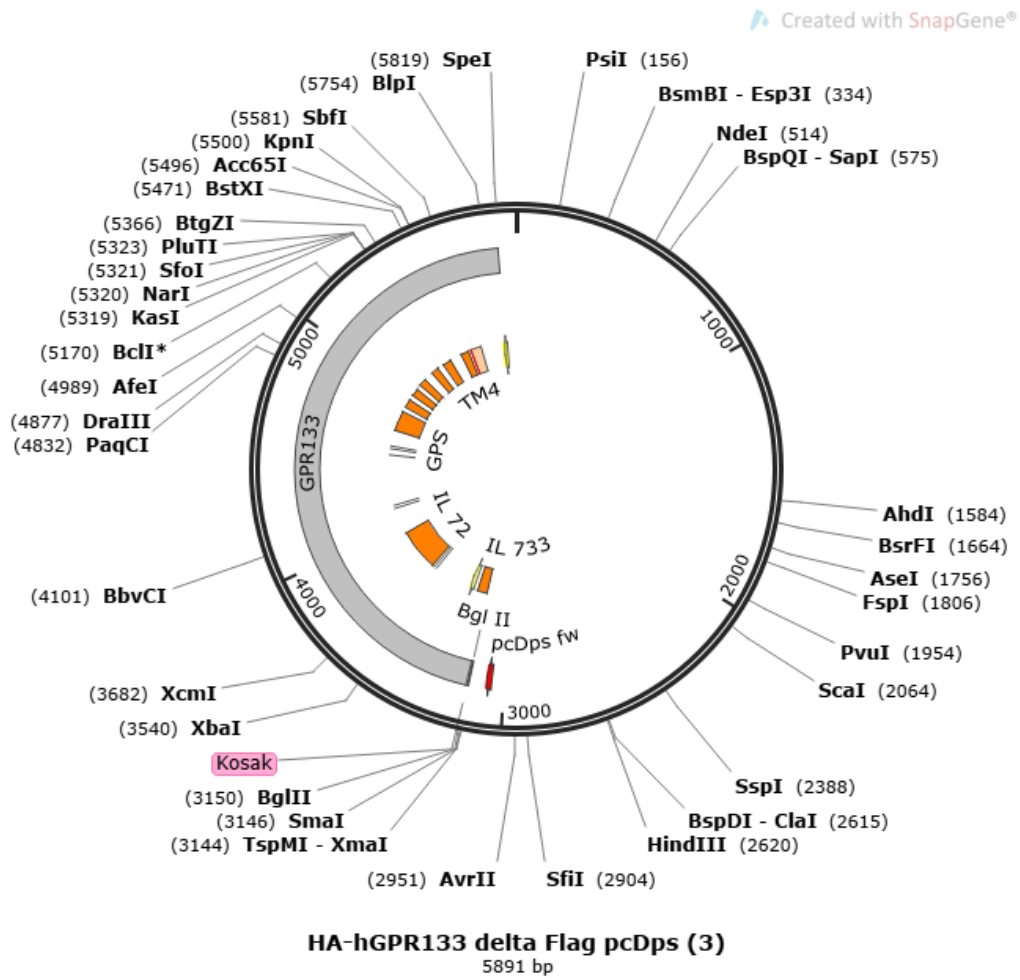


Figure 2.1 The plasmid carrying full-length ADGRD1/GPR133 receptor with HA and FLAG tag.

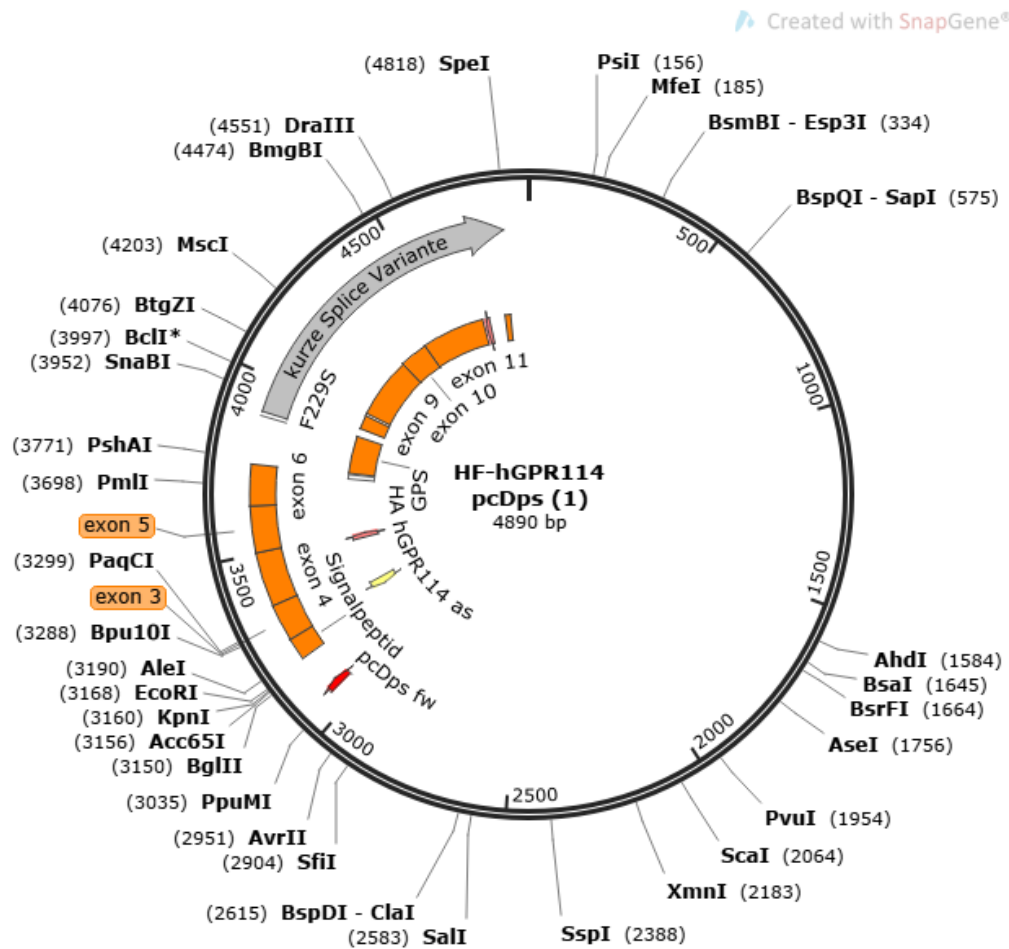


Figure 2.2 The plasmid carrying full-length ADGRG5/GPR114 receptor with HA and FLAG tag.

Insertional PCR includes two successive PCRs. In the first PCR, homologous sequences from the 5' and 3' of mEGFP or NLuc cassettes were amplified by using primer pairs (Table 2.1), and they were flanked by the bases from the directed sites of the ADGRD1 and ADGRG5 cDNA sequences (Table 2.2). The next insertional PCR was to fuse mEGFP or NLuc into the ADGRD1 and ADGRG5 cDNA (

Table 2.3), which uses the first PCR products as primers. The whole plasmid was amplified in this second PCR.

The primers used in the first PCR are to amplify the mEGFP or NLuc with linker sequences with ADGRD1 and ADGRG5 homologous sequences.

Table 2.1 Primers used for the mEGFP and NLuc amplification with GSSG linker. Primers are extended in a 5' to 3' direction.

Primer	Sequence
D1-L- Eins-F	GCCACTCTGCCCACCGCGTCGACCTGTCAGCCGTGGGCAG CAGCGGCGTGAGCAAGGGC
D1-L- Eins-R	CGGCCGCCACTGTGCTGGATATCTGCAGAATTCtcaCTTGTA CAGCTCGTCCATGCCGAG
D1-L- NLins-F	GCCACTCTGCCCACCGCGTCGACCTGTCAGCCGTGGGCAG CAGCGGCGTCTTCACACTCG
D1-L- NLins-R	CGGCCGCCACTGTGCTGGATATCTGCAGAATTCtcaCGCCA GAATGCGTTTCGCACAGCCG
G5-L- Eins-F	ggccttcagctcctcccaacaacacagGGCAGCAGCGGCGTGAGCAAGG GC
G5-L- Eins-R	CGGCCGCCACTGTGCTGGATATCTGCAGAATTCctaCTTGTA CAGCTCGTCCATGCC
G5-L- NLins-F	gaggccttcagctcctcccaacaacacagGGCAGCAGCGGCGTCTTCACA CTCG
G5-L- NLins-R	GGCCGCCACTGTGCTGGATATCTGCAGAATTCctaCGCCAG AATGCGTTTCGCACAGCCGC

Table 2.2 First PCR conditions and component concentration for the mEGFP and NLuc amplification.

Components	20 μL	Final Concentration
Nuclease-free water	5.8-x	
5x Q5 Reaction Buffer	4	1X
2 mM dNTPs	2	200 μ M
Forward Primer	2	0.5 μ M
Reverse Primer	2	0.5 μ M
Template	x	< 1,000 ng
Q5 High-fidelity DNA Polymerase	0.2	0.02 U/ μ l
5x Q5 High GC Enhancer	4	(1X)

98°C 30 s

98°C 10 s

54°C 30 s 35 Cycles

72°C 30 s/kb

72°C 2 m

4°C hold

Thermo Scientific™ GeneJET PCR Purification Kit was used to purify the 1st PCR products bearing the ADGRD1 and AGRG5 homolog sequences before they were used in the insertional PCR.

Table 2.3 Integration PCR conditions and component concentrations to attach first PCR products into ADGRD1 and ADGRG5 cDNA in pcDNA3.1(+). Molar ratio for receptor to amplified mEGFP and NLuc is set to 1:50.

Components	Volume	Final Concentration
Nuclease-free water	9.8-(x+y)	
5x Q5 Reaction Buffer	4	1X
2 mM dNTPs	2	200 μ M
PCR product	y	0.5 μ M
Template	x	80 ng
Q5 High-fidelity DNA Polymerase	0.2	0.02 U/ μ l
5x Q5 High GC Enhancer	4	(1X)

98°C 30 s

98°C 10 s

Gradient 30 s 35 Cycles

72°C 30 s/kb

72°C 2 m

4°C hold

Then, 2nd PCR product was digested with the FastDigest DpnI enzyme from Thermo Scientific™ to remove the methylated template plasmid and leave just the freshly generated plasmid (Table 2.4). DpnI enzyme only cleaves the site when methylated by detecting the 'Gm6A/TC-3'. The template was cleaved in the presence of DpnI enzyme since it has previously been methylated and is extracted from the DH5 α strain of *E. coli*.

Table 2.4 Digestion with DpnI components

Component	Volume
10X FastDigest Buffer	2.3
FastDigest DpnI	1
PCR mixture	20

After the digestion occurs, the mixture was used for transformation by using competent DH5 α strain of *E. coli*. Under the aseptic conditions, competent cells are thawed on ice for around five minutes. Then, 5 μ L of mixture had been put in to the 50 μ L of competent cells. Mixture and cells are gently mixed by flicking the tube followed by incubation on ice for 30 minutes. After incubation, heat shock at 42°C for 45 seconds is applied. After that, cells were incubated on the ice for 5 more minutes. The total volume is completed to 1 mL by adding Super Optimal Broth with catabolite repression (SOC), and then cells were grown at the 37°C for 1 hour with a constant shake. Cells were centrifuged at 6000 rpm for 3 minutes. 800 μ L of the supernatant was discarded. Pellet was resuspended with the remaining supernatant and inoculated on to Ampicillin selective agar plates by spreading. Inoculated plates were incubated overnight at 37°C.

After colonies were formed on the Ampicillin selective plates, colonies were selected, and the 1/3 of the colony is transferred to the 14.3 μ L of nuclease-free water and at the 98°C they were denaturated for 3 minutes. Denaturated colonies were used for the colony PCR to confirm (Table 2.5,

Table 2.6).

Table 2.5 Primers used for the colony PCR. Primers are extended in a 5' to 3' direction.

Primer	Sequence
seqp31-1f	GTGTACGGTGGGAGGTCTAT
seqp31-1r	AGGAAAGGACAGTGGGAGTG
Seqd1-2358F	CTTGCTGTCAACGGTTGTG
Seqg5-1453F	CTTTTGGCGTCTTCCTGCT
seqCherry412r	cttcttctgcattacggggc

Table 2.6 Colony PCR conditions and component concentrations.

Component	Volume	Final Concentration
Water	14.3	
10X PCR Buffer, -Mg	2	1X
50 mM MgCl ₂	0.6	
2 mM dNTPs	2	200 μM each
Forward Primer	0.5	0.5 μM
Reverse Primer	0.5	0.5 μM
Taq DNA Polymerase (5 U/μL)	0.1	3%

94°C 3m

94°C 45s

55°C 30s 35cycles

72°C 90 s/kb

72°C 10m

4°C hold

After colony PCR, products were run on 1% agarose gel. Colonies that have the correct insert size were inoculated into Ampicillin selective Luria-Bertani (LB) broth and let it grow overnight at 37°C with a constant shake.

Plasmids were purified from the inoculated LB by using Thermo Scientific™ GeneJET Plasmid Miniprep kit. In order to determine whether the plasmid includes the desired insert, plasmids were cut with double restriction enzyme digestion and digests were run on 1% agarose gel (Table 2.7).

Table 2.7 Control digestion with restriction enzymes for the conformation of the positive inserts.

Component	Volume
Nuclease-free water	9.1
10 FastDigest Green Buffer	2
FastDigest KpnI	0.2
FastDigest XbaI	0.2
Plasmid	4

Positive constructs were sent for sequencing and correct constructs are used in further experiments.

2.2 Cell culture

2.2.1 HEK 293 maintenance, passage, seeding into culture vessels

For the grown of the HEK 293 cells, complete medium DMEM; ThermoFisher Scientific, USA), 10% fetal bovine serum (FBS; ThermoFisher Scientific, USA), and 1% penicillin/streptomycin (Pen/Strep; ThermoFisher Scientific, USA) was used to culture it. The cells were maintained in a rectangular-shaped canted neck 25 cm² cell culture flask at humidified 37°C and 5% CO₂ conditions. To ensure the aseptic conditions, all mammalian cell culture operations were carried out in a laminar-flow hood, and all chemicals and equipment were kept in a way that preserved their sterility. Twice a week, cells undergo subculture as soon as they become confluent around 80-90%. Confluent had their whole medium aspirated before quickly washed with 3 mL of prewarmed 1X Dulbecco's Phosphate Buffered Saline (DPBS, Biological Industries, Israel). ThermoFisher Scientific, USA) supplied 1 ml of TrypLE™ Express enzyme (ThermoFisher Scientific, USA), which was pre-warmed before being incubated at 37°C for 5 minutes to release cells from the bottom of the flask. Once the cell layer dispersed, the flask was examined using a ZEISS Axio

Vert.A1 inverted microscope (Zeiss, Germany). To dilute the TrypLE™ Express enzyme, cells were resuspended with a pre-warmed complete media and gently aspirated. To remove the enzyme, aspirated cells were put into a 50 mL conical bottom tube (made by Greiner Bio-One in Austria) and spun down for 3 minutes at 900 rpm. After carefully removing the supernatant, the cell pellet was separated from the tube by lightly tapping it. With 5 mL of fresh pre-warmed complete media, cells reconstituted. By using a hemocytometer, cell counter, and Trypan Blue were used to count the total number of cells and assess their viability percentage. 20 µL sample from a cell stock was combined with 20 µL of Trypan Blue, and the mixture was then incubated for one to two minutes. The hemocytometer was the loaded with 10 µL of Trypan Blue-treated cells, and the living and dead cells were counted in four sets of 16 corners that had been chosen.

$$Total\ cells/mL = \frac{Total\ live\ cell\ counted * Dilution\ factor * 10^4}{Number\ of\ squares\ counted}$$

Cell viability (%)

$$= \frac{Average\ live\ cell\ counted}{Average\ live\ cell\ counted + Average\ dead\ cell\ counted} * 100$$

As a subculture and suitable culture vessel for future transfection containing new, pre-warmed complete media, enough resuspended cells were transferred to a fresh 25 cm² cell culture flask (Table 2.8). To disseminate cells equally, the flask and vessel were shaken back and forth and side to side multiple times. Cells were incubated at 37°C and 5% CO₂ in a humidified atmosphere.

Table 2.8 Seeding densities of HEK 293 cells into vessels.

Culture vessels	Seeding density	Final volume
T-25	0.50×10^6	5 mL
35-mm dish	0.25×10^6 or 0.50×10^6	2 mL
24-well plate	0.20×10^6	0.5 mL
96-well plate	0.01×10^6	0.1 mL

2.2.2 Transient plasmid transfection of HEK 293 cells

Using PLUS Reagent and Invitrogen Lipofectamine LTX Reagent, transient transfection was carried out. In Gibco™ Opti-MEM™ Reduced Serum Medium with Phenol Red, the required quantity of DNA was diluted, and PLUS™ Reagent was added. Opti-MEM™ was also used to dilute Lipofectamine™ LTX Reagent into a different tube (Table 2.9).

Table 2.9 Transient transfection reagents for the vessels.

Culture vessels	DNA (ng/μL)	Opti-MEM in each mix (μL)	PLUS™ (μL)	LTX (μL)	Opti-MEM onto cells (μL)	Complete medium (μL)
35-mm	500	100	4	4	1000	1000
24-well	200	50	2	2	100	300
96-well	100	9.75	0.25	0.25	30	50

The Opti-MEM – DNA - PLUS™ combination was combined with the Opti-MEM – LTX mixture, and the entire mixture was incubated for 30 minutes at room temperature. Pre-warmed Opti-MEM was poured onto the cells after the culture media on top of them had been removed and washed with 1X PBS after it had warmed up. The mixture and plasmid DNA were carefully dropped into the cells one at a time. For three hours, the culture vessel was kept in the CO₂ incubator. The transfected cells were added the complete medium and they underwent a 48-hour incubation at 37°C and 5% CO₂ incubator.

2.3 Western blotting

Per each 35-mm cell culture dish 0.5×10^6 HEK 293 cells were seeded (see 2.2.1). Cells were transfected with receptor constructs (see 2.2.2) and they were incubated for 48 hours in incubator.

2.3.1 Sample preparation and protein harvesting

After 48 hours of incubation, dishes were set on ice and the culture media was removed. The cells were washed with 500 μ L of 1X PBS. After washing the cells were lysed using ice-cold 1X Radioimmunoprecipitation (RIPA) buffer and scraped with a cell scraper. Cell lysates were put into ice-cold microcentrifuge tubes, and they were kept on ice for 15 minutes. Then, the lysates were gently sonicated with Elmasonic S 80 (H) for 8 cycles of 15 seconds on and 60 seconds off to shear the chromatin. At 4°C and 15000 g for 10 minutes, tubes were centrifuged. After the centrifuging step, supernatant carefully transferred to another ice-cold microcentrifuge tube. Pierce™ BCA Assay Kit (Thermo Fisher Scientific, USA) was used to determine the total protein content.

2.3.2 Cell loading and SDS-PAGE

4X Laemmli buffer was used to dilute the cell lysates. For 30 minutes Laemmli added lysates were incubated at 37°C. Wells were filled with 20 μ L of lysates and a molecular weight marker. Until the dye reached the reference line, samples were run in the SDS-PAGE gel at 100 V. The gel was delicately removed from the cassette at the end of the run and soaked in the Mili-Q® ultrapure water.

2.3.3 Protein Transfer

Gel was transferred into a 1X transfer buffer and incubated for 15 minutes. Meanwhile, The PVDF membrane (Immobilon[®]-PSQ PVDF Membrane) was activated in methanol for 30 seconds and then incubated in Mili-Q[®] ultrapure water for 5 minutes. Then, the membrane was incubated in the 1X transfer buffer for 5 minutes. To make a wet transfer, onto the black part of cage a sponge dipped into 1X transfer buffer, and on top of it 1X transfer buffer soaked watman paper was layered. The gel was layered and then activated PVDF membrane was put on top of it without making any air bubbled. Soaked watman paper was put on top of the membrane and 3 sponges were added at last. Then the cassette was closed. 1X ice-cold transfer buffer was put into the tank and transferred occurred in Hoefer SE300-10A-1.0 Minive Complete Vertical Electrophoresis System at 4°C for 1 hour at constant 400 mA.

2.3.4 Antibody probing

After the transfer, the PVDF membrane was incubated with Blocking buffer for 1 hour on a rocker at room temperature. Following blocking, the membrane was washed with 1X TBST for 10 minutes 3 times in a row. After washing, it is incubated at 4°C on a rocker with HA antibody (HA-Tag (F-7) 200 µg/ml (Santa Cruz BT, USA) in TBST (1:500)) overnight. The very next day, membrane was washed with 1X TBST for 10 minutes 3 times in a row. Then the membrane was exposed to SuperSignal[™] West Pico PLUS Chemiluminescent Substrate (ThermoFisher Scientific, USA) and the image was acquired using BIO-RAD ChemiDoc MP Imaging System (BioRad, USA).

2.4 Confocal microscopy

Positively built mEGFP tagged ADGRD1 and ADGRG5 constructs were seeded and transfected into glass-bottom 35mm dishes for live-cell imaging (see 2.2.1, 2.2.2). Images were taken by exciting the fluorophore in the mEGFP tagged receptors with a laser beam at 488 nm and the emission was collected between 493 – 586 nm and GAP43-mCherry (Membrane marker) or Seq61b-mApple (ER marker) with a laser beam at 594 nm and the emission was collected in between 599 – 754 nm using Zeiss LSM880 Laser Scanning Confocal Microscope equipped with Zeiss 63x/1.4 Plan Apochrome Oil DIC objective (Stem Cell Institute, Ankara University, Turkey) to observe the localization and expression in the HEK 293 cells.

2.5 BRET assay

Into black 96-well microplate, HEK 293 cells were seeded (see 2.2.1). After 24 hours, they are co-transfected with 50 ng of NLuc tagged receptors as BRET donor and 50 ng of mEGFP tagged receptors as BRET acceptor according to transfection protocol (see 2.2.2). On then day of the assay, 1:1000 of Furimazine 48 (Promega, USA) was diluted in HBSS. After removing the medium from cells, 100 μ L of the Furimazine-HBSS solution was added to each well. NanoBRET was measured using the Mithras² LB 943 Multimode Microplate Reader (Berthold Technologies, Germany) and data were collected with MicroWin 2010. Measurements were conducted using the 460m70 filter for NLuc emission and the 515m40 filter for mEGFP emission.

2.5.1 BRET saturation assay

According to the transfection protocol described, HEK 293 cells were seeded in a black 96-well microplate and co-transfected with a constant amount of NLuc tagged receptor as a BRET donor (10 ng) both in the absence and presence of increasing the amount of mEGFP tagged receptor as a BRET acceptor (0, 10, 20, 40, 60, 80, 100, 160, 200 ng) (see 2.2.1, 2.2.2). 48 hours after transfection, Furimazine-HBSS solution was prepared by diluting Furimazine in HBSS by the ratio of 1:1000. Media upon cells were discarded from the wells and 100 μ L Furimazine-HBSS solution was added on to the cells. Using Mithras² LB 943 Multimode Microplate Reader (Berthold Technologies, Germany) and MicroWin 2010, NanoBRET was directly measured. Measurements were conducted using the 460m70 filter for NLuc emission and the 515m40 filter for mEGFP.

2.5.2 BRET competition assay

HEK 293 cells were seeded in a black 96-well microplate and co-transfected with constant quantity of NLuc tagged receptor as a BRET donor (10 ng) and mEGFP tagged receptor as a BRET acceptor (10 ng), while the quantity of the untagged receptor as competitor increased (0, 10, 20, 40, 60 ng) (see 2.2.1, 2.2.2). Furimazine-HBSS solution was made 48 hours after transfection by diluting Furimazine in HBSS by a factor of 1:1000. 100 μ L of Furimazine-HBSS solution was put on top of the cells after the media surrounding the cells in the wells was removed. NanoBRET was directly measured using the Mithras² LB 943 Multimode Microplate Reader (Berthold Technologies, Germany) and MicroWin 2010. The 460m70 filter for NLuc emission and the 515m40 filter for mEGFP were used in the measurements.

2.6 FRET assay

HEK 293 cells were seeded into 35mm glass-bottom dishes. 24 hours after seeding, cells were transfected with 500 ng of mEGFP tagged receptor as FRET donor and 500 ng of mCherry tagged receptor as FRET acceptor according to the transfection protocol. In the assay day, transfected cells were imaged using Zeiss LSM880 Laser Scanning Confocal Microscope equipped with Zeiss 63x/1.4 Plan Apochrome Oil DIC objective (Stem Cell Institute, Ankara University, Turkey). For donor channel, images were taken by exciting the mEGFP with a laser beam at 488 nm. Emission of the donor channel, emission was collected between 493 – 586 nm. For acceptor channel, mCherry was excited by using a 594 nm laser and the emission was collected in between 599 – 754 nm. For the FRET channel, 488 nm laser beam was used for the excitation and for the emission 599 – 754 nm is used. For the FRET calculations, Zeiss Zen module FRET plus Macro was used with Xia et.al. method. The donor coefficients and the acceptor coefficients were gathered with using only donor and only acceptor transfected cells.

CHAPTER 3

RESULTS

3.1 Construction of bioluminescent and fluorescent tagged receptors

NLuc, mEGFP, or mCherry-tagged receptors were constructed using the insertional PCR method. In the first PCR, NLuc, mEGFP, and mCherry were amplified by inserting a homologous flanking region of the ADGRD1 or ADGRG5 and linker (GSSG). In the second PCR, first PCR products were used as primers to be inserted into ADGRD1 and ADGRG5. Second PCR products were digested with DpnI enzyme to get rid of the template DNA and used in *E. coli* transformation. Colonies were selected and underwent colony PCR to confirm correct insertion size. Colony PCR products were loaded on 1% gel (Figure 3.1, Figure 3.2, Figure 3.3).

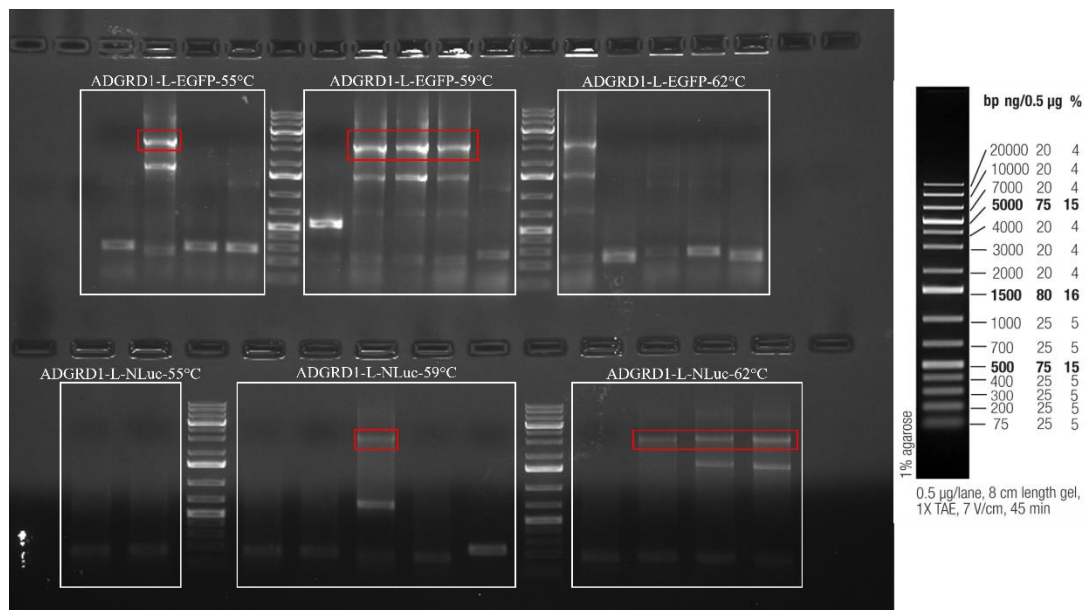


Figure 3.1 Agarose gel electrophoresis image of colony PCR for ADGRD1 cDNAs tagged with EGFP carrying linker (3378 bp) or NLuc carrying linker (3174 bp) in the C-tail. Red boxes indicate the plasmid and insert with the correct size. Primers used are seqp31-1f and seqp31-1r. DNA ladder is Invitrogen™ 1 kb Plus DNA Ladder.

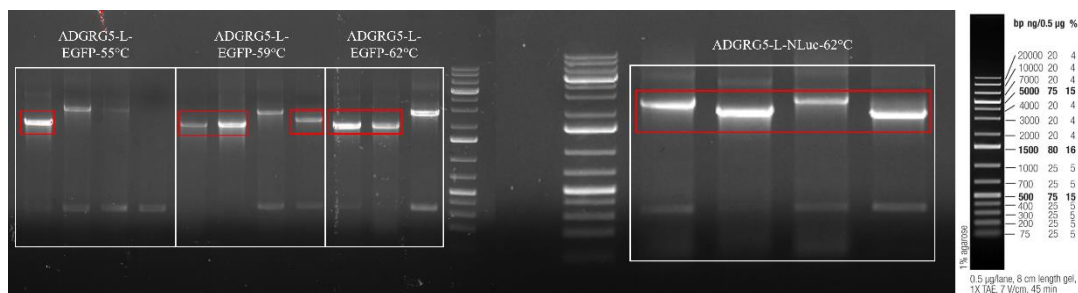


Figure 3.2 Agarose gel electrophoresis image of colony PCR for ADGRG5 cDNAs tagged with EGFP carrying linker (2316 bp) or NLuc carrying linker (2109 bp) in the C-tail. Red boxes indicate the plasmid and insert with the correct size. Primers used are seqp31-1f and seqp31-1r. DNA ladder is Invitrogen™ 1 kb Plus DNA Ladder.

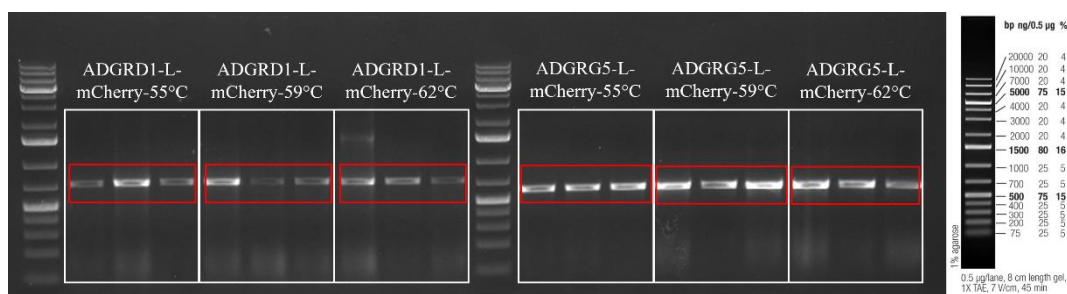


Figure 3.3 Agarose gel electrophoresis image of colony PCR for ADGRD1 cDNAs tagged with mCherry carrying linker (3369 bp) or ADGRG5 cDNAs tagged with mCherry carrying linker (2307 bp) in the C-tail. Red boxes indicate the plasmid and insert with the correct size. Primers used are Seqd1-2358F, Seqg5-1453F and seqCherry412r. DNA ladder is Invitrogen™ 1 kb Plus DNA Ladder.

Colonies which carry the correct insert according to colony PCR were inoculated in LB broth and grown for 16 hours. Then plasmids were isolated using GeneJET Plasmid Miniprep Kit (Thermo Scientific, USA). To make sure the plasmids carry the correct cDNA size, ADGRD1 constructs were digested with NheI and EcoRV, ADGRG5 constructs were digested with NheI and NotI and then run on 1% agarose gel (Figure 3.4, Figure 3.5, Figure 3.6).

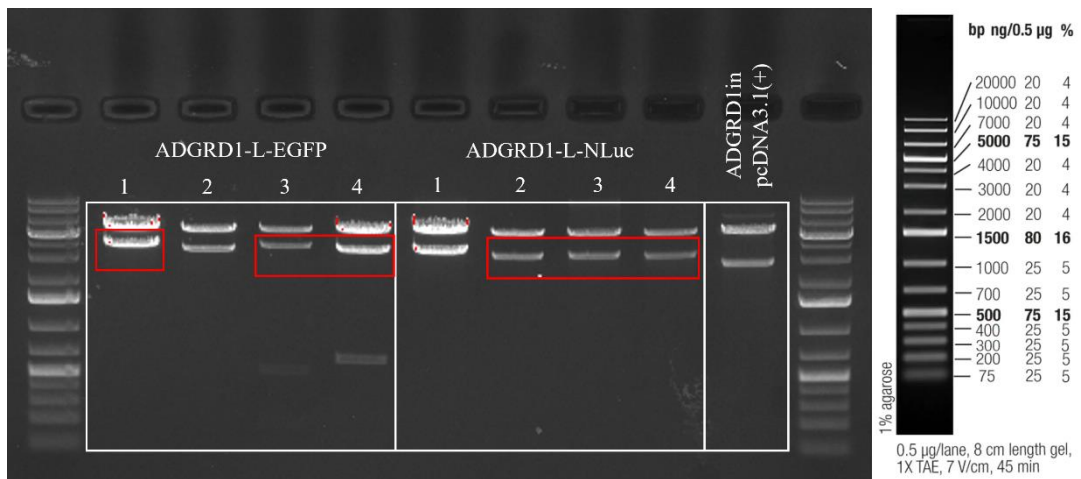


Figure 3.4 Agarose gel image of insertional PCR products after restriction enzyme (NheI-EcoRV) digestion to control the size of the EGFP and NLuc tagged ADGRD1 on C-terminus. The size of EGFP tagged ADGRD1 cDNAs is 3378 bp and NLuc tagged ADGRD1 cDNAs is 3174 bp. Red boxes indicate the plasmid and insert with the correct size. DNA ladder is Invitrogen™ 1 kb Plus DNA Ladder.

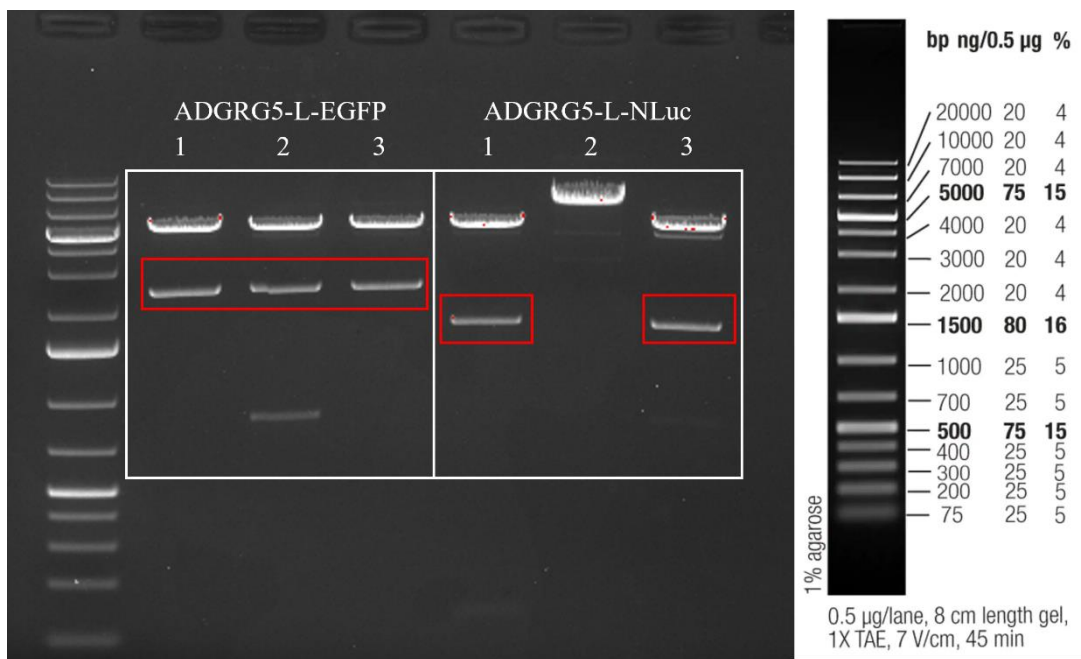


Figure 3.5 Agarose gel image of insertional PCR products after restriction enzyme (NheI-NotI) digestion to control the size of the EGFP and NLuc tagged ADGRG5 on C-terminus. The size of EGFP tagged ADGRG5 cDNAs is 2316 bp and NLuc tagged ADGRG5 cDNAs is 2109 bp. Red boxes indicate the plasmid and insert with the correct size. DNA ladder is Invitrogen™ 1 kb Plus DNA Ladder.

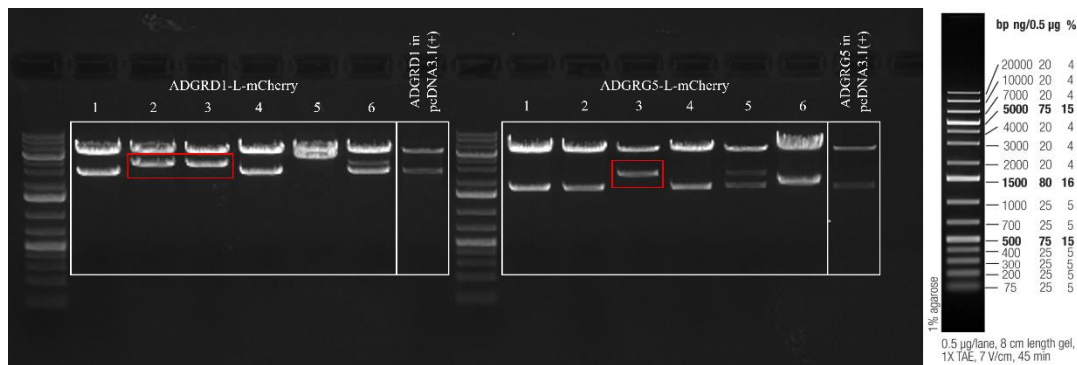


Figure 3.6 Agarose gel image of insertional PCR products after restriction enzyme (NheI-EcoRV&NheI-NotI) digestion to control the size of the EGFP and NLuc tagged ADGRG5 on C-terminus. The size of mCherry tagged ADGRD1 cDNAs is 3369 bp and mCherry tagged ADGRG5 cDNAs is 2307 bp. Red boxes indicate the plasmid and insert with the correct size. DNA ladder is Invitrogen™ 1 kb Plus DNA Ladder.

Furthermore, plasmids with correct sizes were verified by Sanger sequencing to continue the cell culture experiments.

3.2 Laser scanning confocal microscopy imaging

In confocal microscopy imaging, reduced background signal can be achieved which gives a better resolution since confocal microscopes eliminates the out of focus signal with the help of a pinhole. With that information in hand, mEGFP tagged receptors were imaged using laser scanning confocal microscope. mEGFP tagged receptors were co-transfected with a plasma membrane marker GAP43-mCherry to observe localization in the plasma membrane and with ER marker mApple-Sec61b to observe the localization in the ER in HEK 293 cells. After 48 hours of co-transfection of mEGFP tagged ADGRD1 and ADGRG5 constructs were imaged in 35-mm glass-bottom dishes. Live cells were imaged in CO₂ incubation using Zeiss 63x/1.4 Plan Apochrome Oil DIC objective. EGFP was excited at 488 nm laser line and its emission was collected in between 493 – 586 nm while mCherry and mApple were excited at 594 nm laser line and their emissions were collected in between 599-754.

EGFP tagged ADGRD1 constructs were imaged with both ER-marker-mApple and PM-marker-mCherry (Figure 3.7).

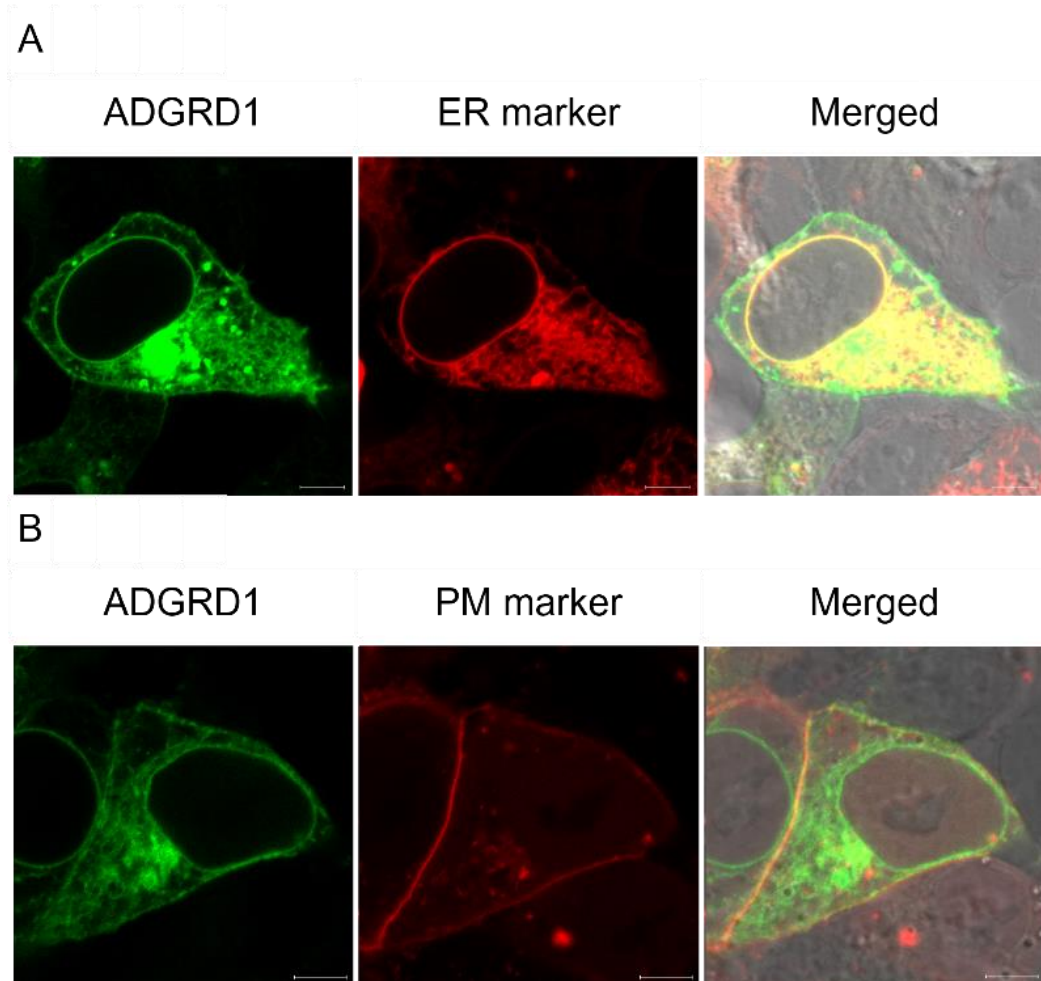


Figure 3.7 Laser scanning confocal microscopy images of ADGRD1-L-EGFP with Seq61b-mApple (A) and with GAP43-mCherry (B). Scale bar corresponds to 5 μ m

EGFP tagged ADGRG5 constructs images with ER-marker-mApple and PM-marker-mCherry were acquired (Figure 3.8).

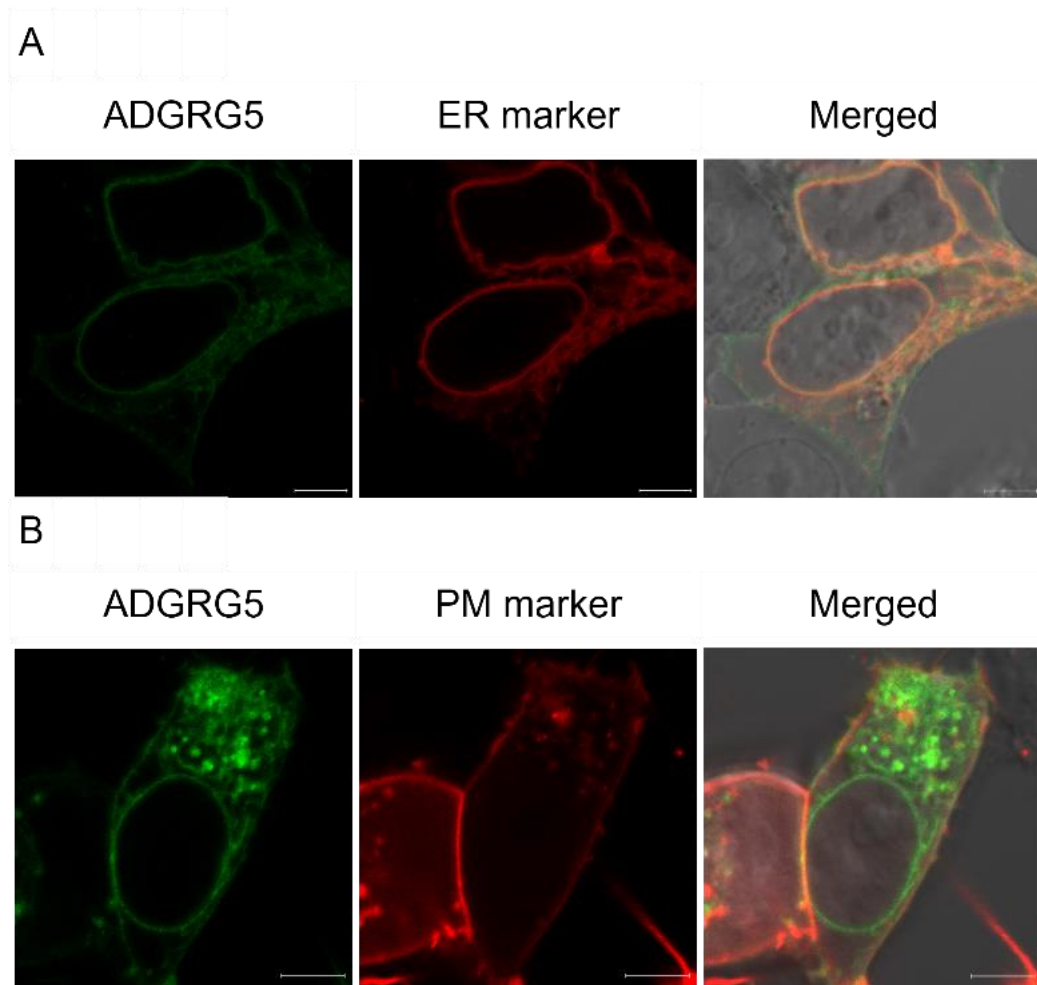


Figure 3.8 Laser scanning confocal microscopy images of ADGRG5-L-EGFP with Seq61b-mApple (A) and with GAP43-mCherry (B). Scale bar corresponds to 5 μ m

3.3 Western Blot

Tagged and untagged constructs of ADGRD1 and ADGRG5 were transfected in HEK 293 cells. After 48 hours of transfection, they were harvested for protein extraction. Each harvest was loaded on each well with Laemmli buffer to resolve on SDS-PAGE. After resolving, SDS gels were transferred to the PVDF membrane by wet transfer. The membrane was probed with Anti-HA antibody followed by the

blocking step. The blot was imaged by incubating the membrane with SuperSignal™ West Pico PLUS Chemiluminescent Substrate (Thermo Scientific, USA).

Anti-HA antibody probed ADGRD1 blot was imaged, and all bands were resolved between 75-100 KDa (Figure 3.9).

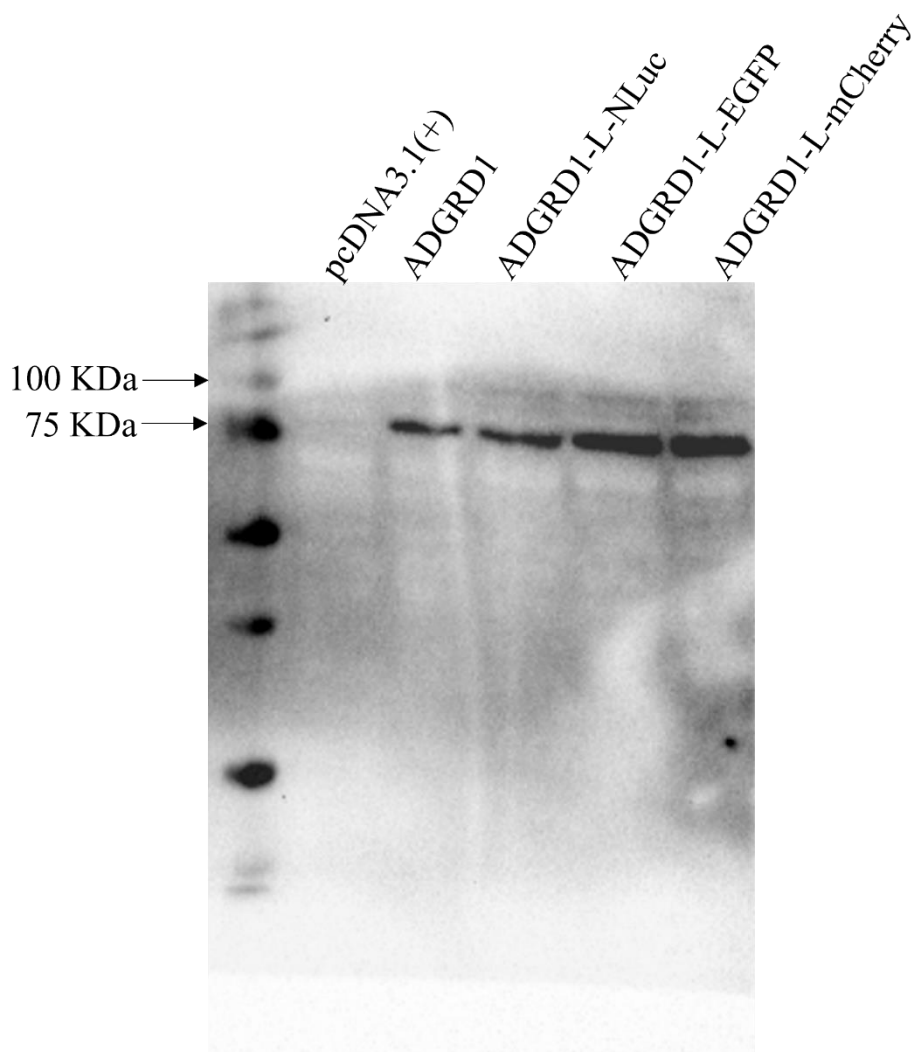


Figure 3.9 The immunoblot image of ADGRD1 constructs. Bands were detected with Anti-HA antibody. Protein marker is Precision Plus Protein™ All Blue Prestained Protein Standards #1610373 (Bio-Rad).

Anti-HA antibody probed ADGRG5 blot was imaged, and all bands were resolved approximately in line with the 75 KDa ladder band as expected (Figure 3.10).

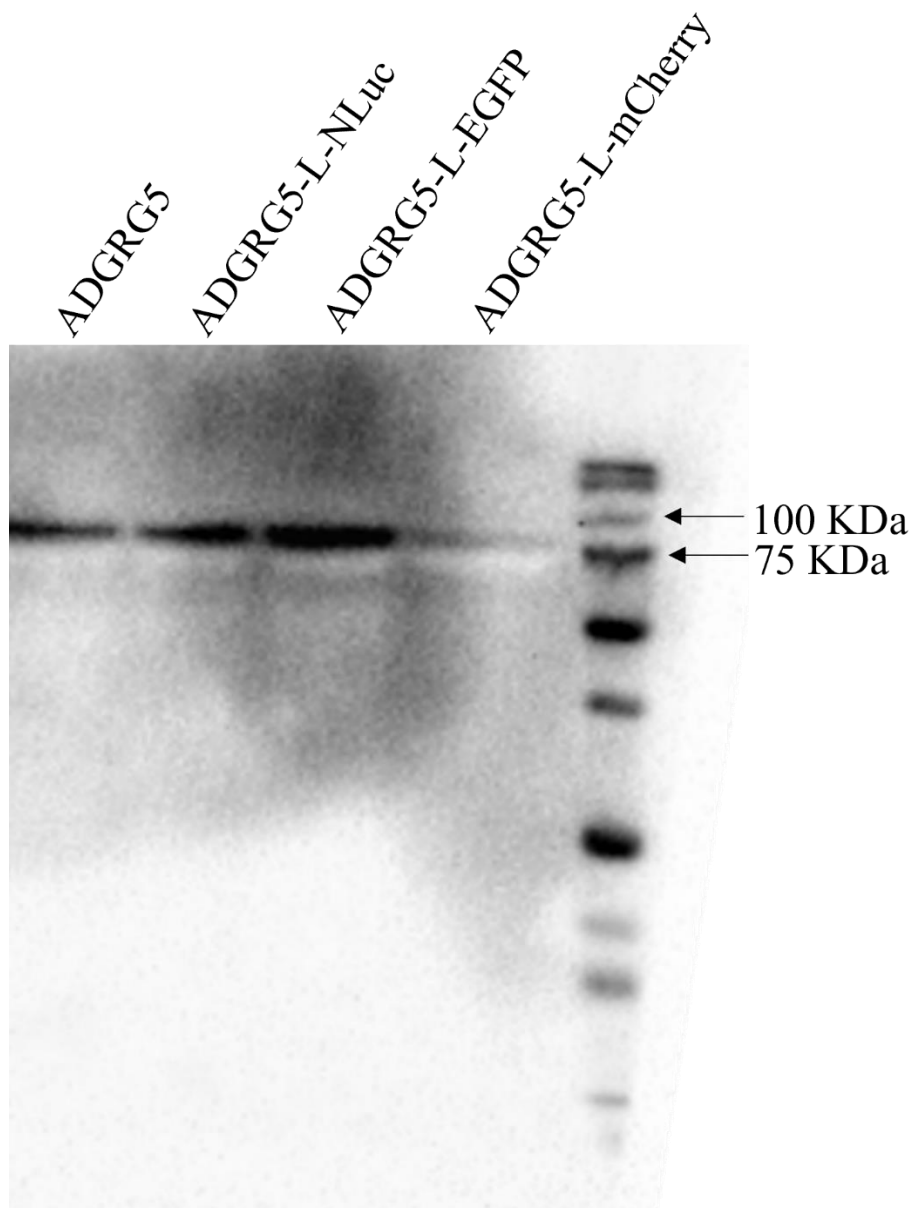


Figure 3.10 The immunoblot image of ADGRG5 constructs. Bands were detected with Anti-HA antibody. Protein marker is Precision Plus Protein™ All Blue Prestained Protein Standards #1610373 (Bio-Rad).

3.4 BRET

3.4.1 NanoBRET

In the BRET assay, NLuc tagged receptors (BRET donor) and mEGFP tagged receptors (BRET acceptor) were co-transfected into HEK 293 cells with a ratio equal to 1:1. HBSS solution containing furimazine as a substrate for NLuc was added onto cells. Energy transfer was measured by using 460m70 for NLuc and 515m40 filters for mEGFP. Emission measured from the EGFP filter were divided by the measurement from the NLuc filter which gives the BRET ratio. The overlap of For calculating the NetBRET, NLuc emission measured at the EGFP filter which is called the bleed-through signal was subtracted from the measured BRET ratio. Cells expressing only the NLuc tagged receptors were used as bleed-through control. Net BRET was calculated using a following formula:

$$Net\ BRET = \frac{EGFP}{NLuc} - Bleed - through$$

The bleed-through of the NLuc was calculated as 0.15. Net BRET results of the ADGRD1 calculated as 0.051 while Net BRET of the ADGRG5 calculated as 0.059 (Figure 3.11).

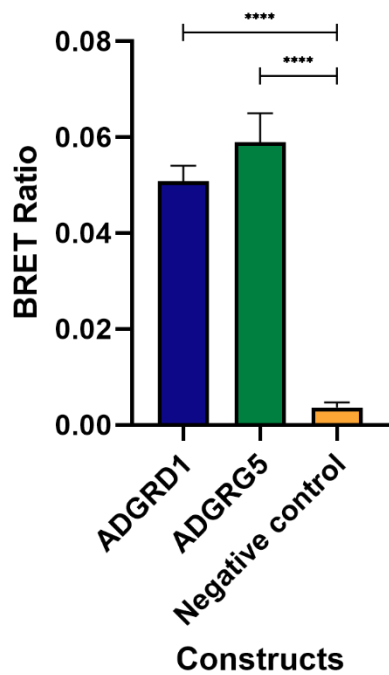


Figure 3.11 The Net BRET ratios of ADGRD1, ADGRG5 and negative control. Respectively, ADGRD1-L-EGFP and ADGRD1-L-NLuc; ADGRG5-L-EGFP and ADGRG5-L-NLuc; EGFP and ADGRG5-L-NLuc. $p < 0.05$. $n = 9$.

Moreover, to observe the shift in EGFP emission, each well underwent spectral scanning. Emissions were gathered from 400 nm to 600 nm in every 5 nm. The data from spectral scanning was graphed (Figure 3.12).

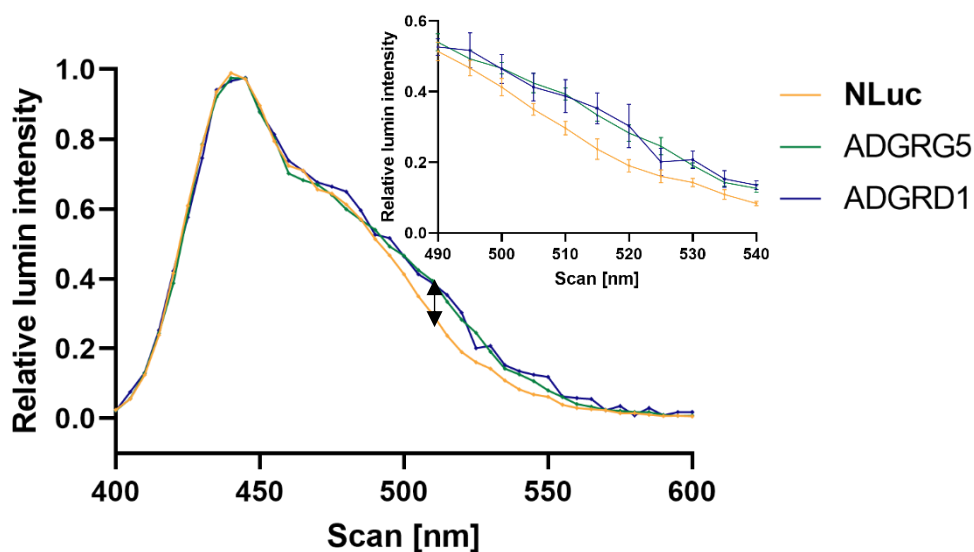


Figure 3.12 Spectral scanning data of ADGRD1, ADGRG5 and NLuc. Respectively, ADGRD1-L-EGFP and ADGRD1-L-NLuc; ADGRG5-L-EGFP and ADGRG5-L-NLuc; NLuc. Black arrow indicated the shift. n=6.

3.4.2 Saturation assay

In the BRET saturation assay, HEK 293 cells were co-transfected with a constant amount of NLuc tagged receptors and increasing amount of mEGFP tagged receptors. This method is used to eliminate the bystander BRET and to make sure that Net BRET measured is a result of the specific receptor interactions rather than random molecular collisions. The data from the samples were averaged and non-linear regression curve was plotted according to their Net BRET results using GraphPad Prism 8 (Figure 3.13).

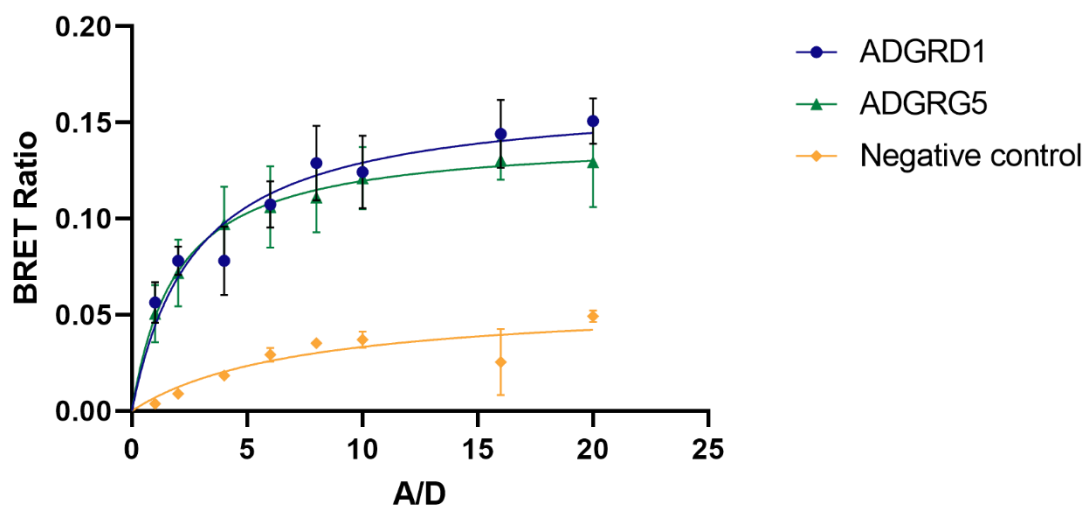


Figure 3.13 Saturation BRET assay for ADGRD1, ADGRG5 and negative control. Respectively, ADGRD1-L-EGFP and ADGRD1-L-NLuc; ADGRG5-L-EGFP and ADGRG5-L-NLuc; EGFP and ADGRG5-L-NLuc. A: acceptor, D: donor. n=9.

According to non-linear curves of saturation BRET, BRET₅₀ values were gathered by using nonlinear regression from (Borroto-Escuela *et al.*, 2013). The results can be found in Table 3.1.

Table 3.1 BRET₅₀ value comparison from saturation BRET assay for ADGRD1, ADGRG5 and negative control. Respectively, ADGRD1-L-EGFP and ADGRD1-L-NLuc; ADGRG5-L-EGFP and ADGRG5-L-NLuc; EGFP and ADGRG5-L-NLuc. p<0.05. n=9

BRET ₅₀	ADGRD1	ADGRG5	Negative control
Mean	1.8859	1.9447	17.4385
SD	±0.3936	±0.1954	±5.8363

3.4.3 Competition assay

In the BRET competition assay, HEK 293 cells which are co-expressing a constant amount of NLuc tagged receptors and EGFP tagged receptors with donor to acceptor

ratio amount is equal to 1:10 and increasing amounts of untagged receptors as competitor were used. Net BRET results were averaged, and non-linear regression curve was graphed by using GraphPad Prism 8 (Figure 3.14).

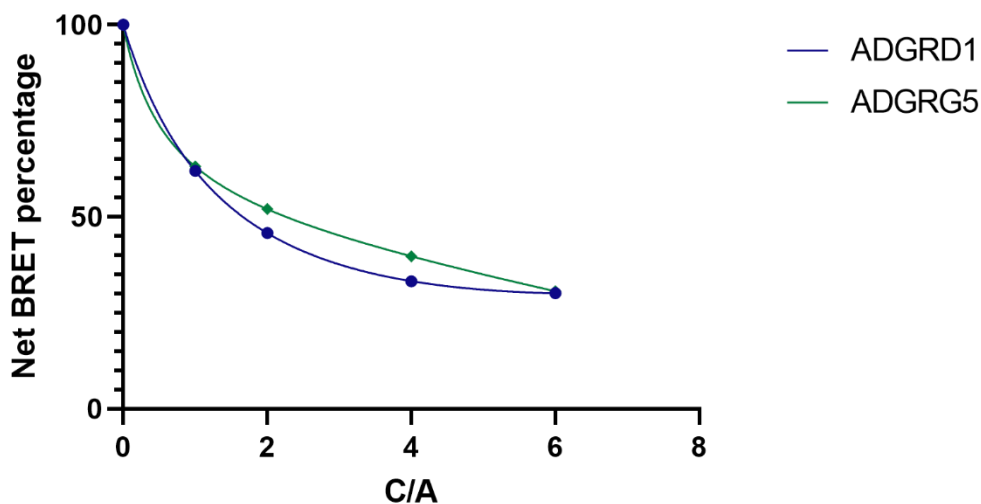


Figure 3.14 Competition BRET assay for ADGRD1 and ADGRG5. Respectively, ADGRD1-L-EGFP and ADGRD1-L-NLuc; ADGRG5-L-EGFP and ADGRG5-L-NLuc. C: competitor, A: acceptor. n=6.

3.5 FRET

FRET constructs were imaged using live cells expressing the tagged receptors in HEK 293 cells on 35-mm glass-bottom dishes by using Zeiss 63x/1.4 Plan Apochrome Oil DIC objective. To calculate the bleed-throughs, cells were transfected only with mEGFP tagged receptors (FRET donor) or only with mCherry tagged receptors (FRET acceptor). For the FRET experiments cells were co-transfected with mEGFP and mCherry tagged receptors. As negative control, GAP43-EGFP and GAP43-mCherry co-transfected cells and as for positive control, GAP43-EGFP-LVPR-mCherry constructs were used. For the FRET analysis, with 3-cube method, images were collected at FRET channel which uses excitation at 488 nm and emissions at 599-754 nm, donor channel uses excitation at 488 nm and

emissions at 493-586 nm, and acceptor channel uses excitation at 594 nm and emissions at 599-754 nm. Donor and acceptor coefficients were calculated using Zeiss Zen module FRET plus Macro (Figure 3.15).



Figure 3.15 FRET parameters gathered from Zeiss LSM880 Laser Scanning Confocal Microscope Zeiss Zen Modul FRET plus Macro using the Xia *et.al.* method settings for donor bleed-through and direct acceptor excitation.

Cells co-expressing mEGFP and mCherry tagged ADGRD1 constructs were imaged (Figure 3.16).

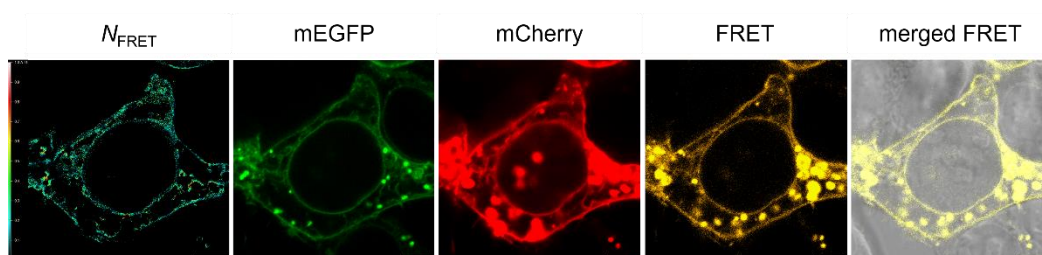


Figure 3.16 Laser scanning confocal microscopy images of ADGRD1 homooligomerization. Each column shows the FRET efficiencies, EGFP channel, mCherry channel, FRET channel and T-PMT and FRET channel merged images in order. Scale bar corresponds to 5 μm .

Cells co-expressing mEGFP and mCherry tagged ADGRG5 in HEK 293 cells were imaged (Figure 3.17).

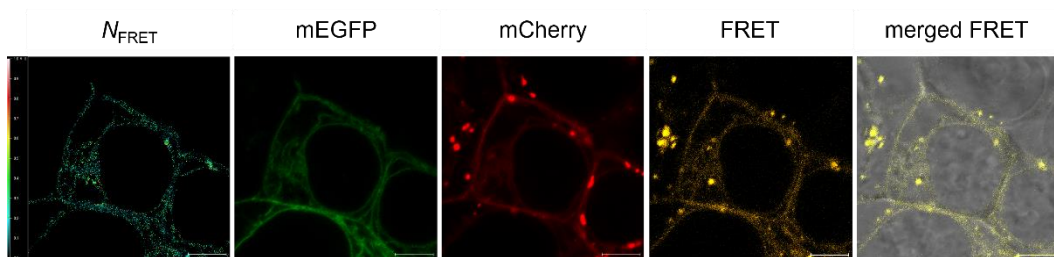


Figure 3.17 Laser scanning confocal microscopy images of ADGRG5 homo-oligomerization. Each column shows the FRET efficiencies, EGFP channel, mCherry channel, FRET channel and T-PMT and FRET channel merged images in order. Scale bar corresponds to 5 μm .

The normalized FRET data as the mean values of each region of interests (ROI) from multiple plasma membrane region after subtracting the background was plotted using GraphPad Prism 8 (Figure 3.18).

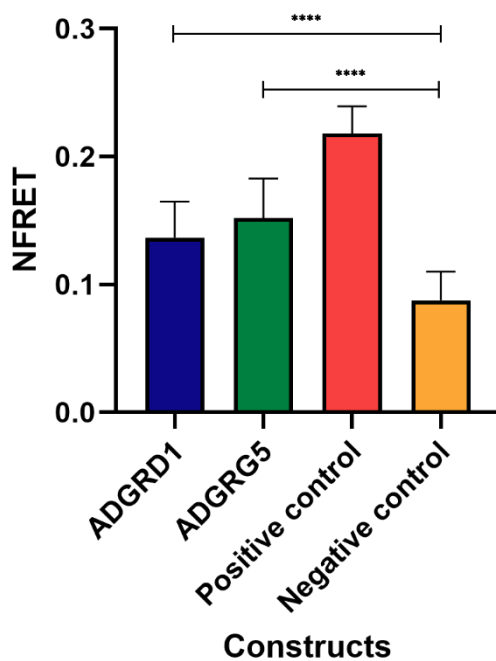


Figure 3.18 N_{FRET} results for ADGRD1, ADGRG5, positive and negative control. Respectively, ADGRD1-L-EGFP and ADGRD1-L-mCherry; ADGRG5-L-EGFP and ADGRG5-L-mCherry; GAP43-EGFP-LVPR-mCherry; GAP43-EGFP and GAP43-mCherry. $p < 0.05$. $n = 25$.

CHAPTER 4

DISCUSSION

4.1 Construction of bioluminescent and fluorescent-tagged receptors

Important part in the tagging of the GPCRs is not to disturb the protein trafficking and localization after inserting a peptide. To understand the dimerization of receptors, according to the literature, C-terminus tagging is the optimum place for a GPCR to be tagged, since GPCR oligomerization is maintained through 7-TM regions (Cvejic & Devi, 1997; Nguyen *et al.*, 2021; Schonbach *et al.*, 2016). Another thing to keep in mind is direct tagging of the receptor, without a linker might affect the receptor function (Bai & Shen, 2006). In this study, both ADGRD1 and ADGRG5 receptors has been tagged with fluorescent or bioluminescent proteins, in their C-terminus with a Gly-Ser-Ser-Gly linker sequence due to its flexibility. Because of small non-polar (Gly) and polar (Ser) amino acids, proteins allow mobility (Chen *et al.*, 2013).

4.2 Western Blot

Western blot experiments showed that all proteins were successfully expressed in the HEK 293 cells. ADGRD1 and ADGRG5 constructs were resolved whether they are wild-type or tagged with bioluminescent or fluorescent proteins. Anti-HA (Santa Cruz BT, USA) antibody detects the peptide sequence introduced to the receptor after signal peptide. Therefore, the bands resolved on the membrane corresponds to the NTF region of ADGRD1 and ADGRG5 receptors. This was probably caused by the presence of SDS in the SDS-PAGE as it will cause proteins

to lose their 3D structure thus possibly lead to the dissociation of the non covalently attached fragments from each other.

4.3 Laser Scanning Confocal Microscopy

After successfully constructing the ADGRD1 and ADGRG5 fusion proteins, HEK 293 cells were co-transfected with mEGFP tagged ADGRD1 or ADGRG5; and their localization was verified with colocalization studies with the membrane and ER markers. The images were acquired by exciting the mEGFP tagged receptors with laser beam at 488 nm, their emissions were gathered at 493 – 586 nm. Markers tagged with mCherry and mApple were excited with a laser beam at 594 nm, and their emissions were gathered in between 599 – 754 nm. According to images gathered, both ADGRD1 and ADGRG5 receptors traffic to the plasma membrane and ER. ER localization of both receptors is also expected due to the ongoing protein synthesis and trafficking during live cell imaging.

Cells expressing only the mEGFP tagged receptors were imaged, since mCherry is very similar to mEGFP according to their protein sequences and overall protein structure. NLuc tagged receptors were not imaged because the confocal microscope used is not suitable for bioluminescence imaging. However, it is expected that the NLuc tagged ADGRD1 and ADGRG5 would give a similar cellular localization.

4.4 BRET

In the BRET measurements, two different optical filters are used to differentiate the donor and acceptor emission signals. In this study, for the donor emission 460m70 filter, which is suitable for NLuc, and for the acceptor emission 515m40 filter, which is suitable for mEGFP were chosen.

According to the results from BRET assay, and spectral scanning after normalizing show that both the ADGRD1 and ADGRG5 receptors forms oligomers. In the

acquired BRET data, compared to negative control, net BRET ratio is significantly higher in the ADGRD1 and ADGRG5. To make a better view, it also can be seen in the spectral scanning data, both of the receptors' energy transfer are increased in the wavelength of the EGFP emission. Altogether, these data suggest the homo-oligomerization of both ADGRD1 and ADGRG5.

4.5 Saturation BRET

To eliminate the false positive signals that might arise due to high protein expression levels, saturation BRET assay was used. In this assay, donor amount remained constant while the acceptor amount was increased to saturate the donor. BRET saturation curve was fitted, which shows that BRET signal increased hyperbolically and saturates after all donor molecules have been occupied with the acceptor molecules. If there is a specific oligomerization and this interaction is independent from the overexpression. ADGRD1 and ADGRG5 receptors would be expected to give hyperbolic curves and that was the case. Significant difference in their BRET₅₀ value from the negative control suggest both receptors oligomerize and their oligomerization is independent from expression level.

4.6 Competition BRET

Another method to assess the specific interactions between proteins is competition BRET assay. In this assay, while the donor and acceptor amount are kept constant, competitor amount which in this case is the amount of untagged receptor is increased. BRET competition curve was fitted. The curve is hyperbolically getting lower while the competitor amount is increasing since untagged receptors compete with donor and acceptor molecules as expected. Data from the competition BRET competition assay supports the homo-oligomerization of ADGRD1 and ADGRG5.

4.7 FRET

To assess the oligomerization of ADGRD1 and ADGRG5 and the location of this receptor oligomers, FRET imaging for ADGRD1 and ADGRG5 were conducted in live cells with laser scanning confocal microscope. Images were taken in the following order for the FRET analysis: (1) FRET channel (ex. 488 nm, em. 599 - 754 nm), donor channel (ex. 488 nm, em. 493 - 586 nm), and (3) acceptor channel (ex. 594 nm, em. 599 - 754 nm). While the donor bleed-through was computed from the images of cells expressing only the donor, acceptor direct excitation was calculated from the images of cells expressing just the acceptor. ADGRD1 and ADGRG5 were shown to localize on the plasma membrane and ER. To calculate the homo-oligomerization on the plasma membrane, regions of interests (ROIs) corresponding to this cellular compartment were drawn. In these areas, N_{FRET} was calculated for each individual pixel. In comparison to BRET, fewer data points were selected in FRET experiments due to the nature of imaging. The calculated N_{FRET} values, however, agree with the BRET findings. FRET studies also suggest, ADGRD1 and ADGRG5 form oligomeric complexes.

CHAPTER 5

CONCLUSION

The presence of GPCR dimerization has been demonstrated with biochemical and physiological techniques. This study's main premise was that ADGRD1 and ADGRG5, like many other GPCR family members, may undergo homo-dimerization. One of the most crucial concerns to be addressed about aGPCRs is how to comprehend their therapeutic potential and functioning significance. As ADGRD1 plays an important role in glioblastoma, and ADGRG5 in immune cells, showing their homo-oligomerization in live cells is a crucial point for their signaling mechanism. In this study, homo-oligomerization of ADGRD1 and ADGRG5 was investigated with BRET and FRET techniques.

By tagging the ADGRD1 and ADGRG5 on their C-terminal domain with a linker, their localization, and expression were evaluated. All tagged receptors were localized on the plasma membrane and in ER possibly due to biosynthesis and trafficking. Expressions of all constructs in HEK 293 cells were shown by Western blot. Homo-dimerization of ADGRD1 and ADGRG5 was tested with BRET and FRET. Bystander BRET was eliminated with saturation and competition BRET assays.

This study shows the ADGRD1 and ADGRG5 homo-dimerization for the first time. Homo-oligomerization results from this study may illuminate the path for the relationship between oligomerization and the signaling mechanism of ADGRD1 and ADGRG5.

REFERENCES

- Achour, L., Kamal, M., Jockers, R., & Marullo, S. (2011). Using Quantitative BRET to Assess G Protein-Coupled Receptor Homo- and Heterodimerization. In L. M. Luttrell & S. S. G. Ferguson (Eds.), *Signal Transduction Protocols* (pp. 183-200). Humana Press.
https://doi.org/10.1007/978-1-61779-160-4_9
- Alexander, S. P., Christopoulos, A., Davenport, A. P., Kelly, E., Marrion, N. V., Peters, J. A., Faccenda, E., Harding, S. D., Pawson, A. J., Sharman, J. L., Southan, C., & Davies, J. A. (2017). THE CONCISE GUIDE TO PHARMACOLOGY 2017/18: G protein-coupled receptors. *British Journal of Pharmacology*, *174*, S17-S129. <https://doi.org/10.1111/bph.13878>
- Angers, S., Salahpour, A., Joly, E., Hilairet, S., Chelsky, D., Dennis, M., & Bouvier, M. (2000). Detection of beta 2-adrenergic receptor dimerization in living cells using bioluminescence resonance energy transfer (BRET). *Proc Natl Acad Sci U S A*, *97*(7), 3684-3689.
<https://doi.org/10.1073/pnas.97.7.3684>
- Araç, D., Boucard, A. A., Bolliger, M. F., Nguyen, J., Soltis, S. M., Südhof, T. C., & Brunker, A. T. (2012). A novel evolutionarily conserved domain of cell-adhesion GPCRs mediates autoproteolysis. *The EMBO Journal*, *31*(6), 1364-1378. <https://doi.org/10.1038/emboj.2012.26>
- Araç, D., & Leon, K. (2020). Chapter 2 - Structure, function and therapeutic potential of adhesion GPCRs. In B. Jastrzebska & P. S. H. Park (Eds.), *GPCRs* (pp. 23-41). Academic Press.
<https://doi.org/https://doi.org/10.1016/B978-0-12-816228-6.00002-7>
- Araç, D., Sträter, N., & Seiradake, E. (2016). Understanding the Structural Basis of Adhesion GPCR Functions. *Handb Exp Pharmacol*, *234*, 67-82.
https://doi.org/10.1007/978-3-319-41523-9_4
- Arpino, J. A. J., Rizkallah, P. J., & Jones, D. D. (2012). Crystal Structure of Enhanced Green Fluorescent Protein to 1.35 Å Resolution Reveals Alternative Conformations for Glu222. *PLoS ONE*, *7*(10), e47132.
<https://doi.org/10.1371/journal.pone.0047132>
- Asher, W. B., Geggier, P., Holsey, M. D., Gilmore, G. T., Pati, A. K., Meszaros, J., Terry, D. S., Mathiasen, S., Kaliszewski, M. J., McCauley, M. D., Govindaraju, A., Zhou, Z., Harikumar, K. G., Jaqaman, K., Miller, L. J., Smith, A. W., Blanchard, S. C., & Javitch, J. A. (2021). Single-molecule FRET imaging of GPCR dimers in living cells. *Nature Methods*, *18*(4), 397-405. <https://doi.org/10.1038/s41592-021-01081-y>
- Ayoub, M. A., Couturier, C., Lucas-Meunier, E., Angers, S., Fossier, P., Bouvier, M., & Jockers, R. (2002). Monitoring of Ligand-independent Dimerization and Ligand-induced Conformational Changes of Melatonin Receptors in Living Cells by Bioluminescence Resonance Energy Transfer. *Journal of*

- Biological Chemistry*, 277(24), 21522-21528.
<https://doi.org/10.1074/jbc.m200729200>
- Ayoub, M. A., & Pflieger, K. D. (2010). Recent advances in bioluminescence resonance energy transfer technologies to study GPCR heteromerization. *Curr Opin Pharmacol*, 10(1), 44-52.
<https://doi.org/10.1016/j.coph.2009.09.012>
- Bai, Y., & Shen, W. C. (2006). Improving the oral efficacy of recombinant granulocyte colony-stimulating factor and transferrin fusion protein by spacer optimization. *Pharm Res*, 23(9), 2116-2121.
<https://doi.org/10.1007/s11095-006-9059-5>
- Baldwin, T. O. (1996). Firefly luciferase: the structure is known, but the mystery remains. *Structure*, 4(3), 223-228.
[https://doi.org/https://doi.org/10.1016/S0969-2126\(96\)00026-3](https://doi.org/https://doi.org/10.1016/S0969-2126(96)00026-3)
- Bayin, N. S., Frenster, J. D., Kane, J. R., Rubenstein, J., Modrek, A. S., Baitalmal, R., Dolgalev, I., Rudzenski, K., Scarabottolo, L., Crespi, D., Redaelli, L., Snuderl, M., Golfinos, J. G., Doyle, W., Pacione, D., Parker, E. C., Chi, A. S., Heguy, A., Macneil, D. J., Shohdy, N., Zagzag, D., & Placantonakis, D. G. (2016). GPR133 (ADGRD1), an adhesion G-protein-coupled receptor, is necessary for glioblastoma growth. *Oncogenesis*, 5(10), e263-e263.
<https://doi.org/10.1038/oncsis.2016.63>
- Bayin, N. S., Modrek, A. S., & Placantonakis, D. G. (2014). Glioblastoma stem cells: Molecular characteristics and therapeutic implications. *World J Stem Cells*, 6(2), 230-238. <https://doi.org/10.4252/wjsc.v6.i2.230>
- Bhudia, N., Desai, S., King, N., Ancellin, N., Grillot, D., Barnes, A. A., & Dowell, S. J. (2020). G Protein-Coupling of Adhesion GPCRs ADGRE2/EMR2 and ADGRE5/CD97, and Activation of G Protein Signalling by an Anti-EMR2 Antibody. *Scientific Reports*, 10(1). <https://doi.org/10.1038/s41598-020-57989-6>
- Bjarnadóttir, T. K., Fredriksson, R., Höglund, P. J., Gloriam, D. E., Lagerström, M. C., & Schiöth, H. B. (2004). The human and mouse repertoire of the adhesion family of G-protein-coupled receptors. *Genomics*, 84(1), 23-33.
<https://doi.org/https://doi.org/10.1016/j.ygeno.2003.12.004>
- Bjarnadóttir, T. K., Geirardsdóttir, K., Ingemansson, M., Mirza, M. A., Fredriksson, R., & Schiöth, H. B. (2007). Identification of novel splice variants of Adhesion G protein-coupled receptors. *Gene*, 387(1-2), 38-48.
<https://doi.org/10.1016/j.gene.2006.07.039>
- Bohnekamp, J., & Schöneberg, T. (2011). Cell Adhesion Receptor GPR133 Couples to Gs Protein. *Journal of Biological Chemistry*, 286(49), 41912-41916. <https://doi.org/10.1074/jbc.c111.265934>
- Borroto-Escuela, D. O., Flajolet, M., Agnati, L. F., Greengard, P., & Fuxe, K. (2013). Bioluminescence resonance energy transfer methods to study G protein-coupled receptor-receptor tyrosine kinase heteroreceptor complexes. *Methods Cell Biol*, 117, 141-164. <https://doi.org/10.1016/b978-0-12-408143-7.00008-6>

- Breit, A., Lagacé, M., & Bouvier, M. (2004). Hetero-oligomerization between beta2- and beta3-adrenergic receptors generates a beta-adrenergic signaling unit with distinct functional properties. *J Biol Chem*, 279(27), 28756-28765. <https://doi.org/10.1074/jbc.M313310200>
- Brzostowski, J. A., Meckel, T., Hong, J., Chen, A., & Jin, T. (2009). Imaging Protein-Protein Interactions by Förster Resonance Energy Transfer (FRET) Microscopy in Live Cells. *Current Protocols in Protein Science*, 56(1). <https://doi.org/10.1002/0471140864.ps1905s56>
- Carrillo, J. J., López-Giménez, J. F., & Milligan, G. (2004). Multiple interactions between transmembrane helices generate the oligomeric alpha1b-adrenoceptor. *Mol Pharmacol*, 66(5), 1123-1137. <https://doi.org/10.1124/mol.104.001586>
- Cevheroğlu, O., Murat, M., Mingu-Akmete, S., & Son, Ç. D. (2021). Ste2p Under the Microscope: the Investigation of Oligomeric States of a Yeast G Protein-Coupled Receptor. *The Journal of Physical Chemistry B*, 125(33), 9526-9536. <https://doi.org/10.1021/acs.jpccb.1c05872>
- Chen, X., Zaro, J. L., & Shen, W. C. (2013). Fusion protein linkers: property, design and functionality. *Adv Drug Deliv Rev*, 65(10), 1357-1369. <https://doi.org/10.1016/j.addr.2012.09.039>
- Cheng, T. Y., Cramb, S. M., Baade, P. D., Youlden, D. R., Nwogu, C., & Reid, M. E. (2016). The International Epidemiology of Lung Cancer: Latest Trends, Disparities, and Tumor Characteristics. *J Thorac Oncol*, 11(10), 1653-1671. <https://doi.org/10.1016/j.jtho.2016.05.021>
- Cvejic, S., & Devi, L. A. (1997). Dimerization of the delta opioid receptor: implication for a role in receptor internalization. *J Biol Chem*, 272(43), 26959-26964. <https://doi.org/10.1074/jbc.272.43.26959>
- Dale, N. C., Johnstone, E. K. M., White, C. W., & Pflieger, K. D. G. (2019). NanoBRET: The Bright Future of Proximity-Based Assays. *Front Bioeng Biotechnol*, 7, 56. <https://doi.org/10.3389/fbioe.2019.00056>
- Davies, J. Q., Chang, G.-W., Yona, S., Gordon, S., Stacey, M., & Lin, H.-H. (2007). The Role of Receptor Oligomerization in Modulating the Expression and Function of Leukocyte Adhesion-G Protein-coupled Receptors. *Journal of Biological Chemistry*, 282(37), 27343-27353. <https://doi.org/10.1074/jbc.m704096200>
- Demberg, L. M., Rothmund, S., Schöneberg, T., & Liebscher, I. (2015). Identification of the tethered peptide agonist of the adhesion G protein-coupled receptor GPR64/ADGRG2. *Biochemical and Biophysical Research Communications*, 464(3), 743-747. <https://doi.org/10.1016/j.bbrc.2015.07.020>
- Ding, W. Q., Cheng, Z. J., McElhiney, J., Kuntz, S. M., & Miller, L. J. (2002). Silencing of secretin receptor function by dimerization with a misspliced variant secretin receptor in ductal pancreatic adenocarcinoma. *Cancer Res*, 62(18), 5223-5229.
- Drinovec, L., Kubale, V., Nøhr Larsen, J., & Vrecl, M. (2012). Mathematical Models for Quantitative Assessment of Bioluminescence Resonance Energy

- Transfer: Application to Seven Transmembrane Receptors Oligomerization [Review]. *Frontiers in Endocrinology*, 3. <https://doi.org/10.3389/fendo.2012.00104>
- Duc, N. M., Kim, H. R., & Chung, K. Y. (2015). Structural mechanism of G protein activation by G protein-coupled receptor. *European Journal of Pharmacology*, 763, 214-222. <https://doi.org/https://doi.org/10.1016/j.ejphar.2015.05.016>
- Ferré, S., Casadó, V., Devi, L. A., Filizola, M., Jockers, R., Lohse, M. J., Milligan, G., Pin, J. P., & Guitart, X. (2014). G protein-coupled receptor oligomerization revisited: functional and pharmacological perspectives. *Pharmacol Rev*, 66(2), 413-434. <https://doi.org/10.1124/pr.113.008052>
- Fischer, L., Wilde, C., Schöneberg, T., & Liebscher, I. (2016). Functional relevance of naturally occurring mutations in adhesion G protein-coupled receptor ADGRD1 (GPR133). *BMC Genomics*, 17(1). <https://doi.org/10.1186/s12864-016-2937-2>
- Foth, B. J., Tsai, I. J., Reid, A. J., Bancroft, A. J., Nichol, S., Tracey, A., Holroyd, N., Cotton, J. A., Stanley, E. J., Zarowiecki, M., Liu, J. Z., Huckvale, T., Cooper, P. J., Grecis, R. K., & Berriman, M. (2014). Whipworm genome and dual-species transcriptome analyses provide molecular insights into an intimate host-parasite interaction. *Nat Genet*, 46(7), 693-700. <https://doi.org/10.1038/ng.3010>
- Frenster, J. D., Inocencio, J. F., Xu, Z., Dhaliwal, J., Alghamdi, A., Zagzag, D., Bayin, N. S., & Placantonakis, D. G. (2017). GPR133 Promotes Glioblastoma Growth in Hypoxia. *Neurosurgery*, 64(CN_suppl_1), 177-181. <https://doi.org/10.1093/neuros/nyx227>
- Frenster, J. D., Kader, M., Kamen, S., Sun, J., Chiriboga, L., Serrano, J., Bready, D., Golub, D., Ravn-Boess, N., Stephan, G., Chi, A. S., Kurz, S. C., Jain, R., Park, C. Y., Fenyó, D., Liebscher, I., Schöneberg, T., Wiggin, G., Newman, R., Barnes, M., Dickson, J. K., Macneil, D. J., Huang, X., Shohdy, N., Snuderl, M., Zagzag, D., & Placantonakis, D. G. (2020). Expression profiling of the adhesion G protein-coupled receptor GPR133 (ADGRD1) in glioma subtypes. *Neuro-Oncology Advances*, 2(1). <https://doi.org/10.1093/noajnl/vdaa053>
- Frenster, J. D., Stephan, G., Ravn-Boess, N., Bready, D., Wilcox, J., Kieslich, B., Wilde, C., Sträter, N., Wiggin, G. R., Liebscher, I., Schöneberg, T., & Placantonakis, D. G. (2021). Functional impact of intramolecular cleavage and dissociation of adhesion G protein-coupled receptor GPR133 (ADGRD1) on canonical signaling. *J Biol Chem*, 296, 100798. <https://doi.org/10.1016/j.jbc.2021.100798>
- Gabilondo, A. M., Meana, J. J., Barturen, F., Sastre, M., & García-Sevilla, J. A. (1994). mu-Opioid receptor and alpha 2-adrenoceptor agonist binding sites in the postmortem brain of heroin addicts. *Psychopharmacology (Berl)*, 115(1-2), 135-140. <https://doi.org/10.1007/bf02244763>
- Goin, J. C., & Nathanson, N. M. (2006). Quantitative analysis of muscarinic acetylcholine receptor homo- and heterodimerization in live cells:

- regulation of receptor down-regulation by heterodimerization. *J Biol Chem*, 281(9), 5416-5425. <https://doi.org/10.1074/jbc.M507476200>
- González-Maeso, J. (2011). GPCR oligomers in pharmacology and signaling. *Molecular Brain*, 4(1), 20. <https://doi.org/10.1186/1756-6606-4-20>
- Gupte, J., Swaminath, G., Danao, J., Tian, H., Li, Y., & Wu, X. (2012). Signaling property study of adhesion G-protein-coupled receptors. *FEBS Lett*, 586(8), 1214-1219. <https://doi.org/10.1016/j.febslet.2012.03.014>
- Gurevich, V. V., & Gurevich, E. V. (2008). Rich tapestry of G protein-coupled receptor signaling and regulatory mechanisms. *Mol Pharmacol*, 74(2), 312-316. <https://doi.org/10.1124/mol.108.049015>
- Hall, M. P., Unch, J., Binkowski, B. F., Valley, M. P., Butler, B. L., Wood, M. G., Otto, P., Zimmerman, K., Vidugiris, G., Machleidt, T., Robers, M. B., Benink, H. A., Eggers, C. T., Slater, M. R., Meisenheimer, P. L., Klaubert, D. H., Fan, F., Encell, L. P., & Wood, K. V. (2012). Engineered Luciferase Reporter from a Deep Sea Shrimp Utilizing a Novel Imidazopyrazinone Substrate. *ACS Chemical Biology*, 7(11), 1848-1857. <https://doi.org/10.1021/cb3002478>
- Hamann, J., Aust, G., Araç, D., Engel, F. B., Formstone, C., Fredriksson, R., Hall, R. A., Harty, B. L., Kirchhoff, C., Knapp, B., Krishnan, A., Liebscher, I., Lin, H. H., Martinelli, D. C., Monk, K. R., Peeters, M. C., Piao, X., Prömel, S., Schöneberg, T., Schwartz, T. W., Singer, K., Stacey, M., Ushkaryov, Y. A., Vallon, M., Wolfrum, U., Wright, M. W., Xu, L., Langenhan, T., & Schiöth, H. B. (2015). International Union of Basic and Clinical Pharmacology. XCIV. Adhesion G protein-coupled receptors. *Pharmacol Rev*, 67(2), 338-367. <https://doi.org/10.1124/pr.114.009647>
- Hamdan, F. F., Percherancier, Y., Breton, B., & Bouvier, M. (2006). Monitoring protein-protein interactions in living cells by bioluminescence resonance energy transfer (BRET). *Curr Protoc Neurosci*, Chapter 5, Unit 5.23. <https://doi.org/10.1002/0471142301.ns0523s34>
- Hauser, A. S., Chavali, S., Masuho, I., Jahn, L. J., Martemyanov, K. A., Gloriam, D. E., & Babu, M. M. (2018). Pharmacogenomics of GPCR Drug Targets. *Cell*, 172(1-2), 41-54.e19. <https://doi.org/10.1016/j.cell.2017.11.033>
- Henderson, R., & Unwin, P. N. T. (1975). Three-dimensional model of purple membrane obtained by electron microscopy. *Nature*, 257(5521), 28-32. <https://doi.org/10.1038/257028a0>
- Huang, Y. S., Chiang, N. Y., Hu, C. H., Hsiao, C. C., Cheng, K. F., Tsai, W. P., Yona, S., Stacey, M., Gordon, S., Chang, G. W., & Lin, H. H. (2012). Activation of myeloid cell-specific adhesion class G protein-coupled receptor EMR2 via ligation-induced translocation and interaction of receptor subunits in lipid raft microdomains. *Mol Cell Biol*, 32(8), 1408-1420. <https://doi.org/10.1128/mcb.06557-11>
- Iguchi, T., Sakata, K., Yoshizaki, K., Tago, K., Mizuno, N., & Itoh, H. (2008). Orphan G protein-coupled receptor GPR56 regulates neural progenitor cell migration via a G alpha 12/13 and Rho pathway. *J Biol Chem*, 283(21), 14469-14478. <https://doi.org/10.1074/jbc.M708919200>

- James, J. R., Oliveira, M. I., Carmo, A. M., Iaboni, A., & Davis, S. J. (2006). A rigorous experimental framework for detecting protein oligomerization using bioluminescence resonance energy transfer. *Nat Methods*, 3(12), 1001-1006. <https://doi.org/10.1038/nmeth978>
- Kammerer, R. A., Frank, S., Schulthess, T., Landwehr, R., Lustig, A., & Engel, J. (1999). Heterodimerization of a functional GABAB receptor is mediated by parallel coiled-coil alpha-helices. *Biochemistry*, 38(40), 13263-13269. <https://doi.org/10.1021/bi991018t>
- Kim, Y. K., Moon, S., Hwang, M. Y., Kim, D.-J., Oh, J. H., Kim, Y. J., Han, B.-G., Lee, J.-Y., & Kim, B.-J. (2013). Gene-based copy number variation study reveals a microdeletion at 12q24 that influences height in the Korean population. *Genomics*, 101(2), 134-138. <https://doi.org/https://doi.org/10.1016/j.ygeno.2012.11.002>
- Kishore, A., Purcell, R. H., Nassiri-Toosi, Z., & Hall, R. A. (2016). Stalk-dependent and Stalk-independent Signaling by the Adhesion G Protein-coupled Receptors GPR56 (ADGRG1) and BAI1 (ADGRB1). *Journal of Biological Chemistry*, 291(7), 3385-3394. <https://doi.org/10.1074/jbc.m115.689349>
- Knierim, A. B., Röthe, J., Çakir, M. V., Lede, V., Wilde, C., Liebscher, I., Thor, D., & Schöneberg, T. (2019). Genetic basis of functional variability in adhesion G protein-coupled receptors. *Scientific Reports*, 9(1), 11036. <https://doi.org/10.1038/s41598-019-46265-x>
- Kovacs, P., & Schöneberg, T. (2016). The Relevance of Genomic Signatures at Adhesion GPCR Loci in Humans. *Handb Exp Pharmacol*, 234, 179-217. https://doi.org/10.1007/978-3-319-41523-9_9
- Krishnan, A., Nijmeijer, S., de Graaf, C., & Schiöth, H. B. (2016). Classification, Nomenclature, and Structural Aspects of Adhesion GPCRs. In T. Langenhan & T. Schöneberg (Eds.), *Adhesion G Protein-coupled Receptors: Molecular, Physiological and Pharmacological Principles in Health and Disease* (pp. 15-41). Springer International Publishing. https://doi.org/10.1007/978-3-319-41523-9_2
- Kurbegovic, A., Kim, H., Xu, H., Yu, S., Cruanès, J., Maser, R. L., Boletta, A., Trudel, M., & Qian, F. (2014). Novel functional complexity of polycystin-1 by GPS cleavage in vivo: role in polycystic kidney disease. *Mol Cell Biol*, 34(17), 3341-3353. <https://doi.org/10.1128/mcb.00687-14>
- Lagerström, M. C., & Schiöth, H. B. (2008). Structural diversity of G protein-coupled receptors and significance for drug discovery. *Nature Reviews Drug Discovery*, 7(4), 339-357. <https://doi.org/10.1038/nrd2518>
- Langenhan, T., Aust, G., & Hamann, J. (2013). Sticky signaling--adhesion class G protein-coupled receptors take the stage. *Sci Signal*, 6(276), re3. <https://doi.org/10.1126/scisignal.2003825>
- Latek, D., Modzelewska, A., Trzaskowski, B., Palczewski, K., & Filipek, S. (2012). G protein-coupled receptors--recent advances. *Acta biochimica Polonica*, 59(4), 515-529. <https://pubmed.ncbi.nlm.nih.gov/23251911>
- <https://www.ncbi.nlm.nih.gov/pmc/articles/PMC4322417/>

- Li, Z., Bao, S., Wu, Q., Wang, H., Eyler, C., Sathornsumetee, S., Shi, Q., Cao, Y., Lathia, J., McLendon, R. E., Hjelmeland, A. B., & Rich, J. N. (2009). Hypoxia-inducible factors regulate tumorigenic capacity of glioma stem cells. *Cancer Cell*, *15*(6), 501-513. <https://doi.org/10.1016/j.ccr.2009.03.018>
- Liebscher, I., Schön, J., Sarah, Fischer, L., Auerbach, N., Lilian, Mogha, A., Cöster, M., Simon, K.-U., Rothmund, S., Kelly, & Schöneberg, T. (2014). A Tethered Agonist within the Ectodomain Activates the Adhesion G Protein-Coupled Receptors GPR126 and GPR133. *Cell Reports*, *9*(6), 2018-2026. <https://doi.org/10.1016/j.celrep.2014.11.036>
- Lin, H. H., Chang, G. W., Davies, J. Q., Stacey, M., Harris, J., & Gordon, S. (2004). Autocatalytic cleavage of the EMR2 receptor occurs at a conserved G protein-coupled receptor proteolytic site motif. *J Biol Chem*, *279*(30), 31823-31832. <https://doi.org/10.1074/jbc.M402974200>
- Lin, H. H., Stacey, M., Yona, S., & Chang, G. W. (2010). GPS proteolytic cleavage of adhesion-GPCRs. *Adv Exp Med Biol*, *706*, 49-58. https://doi.org/10.1007/978-1-4419-7913-1_4
- Lv, M., Li, X., Tian, W., Yang, H., & Zhou, B. (2022). ADGRD1 as a Potential Prognostic and Immunological Biomarker in Non-Small-Cell Lung Cancer. *BioMed Research International*, *2022*, 1-17. <https://doi.org/10.1155/2022/5699892>
- Marquis, J. F., LaCourse, R., Ryan, L., North, R. J., & Gros, P. (2009). Disseminated and rapidly fatal tuberculosis in mice bearing a defective allele at IFN regulatory factor 8. *J Immunol*, *182*(5), 3008-3015. <https://doi.org/10.4049/jimmunol.0800680>
- Marroni, F., Pfeufer, A., Aulchenko, Y. S., Franklin, C. S., Isaacs, A., Pichler, I., Wild, S. H., Oostra, B. A., Wright, A. F., Campbell, H., Witteman, J. C., KäÄB, S., Hicks, A. A., Gyllensten, U., Rudan, I., Meitinger, T., Pattaro, C., Van Duijn, C. M., Wilson, J. F., & Pramstaller, P. P. (2009). A Genome-Wide Association Scan of RR and QT Interval Duration in 3 European Genetically Isolated Populations. *Circulation: Cardiovascular Genetics*, *2*(4), 322-328. <https://doi.org/10.1161/circgenetics.108.833806>
- Martínez-Muñoz, L., Rodríguez-Frade, J. M., & Mellado, M. (2016). Use of Resonance Energy Transfer Techniques for In Vivo Detection of Chemokine Receptor Oligomerization. In T. Jin & D. Hereld (Eds.), *Chemotaxis: Methods and Protocols* (pp. 341-359). Springer New York. https://doi.org/10.1007/978-1-4939-3480-5_24
- Maurel, D., Comps-Agrar, L., Brock, C., Rives, M. L., Bourrier, E., Ayoub, M. A., Bazin, H., Tinel, N., Durroux, T., Prézeau, L., Trinquet, E., & Pin, J. P. (2008). Cell-surface protein-protein interaction analysis with time-resolved FRET and snap-tag technologies: application to GPCR oligomerization. *Nat Methods*, *5*(6), 561-567. <https://doi.org/10.1038/nmeth.1213>
- McMillan, D. R., & White, P. C. (2010). Studies on the very large G protein-coupled receptor: from initial discovery to determining its role in

- sensorineural deafness in higher animals. *Adv Exp Med Biol*, 706, 76-86. https://doi.org/10.1007/978-1-4419-7913-1_6
- Mercier, J. F., Salahpour, A., Angers, S., Breit, A., & Bouvier, M. (2002). Quantitative assessment of beta 1- and beta 2-adrenergic receptor homo- and heterodimerization by bioluminescence resonance energy transfer. *J Biol Chem*, 277(47), 44925-44931. <https://doi.org/10.1074/jbc.M205767200>
- Mo, X. L., & Fu, H. (2016). BRET: NanoLuc-Based Bioluminescence Resonance Energy Transfer Platform to Monitor Protein-Protein Interactions in Live Cells. *Methods Mol Biol*, 1439, 263-271. https://doi.org/10.1007/978-1-4939-3673-1_17
- Moreno, J. L., Holloway, T., Albizu, L., Sealton, S. C., & González-Maeso, J. (2011). Metabotropic glutamate mGlu2 receptor is necessary for the pharmacological and behavioral effects induced by hallucinogenic 5-HT2A receptor agonists. *Neurosci Lett*, 493(3), 76-79. <https://doi.org/10.1016/j.neulet.2011.01.046>
- Nazarko, O., Kibrom, A., Winkler, J., Leon, K., Stoveken, H., Salzman, G., Merdas, K., Lu, Y., Narkhede, P., Tall, G., Prömel, S., & Araç, D. (2018). A Comprehensive Mutagenesis Screen of the Adhesion GPCR Latrophilin-1/ADGRL1. *iScience*, 3, 264-278. <https://doi.org/10.1016/j.isci.2018.04.019>
- Ng, S. Y., Lee, L. T., & Chow, B. K. (2012). Receptor oligomerization: from early evidence to current understanding in class B GPCRs. *Front Endocrinol (Lausanne)*, 3, 175. <https://doi.org/10.3389/fendo.2012.00175>
- Nguyen, K. D. Q., Vigers, M., Sefah, E., Seppälä, S., Hoover, J. P., Schonenbach, N. S., Mertz, B., O'Malley, M. A., & Han, S. (2021). Homo-oligomerization of the human adenosine A(2A) receptor is driven by the intrinsically disordered C-terminus. *eLife*, 10. <https://doi.org/10.7554/eLife.66662>
- Paavola, K. J., Stephenson, J. R., Ritter, S. L., Alter, S. P., & Hall, R. A. (2011). The N terminus of the adhesion G protein-coupled receptor GPR56 controls receptor signaling activity. *J Biol Chem*, 286(33), 28914-28921. <https://doi.org/10.1074/jbc.M111.247973>
- Padilla-Parra, S., & Tramier, M. (2012). FRET microscopy in the living cell: Different approaches, strengths and weaknesses [<https://doi.org/10.1002/bies.201100086>]. *BioEssays*, 34(5), 369-376. <https://doi.org/https://doi.org/10.1002/bies.201100086>
- Paila, Y. D., Komrabail, M., Krishnamoorthy, G., & Chattopadhyay, A. (2011). Oligomerization of the Serotonin1A Receptor in Live Cells: A Time-Resolved Fluorescence Anisotropy Approach. *The Journal of Physical Chemistry B*, 115(39), 11439-11447. <https://doi.org/10.1021/jp201458h>
- Pakhomov, A. A., & Martynov, V. I. (2008). GFP family: structural insights into spectral tuning. *Chem Biol*, 15(8), 755-764. <https://doi.org/10.1016/j.chembiol.2008.07.009>
- Peng, Y.-M., Van De Garde, M. D. B., Cheng, K.-F., Baars, P. A., Remmerswaal, E. B. M., Van Lier, R. A. W., Mackay, C. R., Lin, H.-H., & Hamann, J.

- (2011). Specific expression of GPR56 by human cytotoxic lymphocytes. *Journal of Leukocyte Biology*, 90(4), 735-740.
<https://doi.org/10.1189/jlb.0211092>
- Pfleger, K. D., & Eidne, K. A. (2006). Illuminating insights into protein-protein interactions using bioluminescence resonance energy transfer (BRET). *Nat Methods*, 3(3), 165-174. <https://doi.org/10.1038/nmeth841>
- Pierce, K. L., Premont, R. T., & Lefkowitz, R. J. (2002). Seven-transmembrane receptors. *Nat Rev Mol Cell Biol*, 3(9), 639-650.
<https://doi.org/10.1038/nrm908>
- Ping, Y.-Q., Xiao, P., Yang, F., Zhao, R.-J., Guo, S.-C., Yan, X., Wu, X., Zhang, C., Lu, Y., Zhao, F., Zhou, F., Xi, Y.-T., Yin, W., Liu, F.-Z., He, D.-F., Zhang, D.-L., Zhu, Z.-L., Jiang, Y., Du, L., Feng, S.-Q., Schöneberg, T., Liebscher, I., Xu, H. E., & Sun, J.-P. (2022). Structural basis for the tethered peptide activation of adhesion GPCRs. *Nature*.
<https://doi.org/10.1038/s41586-022-04619-y>
- Prömel, S., Langenhan, T., & Araç, D. (2013). Matching structure with function: the GAIN domain of adhesion-GPCR and PKD1-like proteins. *Trends in pharmacological sciences*, 34(8), 470-478.
<https://doi.org/10.1016/j.tips.2013.06.002>
- Qu, X., Qiu, N., Wang, M., Zhang, B., Du, J., Zhong, Z., Xu, W., Chu, X., Ma, L., Yi, C., Han, S., Shui, W., Zhao, Q., & Wu, B. (2022). Structural basis of tethered agonism of the adhesion GPCRs ADGRD1 and ADGRF1. *Nature*.
<https://doi.org/10.1038/s41586-022-04580-w>
- Rizzo, M. J., & Johnson, E. C. (2020). Homodimerization of Drosophila Class A neuropeptide GPCRs: Evidence for conservation of GPCR dimerization throughout metazoan evolution. *Biochemical and Biophysical Research Communications*, 523(2), 322-327.
<https://doi.org/https://doi.org/10.1016/j.bbrc.2019.12.019>
- Salzman, Gabriel S., Ackerman, Sarah D., Ding, C., Koide, A., Leon, K., Luo, R., Stoveken, Hannah M., Fernandez, Celia G., Tall, Gregory G., Piao, X., Monk, Kelly R., Koide, S., & Araç, D. (2016). Structural Basis for Regulation of GPR56/ADGRG1 by Its Alternatively Spliced Extracellular Domains. *Neuron*, 91(6), 1292-1304.
<https://doi.org/https://doi.org/10.1016/j.neuron.2016.08.022>
- Salzman, G. S., Zhang, S., Gupta, A., Koide, A., Koide, S., & Araç, D. (2017). *Stachel*-independent modulation of GPR56/ADGRG1 signaling by synthetic ligands directed to its extracellular region. *Proceedings of the National Academy of Sciences*, 114(38), 10095-10100.
<https://doi.org/doi:10.1073/pnas.1708810114>
- Schiöth, H. B., Nordström, K. J., & Fredriksson, R. (2010). The adhesion GPCRs; gene repertoire, phylogeny and evolution. *Adv Exp Med Biol*, 706, 1-13.
https://doi.org/10.1007/978-1-4419-7913-1_1
- Schonenbach, N. S., Hussain, S., & O'Malley, M. A. (2015). Structure and function of G protein-coupled receptor oligomers: implications for drug discovery.

- Wiley Interdiscip Rev Nanomed Nanobiotechnol, 7(3), 408-427.
<https://doi.org/10.1002/wnan.1319>
- Schonenbach, N. S., Rieth, M. D., Han, S., & O'Malley, M. A. (2016). Adenosine A2a receptors form distinct oligomers in protein detergent complexes. *FEBS Lett*, 590(18), 3295-3306. <https://doi.org/10.1002/1873-3468.12367>
- Sekar, R. B., & Periasamy, A. (2003). Fluorescence resonance energy transfer (FRET) microscopy imaging of live cell protein localizations. *J Cell Biol*, 160(5), 629-633. <https://doi.org/10.1083/jcb.200210140>
- Singh, S. K., Hawkins, C., Clarke, I. D., Squire, J. A., Bayani, J., Hide, T., Henkelman, R. M., Cusimano, M. D., & Dirks, P. B. (2004). Identification of human brain tumour initiating cells. *Nature*, 432(7015), 396-401. <https://doi.org/10.1038/nature03128>
- Skruzny, M., Pohl, E., & Abella, M. (2019). FRET Microscopy in Yeast. *Biosensors*, 9(4).
- Stacey, M., Chang, G. W., Davies, J. Q., Kwakkenbos, M. J., Sanderson, R. D., Hamann, J., Gordon, S., & Lin, H. H. (2003). The epidermal growth factor-like domains of the human EMR2 receptor mediate cell attachment through chondroitin sulfate glycosaminoglycans. *Blood*, 102(8), 2916-2924. <https://doi.org/10.1182/blood-2002-11-3540>
- Stephan, G., Frenster, J. D., Liebscher, I., & Placantonakis, D. G. (2022). Activation of the adhesion G protein-coupled receptor GPR133 by antibodies targeting its N-terminus. *Journal of Biological Chemistry*, 298(6), 101949. <https://doi.org/10.1016/j.jbc.2022.101949>
- Stoveken, H. M., Hajduczuk, A. G., Xu, L., & Tall, G. G. (2015). Adhesion G protein-coupled receptors are activated by exposure of a cryptic tethered agonist. *Proceedings of the National Academy of Sciences*, 112(19), 6194-6199. <https://doi.org/doi:10.1073/pnas.1421785112>
- Stoveken, H. M., Larsen, S. D., Smrcka, A. V., & Tall, G. G. (2018). Gedunin- and Khivorin-Derivatives Are Small-Molecule Partial Agonists for Adhesion G Protein-Coupled Receptors GPR56/ADGRG1 and GPR114/ADGRG5. *Mol Pharmacol*, 93(5), 477-488. <https://doi.org/10.1124/mol.117.111476>
- Stupp, R., Mason, W. P., van den Bent, M. J., Weller, M., Fisher, B., Taphoorn, M. J., Belanger, K., Brandes, A. A., Marosi, C., Bogdahn, U., Curschmann, J., Janzer, R. C., Ludwin, S. K., Gorlia, T., Allgeier, A., Lacombe, D., Cairncross, J. G., Eisenhauer, E., & Mirimanoff, R. O. (2005). Radiotherapy plus concomitant and adjuvant temozolomide for glioblastoma. *N Engl J Med*, 352(10), 987-996. <https://doi.org/10.1056/NEJMoa043330>
- Tan, C. M., Brady, A. E., Nickols, H. H., Wang, Q., & Limbird, L. E. (2004). Membrane trafficking of G protein-coupled receptors. *Annu Rev Pharmacol Toxicol*, 44, 559-609. <https://doi.org/10.1146/annurev.pharmtox.44.101802.121558>
- Terrillon, S., Durroux, T., Mouillac, B., Breit, A., Ayoub, M. A., Taulan, M., Jockers, R., Barberis, C., & Bouvier, M. (2003). Oxytocin and vasopressin

V1a and V2 receptors form constitutive homo- and heterodimers during biosynthesis. *Mol Endocrinol*, 17(4), 677-691.

<https://doi.org/10.1210/me.2002-0222>

- Tönjes, A., Koriath, M., Schleinitz, D., Dietrich, K., Böttcher, Y., Rayner, N. W., Almgren, P., Enigk, B., Richter, O., Rohm, S., Fischer-Rosinsky, A., Pfeiffer, A., Hoffmann, K., Krohn, K., Aust, G., Spranger, J., Groop, L., Blüher, M., Kovacs, P., & Stumvoll, M. (2009). Genetic variation in GPR133 is associated with height: genome wide association study in the self-contained population of Sorbs. *Human molecular genetics*, 18(23), 4662-4668. <https://doi.org/10.1093/hmg/ddp423>
- Venter, J. C., Adams, M. D., Myers, E. W., Li, P. W., Mural, R. J., Sutton, G. G., Smith, H. O., Yandell, M., Evans, C. A., Holt, R. A., Gocayne, J. D., Amanatides, P., Ballew, R. M., Huson, D. H., Wortman, J. R., Zhang, Q., Kodira, C. D., Zheng, X. H., Chen, L., Skupski, M., Subramanian, G., Thomas, P. D., Zhang, J., Gabor Miklos, G. L., Nelson, C., Broder, S., Clark, A. G., Nadeau, J., McKusick, V. A., Zinder, N., Levine, A. J., Roberts, R. J., Simon, M., Slayman, C., Hunkapiller, M., Bolanos, R., Delcher, A., Dew, I., Fasulo, D., Flanigan, M., Florea, L., Halpern, A., Hannenhalli, S., Kravitz, S., Levy, S., Mobarry, C., Reinert, K., Remington, K., Abu-Threideh, J., Beasley, E., Biddick, K., Bonazzi, V., Brandon, R., Cargill, M., Chandramouliswaran, I., Charlab, R., Chaturvedi, K., Deng, Z., Di Francesco, V., Dunn, P., Eilbeck, K., Evangelista, C., Gabrielian, A. E., Gan, W., Ge, W., Gong, F., Gu, Z., Guan, P., Heiman, T. J., Higgins, M. E., Ji, R. R., Ke, Z., Ketchum, K. A., Lai, Z., Lei, Y., Li, Z., Li, J., Liang, Y., Lin, X., Lu, F., Merkulov, G. V., Milshina, N., Moore, H. M., Naik, A. K., Narayan, V. A., Neelam, B., Nusskern, D., Rusch, D. B., Salzberg, S., Shao, W., Shue, B., Sun, J., Wang, Z., Wang, A., Wang, X., Wang, J., Wei, M., Wides, R., Xiao, C., Yan, C., Yao, A., Ye, J., Zhan, M., Zhang, W., Zhang, H., Zhao, Q., Zheng, L., Zhong, F., Zhong, W., Zhu, S., Zhao, S., Gilbert, D., Baumhueter, S., Spier, G., Carter, C., Cravchik, A., Woodage, T., Ali, F., An, H., Awe, A., Baldwin, D., Baden, H., Barnstead, M., Barrow, I., Beeson, K., Busam, D., Carver, A., Center, A., Cheng, M. L., Curry, L., Danaher, S., Davenport, L., Desilets, R., Dietz, S., Dodson, K., Doup, L., Ferriera, S., Garg, N., Gluecksmann, A., Hart, B., Haynes, J., Haynes, C., Heiner, C., Hladun, S., Hostin, D., Houck, J., Howland, T., Ibegwam, C., Johnson, J., Kalush, F., Kline, L., Koduru, S., Love, A., Mann, F., May, D., McCawley, S., McIntosh, T., McMullen, I., Moy, M., Moy, L., Murphy, B., Nelson, K., Pfannkoch, C., Pratts, E., Puri, V., Qureshi, H., Reardon, M., Rodriguez, R., Rogers, Y. H., Romblad, D., Ruhfel, B., Scott, R., Sitter, C., Smallwood, M., Stewart, E., Strong, R., Suh, E., Thomas, R., Tint, N. N., Tse, S., Vech, C., Wang, G., Wetter, J., Williams, S., Williams, M., Windsor, S., Winn-Deen, E., Wolfe, K., Zaveri, J., Zaveri, K., Abril, J. F., Guigó, R., Campbell, M. J., Sjolander, K. V., Karlak, B., Kejariwal, A., Mi, H., Lazareva, B., Hatton, T., Narechania, A., Diemer, K., Muruganujan, A., Guo, N., Sato, S., Bafna, V., Istrail, S.,

- Lippert, R., Schwartz, R., Walenz, B., Yooseph, S., Allen, D., Basu, A., Baxendale, J., Blick, L., Caminha, M., Carnes-Stine, J., Caulk, P., Chiang, Y. H., Coyne, M., Dahlke, C., Deslattes Mays, A., Dombroski, M., Donnelly, M., Ely, D., Esparham, S., Fosler, C., Gire, H., Glanowski, S., Glasser, K., Glodek, A., Gorokhov, M., Graham, K., Gropman, B., Harris, M., Heil, J., Henderson, S., Hoover, J., Jennings, D., Jordan, C., Jordan, J., Kasha, J., Kagan, L., Kraft, C., Levitsky, A., Lewis, M., Liu, X., Lopez, J., Ma, D., Majoros, W., McDaniel, J., Murphy, S., Newman, M., Nguyen, T., Nguyen, N., Nodell, M., Pan, S., Peck, J., Peterson, M., Rowe, W., Sanders, R., Scott, J., Simpson, M., Smith, T., Sprague, A., Stockwell, T., Turner, R., Venter, E., Wang, M., Wen, M., Wu, D., Wu, M., Xia, A., Zandieh, A., & Zhu, X. (2001). The sequence of the human genome. *Science*, *291*(5507), 1304-1351. <https://doi.org/10.1126/science.1058040>
- Villardaga, J. P., Nikolaev, V. O., Lorenz, K., Ferrandon, S., Zhuang, Z., & Lohse, M. J. (2008). Conformational cross-talk between alpha2A-adrenergic and mu-opioid receptors controls cell signaling. *Nat Chem Biol*, *4*(2), 126-131. <https://doi.org/10.1038/nchembio.64>
- Vizurraga, A., Adhikari, R., Yeung, J., Yu, M., & Tall, G. G. (2020). Mechanisms of adhesion G protein-coupled receptor activation. *Journal of Biological Chemistry*, *295*(41), 14065-14083. <https://doi.org/10.1074/jbc.rev120.007423>
- Vrecl, M., Drinovec, L., Elling, C., & Heding, A. (2006). Opsin oligomerization in a heterologous cell system. *J Recept Signal Transduct Res*, *26*(5-6), 505-526. <https://doi.org/10.1080/10799890600932253>
- Wang, X. J., Zhang, D. L., Xu, Z. G., Ma, M. L., Wang, W. B., Li, L. L., Han, X. L., Huo, Y., Yu, X., & Sun, J. P. (2014). Understanding cadherin EGF LAG seven-pass G-type receptors. *J Neurochem*, *131*(6), 699-711. <https://doi.org/10.1111/jnc.12955>
- Wei, W., Hackmann, K., Xu, H., Germino, G., & Qian, F. (2007). Characterization of cis-autoproteolysis of polycystin-1, the product of human polycystic kidney disease 1 gene. *J Biol Chem*, *282*(30), 21729-21737. <https://doi.org/10.1074/jbc.M703218200>
- White, J. P., Wrann, C. D., Rao, R. R., Nair, S. K., Jedrychowski, M. P., You, J.-S., Martínez-Redondo, V., Gygi, S. P., Ruas, J. L., Hornberger, T. A., Wu, Z., Glass, D. J., Piao, X., & Spiegelman, B. M. (2014). G protein-coupled receptor 56 regulates mechanical overload-induced muscle hypertrophy. *Proceedings of the National Academy of Sciences of the United States of America*, *111*(44), 15756-15761. <https://doi.org/10.1073/pnas.1417898111>
- Whorton, M. R., Bokoch, M. P., Rasmussen, S. G., Huang, B., Zare, R. N., Kobilka, B., & Sunahara, R. K. (2007). A monomeric G protein-coupled receptor isolated in a high-density lipoprotein particle efficiently activates its G protein. *Proc Natl Acad Sci U S A*, *104*(18), 7682-7687. <https://doi.org/10.1073/pnas.0611448104>

- Wilde, C., Fischer, L., Lede, V., Kirchberger, J., Rothmund, S., Schöneberg, T., & Liebscher, I. (2016). The constitutive activity of the adhesion GPCR GPR114/ADGRG5 is mediated by its tethered agonist. *The FASEB Journal*, 30(2), 666-673. <https://doi.org/10.1096/fj.15-276220>
- Wu, P., & Brand, L. (1994). Resonance energy transfer: methods and applications. *Anal Biochem*, 218(1), 1-13. <https://doi.org/10.1006/abio.1994.1134>
- Xia, Z., & Liu, Y. (2001). Reliable and Global Measurement of Fluorescence Resonance Energy Transfer Using Fluorescence Microscopes. *Biophysical Journal*, 81(4), 2395-2402. [https://doi.org/10.1016/S0006-3495\(01\)75886-9](https://doi.org/10.1016/S0006-3495(01)75886-9)
- Yang, J., Wu, S., & Alachkar, H. (2019). Characterization of upregulated adhesion GPCRs in acute myeloid leukemia. *Translational research : the journal of laboratory and clinical medicine*, 212, 26-35. <https://doi.org/10.1016/j.trsl.2019.05.004>
- Yang, L. Y., Liu, X. F., Yang, Y., Yang, L. L., Liu, K. W., Tang, Y. B., Zhang, M., Tan, M. J., Cheng, S. M., Xu, Y. C., Yang, H. Y., Liu, Z. J., Song, G. J., & Huang, W. (2017). Biochemical features of the adhesion G protein-coupled receptor CD97 related to its auto-proteolysis and HeLa cell attachment activities. *Acta Pharmacol Sin*, 38(1), 56-68. <https://doi.org/10.1038/aps.2016.89>
- Yona, S., Lin, H. H., Siu, W. O., Gordon, S., & Stacey, M. (2008). Adhesion-GPCRs: emerging roles for novel receptors. *Trends Biochem Sci*, 33(10), 491-500. <https://doi.org/10.1016/j.tibs.2008.07.005>
- Zhou, L.-L., Jiao, Y., Chen, H.-M., Kang, L.-H., Yang, Q., Li, J., Guan, M., Zhu, G., Liu, F.-Q., Wang, S., Bai, X., & Song, Y.-Q. (2019). Differentially expressed long noncoding RNAs and regulatory mechanism of LINC02407 in human gastric adenocarcinoma. *World journal of gastroenterology*, 25(39), 5973-5990. <https://doi.org/10.3748/wjg.v25.i39.5973>
- Zhu, K., Yan, A., Zhou, F., Zhao, S., Ning, J., Yao, L., Shang, D., & Chen, L. (2022). A Pyroptosis-Related Signature Predicts Overall Survival and Immunotherapy Responses in Lung Adenocarcinoma [Original Research]. *Frontiers in Genetics*, 13. <https://doi.org/10.3389/fgene.2022.891301>

APPENDICES

A. Coding constructs of ADGRD1 and ADGRG5 constructs

ADGRD1 in pcDNA3.1(+)

GCTAGCCCCACCATGGAAAAGCTGCTGCGGCTGTGCTGCTGGTACTCCT
GGCTGCTGCTATTTTATTACAACCTTCAGGTGCGTGGCGTCTACTCCAG
ATCGTACCCCTACGACGTCCCCGACTACGCCAGGACCATCCAGGATT
CAGGTGTTGGCGTCTGCTTCCCATTACTGGCCACTGGAGAATGTGGATG
GGATCCATGAACTTCAGGATAACAACCTGGAGATATTGTGGAAGGGAAGG
TCAACAAAGGCATTTACCTGAAAGAGGAAAAGGGAGTCACGCTTCTCT
ATTACGGCAGGTACAACAGCTCCTGCATCAGCAAGCCAGAGCAGTGTG
GCCCTGAAGGGGTCACGTTTTCTTTTTCTGGAAGACACAAGGAGAACA
GTCTAGACCAATCCCTTCTGCGTATGGGGGACAGGTCATCTCCAATGGG
TTCAAAGTCTGCTCCAGCGGTGGCAGAGGCTCTGTGGAGCTGTATACGC
GGGACAATTCCATGACATGGGAGGCCTCCTTCAGCCCCCAGGCCCCCTA
TTGGACTCATGTCCTATTTACATGGAAATCCAAGGAGGGCCTGAAAGTC
TACGTCAACGGGACCCTGAGCACCTCTGATCCGAGTGGAAAAGTGTCTC
GTGACTATGGAGAGTCCAACGTCAACCTCGTGATAGGGTCTGAGCAGG
ACCAGGCCAAGTGTTATGAGAACGGTGCTTTCGATGAGTTCATCATCTG
GGAGCGGGCTCTGACTCCGGATGAGATCGCCATGTACTTCACTGCTGCC
ATTGGAAAGCATGCTTTATTGTCTTCAACGCTGCCAAGCCTCTTCATGA
CATCCACAGCAAGCCCCGTGATGCCACAGATGCCTACCATCCCATCAT
AACCAACCTGACAGAAGAGAGAAAAACCTTCCAAAGTCCCGGAGTGAT
ACTGAGTTACCTCCAAAATGTATCCCTCAGCTTACCCAGTAAGTCCCTC
TCGGAGCAGACAGCCTTGAATCTCACCAAGACCTTCTTAAAAGCCGTGG
GAGAGATCCTTCTACTGCCTGGTTGGATTGCTCTGTCAGAGGACAGCGC
CGTGGTACTGAGTCTCATCGACACTATTGACACCGTCATGGGCCATGTA

TCCTCCAACCTGCACGGCAGCACGCCCCAGGTCACCGTGGAGGGCTCCT
CTGCCATGGCAGAGTTTTCCGTGGCCAAAATCCTGCCCAAGACCGTGAA
TTCTCCCATTACCGCTTCCCGGCCACGGGCAGAGCTTCATCCAGATC
CCCCACGAGGCCTTCCACAGGCACGCCTGGAGCACCGTCGTGGGTCTGC
TGTACCACAGCATGCACTACTACCTGAACAACATCTGGCCCCGCCACAC
CAAGATCGCGGAGGCCATGCATCACCAGGACTGCCTGCTGTTCCGCCACC
AGCCACCTGATTTCCCTGGAGGTGTCCCCACCACCACCCTGTCTCAGA
ACCTGTCGGGCTCTCCACTCATTACGGTCCACCTCAAGCACAGATTGAC
ACGTAAGCAGCACAGTGAGGCCACCAACAGCAGCAACCGAGTCTTCGT
GTACTGCGCCTTCCCTGGACTTCAGCTCCGGAGAAGGGGTCTGGTCTAAC
CACGGCTGTGCGCTCACGAGAGGAAACCTCACCTACTCCGTCTGCCGCT
GCACTCACCTCACCAACTTTGCCATCCTCATGCAGGTGGTCCCGCTGGA
GCTTGCACGCGGACACCAGGTGGCGCTGTCGTCTATCAGCTATGTGGGC
TGCTCCCTCTCCGTGCTCTGCCTGGTGGCCACGCTGGTCACCTTCGCCGT
GCTGTCTCCGTGAGCACCATCCGGAACCAGCGCTACCACATCCACGCC
AACCTGTCTTCGCCGTGCTGGTGGCCCAGGTCCTGCTGCTCATTAGTTT
CCGCCTCGAGCCGGGCACGACCCCCTGCCAAGTGATGGCCGTGCTCCTA
CACTACTTCTTCCCTGAGTGCCTTCGCATGGATGCTGGTGGAGGGGCTGC
ACCTCTACAGCATGGTGATCAAGGTCTTTGGGTCGGAGGACAGCAAGC
ACCGTTACTACTATGGGATGGGATGGGGTTTTCTCTTCTGATCTGCATC
ATTTCACTGTCATTTGCCATGGACAGTTACGGAACAAGCAACAATTGCT
GGCTGTCGTTGGCGAGTGGCGCCATCTGGGCCTTTGTAGCCCCTGCCCT
GTTTGTCATCGTGGTCAACATTGGCATCCTCATCGCTGTGACCAGAGTC
ATCTCACAGATCAGCGCCGACAACACTACAAGATCCATGGAGACCCCAGT
GCCTTCAAGTTGACAGCCAAGGCAGTGGCCGTGCTGCTGCCCATCCTGG
GTACCTCGTGGGTCTTTGGCGTGCTTGCTGTCAACGGTTGTGCTGTGGTT
TTCCAGTACATGTTTGCCACGCTCAACTCCCTGCAGGGACTGTTTCATATT
CCTCTTTCATTGTCTCCTGAATTCAGAGGTGAGAGCCGCCTTCAAGCAC
AAAACCAAGGTCTGGTCGCTCACGAGCAGCTCTGCCCGCACCTCCAAC
GCGAAGCCCTTCCACTCGGACCTCATGAATGGGACCCGGCCAGGCATG

GCCTCCACCAAGCTCAGCCCTTGGGACAAGAGCAGCCACTCTGCCCACC
GCGTCGACCTGTCAGCCGTGTGAGAATTCTGCAGATATCCAGCACAGTG
GCGGCCGCTCGAGTCTAGAGGGCCCGTTTAAA

ADGRD1-L-EGFP

GCTAGCCCCACCATGGAAAAGCTGCTGCGGCTGTGCTGCTGGTACTCCT
GGCTGCTGCTATTTTATTACAACCTTTCAGGTGCGTGGCGTCTACTCCAG
ATCGTACCCCTACGACGTCCCCGACTACGCCAGGACCATCCAGGATTT
CAGGTGTTGGCGTCTGCTTCCCATTACTGGCCACTGGAGAATGTGGATG
GGATCCATGAACTTCAGGATACAACCTGGAGATATTGTGGAAGGGAAGG
TCAACAAAGGCATTTACCTGAAAGAGGAAAAGGGAGTCACGCTTCTCT
ATTACGGCAGGTACAACAGCTCCTGCATCAGCAAGCCAGAGCAGTGTG
GCCCTGAAGGGGTCACGTTTTCTTTTTCTGGAAGACACAAGGAGAACA
GTCTAGACCAATCCCTTCTGCGTATGGGGGACAGGTCATCTCCAATGGG
TTCAAAGTCTGCTCCAGCGGTGGCAGAGGCTCTGTGGAGCTGTATACGC
GGGACAATTCCATGACATGGGAGGCCTCCTTCAGCCCCCAGGCCCCCTA
TTGGACTCATGTCCTATTTACATGGAAATCCAAGGAGGGCCTGAAAGTC
TACGTCAACGGGACCCTGAGCACCTCTGATCCGAGTGGAAAAGTGTCTC
GTGACTATGGAGAGTCCAACGTCAACCTCGTGATAGGGTCTGAGCAGG
ACCAGGCCAAGTGTTATGAGAACGGTGCTTTCGATGAGTTCATCATCTG
GGAGCGGGCTCTGACTCCGGATGAGATCGCCATGTACTTCACTGCTGCC
ATTGGAAAGCATGCTTTATTGTCTTCAACGCTGCCAAGCCTCTTCATGA
CATCCACAGCAAGCCCCGTGATGCCACAGATGCCTACCATCCCATCAT
AACCAACCTGACAGAAGAGAGAAAAACCTTCCAAAGTCCCAGGAGTGAT
ACTGAGTTACCTCCAAAATGTATCCCTCAGCTTACCCAGTAAGTCCCTC
TCGGAGCAGACAGCCTTGAATCTCACCAAGACCTTCTTAAAAGCCGTGG
GAGAGATCCTTCTACTGCCTGGTTGGATTGCTCTGTCAGAGGACAGCGC
CGTGGTACTGAGTCTCATCGACACTATTGACACCGTCATGGGCCATGTA
TCCTCCAACCTGCACGGCAGCACGCCCCAGGTCACCGTGGAGGGCTCCT

CTGCCATGGCAGAGTTTTCCGTGGCCAAAATCCTGCCCAAGACCGTGAA
TTCTCCATTACCGCTTCCCGGCCACGGGCAGAGCTTCATCCAGATC
CCCCACGAGGCCTTCCACAGGCACGCCTGGAGCACCGTCGTGGGTCTGC
TGTACCACAGCATGCACTACTACCTGAACAACATCTGGCCCGCCACAC
CAAGATCGCGGAGGCCATGCATCACCAGGACTGCCTGCTGTTCCGCCACC
AGCCACCTGATTTCCCTGGAGGTGTCCCCACCACCCACCCTGTCTCAGA
ACCTGTCGGGCTCTCCACTCATTACGGTCCACCTCAAGCACAGATTGAC
ACGTAAGCAGCACAGTGAGGCCACCAACAGCAGCAACCGAGTCTTCGT
GTACTGCGCCTTCCCTGGACTTCAGCTCCGGAGAAGGGGTCTGGTCAAC
CACGGCTGTGCGCTCACGAGAGGAAACCTCACCTACTCCGTCTGCCGCT
GCACTCACCTCACCAACTTTGCCATCCTCATGCAGGTGGTCCCGCTGGA
GCTTGCACGCGGACACCAGGTGGCGCTGTCGTCTATCAGCTATGTGGGC
TGCTCCCTCTCCGTGCTCTGCCTGGTGGCCACGCTGGTCACCTTCGCCGT
GCTGTCCTCCGTGAGCACCATCCGGAACCAGCGCTACCACATCCACGCC
AACCTGTCCTTCGCCGTGCTGGTGGCCAGGTCCCTGCTGCTCATTAGTTT
CCGCCTCGAGCCGGGCACGACCCCTGCCAAGTGATGGCCGTGCTCCTA
CACTACTTCTTCCCTGAGTGCCTTCGCATGGATGCTGGTGGAGGGGCTGC
ACCTCTACAGCATGGTGATCAAGGTCTTTGGGTTCGGAGGACAGCAAGC
ACCGTTACTACTATGGGATGGGATGGGGTTTTCTCTTCTGATCTGCATC
ATTTCACTGTCAATTTGCCATGGACAGTTACGGAACAAGCAACAATTGCT
GGCTGTCGTTGGCGAGTGGCGCCATCTGGGCCTTTGTAGCCCCTGCCCT
GTTTGTCATCGTGGTCAACATTGGCATCCTCATCGCTGTGACCAGAGTC
ATCTCACAGATCAGCGCCGACAACACTACAAGATCCATGGAGACCCCAGT
GCCTTCAAGTTGACAGCCAAGGCAGTGGCCGTGCTGCTGCCCATCCTGG
GTACCTCGTGGGTCTTTGGCGTGCTTGCTGTCAACGGTTGTGCTGTGGTT
TTCCAGTACATGTTTGCCACGCTCAACTCCCTGCAGGGACTGTTTCATATT
CCTCTTTCATTGTCTCCTGAATTCAGAGGTGAGAGCCGCCTTCAAGCAC
AAAACCAAGGTCTGGTCGCTCACGAGCAGCTCTGCCCGCACCTCCAAC
GCGAAGCCCTTCCACTCGGACCTCATGAATGGGACCCGGCCAGGCATG
GCCTCCACCAAGCTCAGCCCTTGGGACAAGAGCAGCCACTCTGCCACC

GCGTCGACCTGTCAGCCGTGGGCAGCAGCGGCGTGAGCAAGGGCGAGG
AGCTGTTACCGGGGTGGTGCCCATCCTGGTCGAGCTGGACGGCGACGT
AAACGGCCACAAGTTCAGCGTGTCCGGCGAGGGCGAGGGCGATGCCAC
CTACGGCAAGCTGACCCTGAAGTTCATCTGCACCACCGGCAAGCTGCCC
GTGCCCTGGCCCACCCTCGTGACCACCCTGACCTACGGCGTGCAGTGCT
TCAGCCGCTACCCCGACCACATGAAGCAGCACGACTTCTTCAAGTCCGC
CATGCCCCGAAGGCTACGTCCAGGAGCGCACCATCTTCTTCAAGGACGA
CGGCAACTACAAGACCCGCGCCGAGGTGAAGTTCGAGGGCGACACCCT
GGTGAACCGCATCGAGCTGAAGGGCATCGACTTCAAGGAGGACGGCAA
CATCCTGGGGCACAAGCTGGAGTACAACACTACAACAGCCACAACGTCTA
TATCATGGCCGACAAGCAGAAGAACGGCATCAAGGTGAACTTCAAGAT
CCGCCACAACATCGAGGACGGCAGCGTGCAGCTCGCCGACCACTACCA
GCAGAACACCCCCATCGGCGACGGCCCCGTGCTGCTGCCCGACAACCA
CTACCTGAGCACCCAGTCCAAGCTTAGCAAAGATCCCAACGAGAAGCG
CGATCACATGGTCCTGCTGGAGTTCGTGACCGCCGCCGGGATCACTCTC
GGCATGGACGAGCTGTACAAGTAGCGGCCGTGCAGATATCCAGCACAG
TGGCGGCCGCTCGAGTCTAGAGGGCCCGTTTAAA

ADGRD1-L-NLuc

GCTAGCCCCACCATGGAAAAGCTGCTGCGGCTGTGCTGCTGGTACTCCT
GGCTGCTGCTATTTTATTACAACCTTTCAGGTGCGTGGCGTCTACTCCAG
ATCGTACCCCTACGACGTCCCCGACTACGCCCAGGACCATCCAGGATTT
CAGGTGTTGGCGTCTGCTTCCCATTACTGGCCACTGGAGAATGTGGATG
GGATCCATGAACTTCAGGATACAACTGGAGATATTGTGGAAGGGAAGG
TCAACAAAGGCATTTACCTGAAAGAGGAAAAGGGAGTCACGCTTCTCT
ATTACGGCAGGTACAACAGCTCCTGCATCAGCAAGCCAGAGCAGTGTG
GCCCTGAAGGGGTCACGTTTTCTTTTTTCTGGAAGACACAAGGAGAACA
GTCTAGACCAATCCCTTCTGCGTATGGGGGACAGGTCATCTCCAATGGG
TTCAAAGTCTGCTCCAGCGGTGGCAGAGGCTCTGTGGAGCTGTATACGC

GGGACAATTCCATGACATGGGAGGCCTCCTTCAGCCCCCAGGCCCTA
TTGGACTCATGTCCTATTTACATGGAAATCCAAGGAGGGCCTGAAAGTC
TACGTCAACGGGACCCTGAGCACCTCTGATCCGAGTGGAAAAGTGTCTC
GTGACTATGGAGAGTCCAACGTCAACCTCGTGATAGGGTCTGAGCAGG
ACCAGGCCAAGTGTTATGAGAACGGTGCTTTCGATGAGTTCATCATCTG
GGAGCGGGCTCTGACTCCGGATGAGATCGCCATGTA CTTC ACTGCTGCC
ATTGGAAAGCATGCTTTATTGTCTTCAACGCTGCCAAGCCTCTTCATGA
CATCCACAGCAAGCCCCGTGATGCCACAGATGCCTACCATCCCATCAT
AACCAACCTGACAGAAGAGAGAAAAACCTTCCAAAGTCCCGGAGTGAT
ACTGAGTTACCTCCAAAATGTATCCCTCAGCTTACCCAGTAAGTCCCTC
TCGGAGCAGACAGCCTTGAATCTCACCAAGACCTTCTTAAAAGCCGTGG
GAGAGATCCTTCTACTGCCTGGTTGGATTGCTCTGTCAGAGGACAGCGC
CGTGGTACTGAGTCTCATCGACACTATTGACACCGTCATGGGCCATGTA
TCCTCCAACCTGCACGGCAGCACGCCCCAGGTCACCGTGGAGGGCTCCT
CTGCCATGGCAGAGTTTTCCGTGGCCAAAATCCTGCCCAAGACCGTGAA
TTCTCCATTACCGCTTCCCGGCCACGGGCAGAGCTTCATCCAGATC
CCCCACGAGGCCTTCCACAGGCACGCCTGGAGCACCGTCGTGGGTCTGC
TGTACCACAGCATGCACTACTACCTGAACAACATCTGGCCCCGCCACAC
CAAGATCGCGGAGGCCATGCATCACCAGGACTGCCTGCTGTTCCGCCACC
AGCCACCTGATTTCCCTGGAGGTGTCCCCACCACCCACCCTGTCTCAGA
ACCTGTCGGGCTCTCCACTCATTACGGTCCACCTCAAGCACAGATTGAC
ACGTAAGCAGCACAGTGAGGCCACCAACAGCAGCAACCGAGTCTTCGT
GTACTGCGCCTTCCCTGGACTTCAGCTCCGGAGAAGGGGTCTGGTTCGAAC
CACGGCTGTGCGCTCACGAGAGGAAACCTCACCTACTCCGTCTGCCGCT
GCACTCACCTCACCAACTTTGCCATCCTCATGCAGGTGGTCCCGCTGGA
GCTTGCACGCGGACACCAGGTGGCGCTGTCTGTCTATCAGCTATGTGGGC
TGCTCCCTCTCCGTGCTCTGCCTGGTGGCCACGCTGGTACCTTCGCCGT
GCTGTCTCCGTGAGCACCATCCGGAACCAGCGCTACCACATCCACGCC
AACCTGTCTTCGCCGTGCTGGTGGCCCAGGTCTGCTGCTCATTAGTTT
CCGCCTCGAGCCGGGCACGACCCCCTGCCAAGTGATGGCCGTGCTCCTA

CACTACTTCTTCCTGAGTGCCTTCGCATGGATGCTGGTGGAGGGGCTGC
ACCTCTACAGCATGGTGATCAAGGTCTTTGGGTCGGAGGACAGCAAGC
ACCGTTACTACTATGGGATGGGATGGGGTTTTCTCTTCTGATCTGCATC
ATTTCACTGTCATTTGCCATGGACAGTTACGGAACAAGCAACAATTGCT
GGCTGTCGTTGGCGAGTGGCGCCATCTGGGCCTTTGTAGCCCCTGCCCT
GTTTGTTCATCGTGGTCAACATTGGCATCCTCATCGCTGTGACCAGAGTC
ATCTCACAGATCAGCGCCGACA ACTACAAGATCCATGGAGACCCCAGT
GCCTTCAAGTTGACAGCCAAGGCAGTGGCCGTGCTGCTGCCATCCTGG
GTACCTCGTGGGTCTTTGGCGTGCTTGCTGTCAACGGTTGTGCTGTGGTT
TTCCAGTACATGTTTGCCACGCTCAACTCCCTGCAGGGACTGTTTCATATT
CCTCTTTCATTGTCTCCTGAATTCAGAGGTGAGAGCCGCCTTCAAGCAC
AAAACCAAGGTCTGGTCGCTCACGAGCAGCTCTGCCCCGACCTCCAAC
GCGAAGCCCTTCCACTCGGACCTCATGAATGGGACCCGGCCAGGCATG
GCCTCCACCAAGCTCAGCCCTTGGGACAAGAGCAGCCACTCTGCCACC
GCGTCGACCTGTCAGCCGTGGGCAGCAGCGGCGTCTTCACACTCGAAG
ATTTGTTGGGGACTGGCGACAGACAGCCGGCTACAACCTGGACCAAG
TCCTTGAACAGGGAGGTGTGTCCAGTTTGTTCAGAATCTCGGGGTGTC
CGTAACTCCGATCCAAAGGATTGTCCTGAGCGGTGAAAATGGGCTGAA
GATCGACATCCATGTCATCATCCCGTATGAAGGTCTGAGCGGCGACCAA
ATGGGCCAGATCGAAAAAATTTTTAAGGTGGTGTACCCTGTGGATGATC
ATCACTTTAAGGTGATCCTGCACTATGGCACACTGGTAATCGACGGGGT
TACGCCGAACATGATCGACTATTTCCGGACGGCCGTATGAAGGCATCGCC
GTGTTTCGACGGCAAAAAGATCACTGTAACAGGGACCCTGTGGAACGGC
AACAAAATTATCGACGAGCGCCTGATCAACCCCGACGGCTCCCTGCTGT
TCCGAGTAACCATCAACGGAGTGACCGGCTGGCGGCTGTGCGAACGCA
TTCTGGCGTAGCGGCCGTGCAGATATCCAGCACAGTGGCGGCCGCTCG
AGTCTAGAGGGCCCGTTTAAA

ADGRD1-L-mCherry

GCTAGCCCCACCATGGAAAAGCTGCTGCGGCTGTGCTGCTGGTACTCCT
GGCTGCTGCTATTTTATTACAACCTTCAGGTGCGTGGCGTCTACTCCAG
ATCGTACCCCTACGACGTCCCCGACTACGCCAGGACCATCCAGGATTT
CAGGTGTTGGCGTCTGCTTCCCATTACTGGCCACTGGAGAATGTGGATG
GGATCCATGAACTTCAGGATACAACCTGGAGATATTGTGGAAGGGAAGG
TCAACAAAGGCATTTACCTGAAAGAGGAAAAGGGAGTCACGCTTCTCT
ATTACGGCAGGTACAACAGCTCCTGCATCAGCAAGCCAGAGCAGTGTG
GCCCTGAAGGGGTCACGTTTTCTTTTTCTGGAAGACACAAGGAGAACA
GTCTAGACCAATCCCTTCTGCGTATGGGGGACAGGTCATCTCCAATGGG
TTCAAAGTCTGCTCCAGCGGTGGCAGAGGCTCTGTGGAGCTGTATACGC
GGGACAATTCCATGACATGGGAGGCCTCCTTCAGCCCCCAGGCCCTA
TTGGACTCATGTCCTATTTACATGGAAATCCAAGGAGGGCCTGAAAGTC
TACGTCAACGGGACCCTGAGCACCTCTGATCCGAGTGGAAAAGTGTCTC
GTGACTATGGAGAGTCCAACGTCAACCTCGTGATAGGGTCTGAGCAGG
ACCAGGCCAAGTGTTATGAGAACGGTGCTTTCGATGAGTTCATCATCTG
GGAGCGGGCTCTGACTCCGGATGAGATCGCCATGTACTTCACTGCTGCC
ATTGGAAGCATGCTTTATTGTCTTCAACGCTGCCAAGCCTCTTCATGA
CATCCACAGCAAGCCCCGTGATGCCACAGATGCCTACCATCCATCAT
AACCAACCTGACAGAAGAGAGAAAAACCTTCCAAAGTCCCGGAGTGAT
ACTGAGTTACCTCCAAAATGTATCCCTCAGCTTACCCAGTAAGTCCCTC
TCGGAGCAGACAGCCTTGAATCTCACCAAGACCTTCTTAAAAGCCGTGG
GAGAGATCCTTCTACTGCCTGGTTGGATTGCTCTGTCAGAGGACAGCGC
CGTGGTACTGAGTCTCATCGACACTATTGACACCGTCATGGGCCATGTA
TCCTCCAACCTGCACGGCAGCACGCCCCAGGTCACCGTGGAGGGCTCCT
CTGCCATGGCAGAGTTTTCCGTGGCCAAAATCCTGCCCAAGACCGTGAA
TTCTCCCATACCGCTTCCCGGCCACGGGCAGAGCTTCATCCAGATC
CCCCACGAGGCCTTCCACAGGCACGCCTGGAGCACCGTCGTGGGTCTGC
TGTACCACAGCATGCACTACTACCTGAACAACATCTGGCCCCGCCACAC
CAAGATCGCGGAGGCCATGCATCACCAGGACTGCCTGCTGTTTCGCCACC

AGCCACCTGATTTCCCTGGAGGTGTCCCCACCACCCACCCTGTCTCAGA
ACCTGTGCGGGCTCTCCACTCATTACGGTCCACCTCAAGCACAGATTGAC
ACGTAAGCAGCACAGTGAGGCCACCAACAGCAGCAACCGAGTCTTCGT
GTACTGCGCCTTCCTGGACTTCAGCTCCGGAGAAGGGGTCTGGTCTGAAC
CACGGCTGTGCGCTCACGAGAGGAAACCTCACCTACTCCGTCTGCCGCT
GCACTCACCTACCAACTTTGCCATCCTCATGCAGGTGGTCCCGCTGGA
GCTTGACGCGGACACCAGGTGGCGCTGTTCGTCTATCAGCTATGTGGGC
TGCTCCCTCTCCGTGCTCTGCCTGGTGGCCACGCTGGTCACCTTCGCCGT
GCTGTCTCCGTGAGCACCATCCGGAACCAGCGCTACCACATCCACGCC
AACCTGTCCTTCGCCGTGCTGGTGGCCCAGGTCCTGCTGCTCATTAGTTT
CCGCCTCGAGCCGGGCACGACCCCCTGCCAAGTGATGGCCGTGCTCCTA
CACTACTTCTTCCTGAGTGCCTTCGCATGGATGCTGGTGGAGGGGCTGC
ACCTCTACAGCATGGTGATCAAGGTCTTTGGGTCTGGAGGACAGCAAGC
ACCGTTACTACTATGGGATGGGATGGGGTTTTCTCTTCTGATCTGCATC
ATTTCACTGTCATTTGCCATGGACAGTTACGGAACAAGCAACAATTGCT
GGCTGTCGTTGGCGAGTGGCGCCATCTGGGCCTTTGTAGCCCCTGCCCT
GTTTGTTCATCGTGGTCAACATTGGCATCCTCATCGCTGTGACCAGAGTC
ATCTCACAGATCAGCGCCGACAACACTACAAGATCCATGGAGACCCCAGT
GCCTTCAAGTTGACAGCCAAGGCAGTGGCCGTGCTGCTGCCCATCCTGG
GTACCTCGTGGGTCTTTGGCGTGCTTGCTGTCAACGGTTGTGCTGTGGTT
TTCCAGTACATGTTTGCCACGCTCAACTCCCTGCAGGGACTGTTTCATATT
CCTCTTTTCATTGTCTCCTGAATTCAGAGGTGAGAGCCGCCTTCAAGCAC
AAAACCAAGGTCTGGTCGCTCACGAGCAGCTCTGCCCCGCACCTCCAAC
GCGAAGCCCTTCCACTCGGACCTCATGAATGGGACCCGGCCAGGCATG
GCCTCCACCAAGCTCAGCCCTTGGGACAAGAGCAGCCACTCTGCCACC
GCGTCGACCTGTCAGCCGTGGGCAGCAGCGGCGTGAGCAAGGGCGAGG
AGGATAACATGGCCATCATCAAGGAGTTCATGCGCTTCAAGGTGCACA
TGGAGGGCTCCGTGAACGGCCACGAGTTCGAGATCGAGGGCGAGGGCG
AGGGCCGCCCTACGAGGGCACCCAGACCGCCAAGCTGAAGGTGACCA
AGGGTGGCCCCCTGCCCTTCGCCTGGGACATCCTGTCCCCTCAGTTCAT

GTACGGCTCCAAGGCCTACGTGAAGCACCCCGCCGACATCCCCGACTA
CTTGAAGCTGTCCTTCCCCGAGGGCTTCAAGTGGGAGCGCGTGATGAAC
TTCGAGGACGGCGGCGTGGTGACCGTGACCCAGGACTCCTCCCTGCAG
GACGGCGAGTTCATCTACAAGGTGAAGCTGCGCGGCACCAACTTCCCCT
CCGACGGCCCCGTAATGCAGAAGAAGACCATGGGCTGGGAGGCCTCCT
CCGAGCGGATGTACCCCGAGGACGGCGCCCTGAAGGGCGAGATCAAGC
AGAGGCTGAAGCTGAAGGACGGCGGCCACTACGACGCTGAGGTCAAGA
CCACCTACAAGGCCAAGAAGCCCGTGCAGCTGCCCCGGCGCCTACAACG
TCAACATCAAGTTGGACATCACCTCCCACAACGAGGACTACACCATCGT
GGAACAGTACGAACGCGCCGAGGGCCGCCACTCCACCGGCGGCATGGA
CGAGCTGTACAAGTAGCGGCCGTGCAGATATCCAGCACAGTGGCGGCC
GCTCGAGTCTAGAGGGCCCGTTTAAA

ADGRG5 in pcDNA3.1(+)

GCTAGCCCCACCATGGATCACTGTGGTGCCCTTTTCCTGTGCCTGTGCCT
TCTGACTTTGCAGAATGCAACAACAGAGACATGGGAATACCCCTACGA
CGTCCCCGACTACGCCGAACCTCTGAGCTACATGGAGAATATGCAGGT
GTCCAGGGGCCGGAGCTCAGTTTTTTTCCTCTCGTCAACTCCACCAGCTG
GAGCAGATGCTACTGAACACCAGCTTCCCAGGCTACAACCTGACCTTGC
AGACACCCACCATCCAGTCTCTGGCCTTCAAGCTGAGCTGTGACTTCTC
TGGCCTCTCGCTGACCAGTGCCACTCTGAAGCGGGTGCCCCAGGCAGG
AGGTCAGCATGCCCCGGGGTCAGCACGCCATGCAGTTCCCCGCCGAGCT
GACCCGGGACGCCTGCAAGACCCGCCCCAGGGAGCTGCGGCTCATCTG
TATCTACTTCTCCAACACCCACTTTTTCAAGGATGAAAACAACCTCATCT
CTGCTGAATAACTACGTCCTGGGGGCCAGCTGAGTCATGGGCACGTG
AACAACTCAGGGATCCTGTGAACATCAGCTTCTGGCACAACCAAAGC
CTGGAAGGCTACACCCTGACCTGTGTCTTCTGGAAGGAGGGAGCCAGG
AAACAGCCCTGGGGGGGCTGGAGCCCTGAGGGCTGTCGTACAGAGCAG
CCCTCCCCTCTCAGGTGCTCTGCCGCTGCAACCACCTCACCTACTTTGC

TGTTCTCATGCAACTCTCCCCAGCCCTGGTCCCTGCAGAGTTGCTGGCA
CCTCTTACGTACATCTCCCTCGTGGGCTGCAGCATCTCCATCGTGGCCTC
GCTGATCACAGTCCTGCTGCACTTCCATTTTCAGGAAGCAGAGTGACTCC
TTAACACGCATCCACATGAACCTGCATGCCTCCGTGCTGCTCCTGAACA
TCGCCTTCCTGCTGAGCCCCGCATTTCGAATGTCTCCTGTGCCCGGGTC
AGCATGCACGGCTCTGGCCGCTGCCCTGCACTACGCGCTGCTCAGCTGC
CTCACCTGGATGGCCATCGAGGGCTTCAACCTCTACCTCCTCCTCGGGC
GTGTCTACAACATCTACATCCGCAGATATGTGTTCAAGCTTGGTGTGCT
AGGCTGGGGGGCCCCAGCCCTCCTGGTGTGCTTTCCCTCTCTGTCAAG
AGCTCGGTATACGGACCCTGCACAATCCCCGTCTTCGACAGCTGGGAGA
ATGGCACAGGCTTCCAGAACATGTCCATATGCTGGGTGCGGAGCCCCGT
GGTGACAGTGTCTGGTCATGGGCTACGGCGGCCTCACGTCCCTCTTC
AACCTGGTGGTGTGCTGGCCTGGGCGCTGTGGACCCTGCGCAGGCTGCGG
GAGCGGGCGGATGCACCAAGTGTCAGGGCCTGCCATGACACTGTCACT
GTGCTGGGCCTCACCGTGCTGCTGGGAACCACCTGGGCCTTGGCCTTCT
TTTCTTTTGGCGTCTTCCTGTGCCCCAGCTGTTCTCTTCACCATCTTAA
ACTCGCTCTACGGTTTCTTCCTTTTCCTGTGGTTCTGCTCCCAGCGGTGC
CGCTCAGAAGCAGAGGCCAAGGCACAGATAGAGGCCTTCAGCTCCTCC
CAAACAACACAGTAGGAATTCTGCAGATATCCAGCACAGTGGCGGCCG
CTCGAGTCTAGAGGGCCCCGTTTAAA

ADGRG5-L-EGFP

GCTAGCCCCACCATGGATCACTGTGGTGCCCTTTTCCTGTGCCTGTGCCT
TCTGACTTTGCAGAATGCAACAACAGAGACATGGGAATACCCCTACGA
CGTCCCCGACTACGCCGAACCTCCTGAGCTACATGGAGAATATGCAGGT
GTCCAGGGGCCGGAGCTCAGTTTTTTCTCTCGTCAACTCCACCAGCTG
GAGCAGATGCTACTGAACACCAGCTTCCCAGGCTACAACCTGACCTTGC
AGACACCCACCATCCAGTCTCTGGCCTTCAAGCTGAGCTGTGACTTCTC
TGGCCTCTCGCTGACCAGTGCCACTCTGAAGCGGGTGCCCCAGGCAGG

AGGTCAGCATGCCCCGGGGTCAGCACGCCATGCAGTTCCCCGCCGAGCT
GACCCGGGACGCCTGCAAGACCCGCCCCAGGGAGCTGCGGCTCATCTG
TATCTACTTCTCCAACACCCACTTTTTCAAGGATGAAAACAACCTCATCT
CTGCTGAATAACTACGTCCTGGGGGCCAGCTGAGTCATGGGCACGTG
AACAACTCAGGGATCCTGTGAACATCAGCTTCTGGCACAACCAAAGC
CTGGAAGGCTACACCCTGACCTGTGTCTTCTGGAAGGAGGGAGCCAGG
AAACAGCCCTGGGGGGGCTGGAGCCCTGAGGGCTGTCGTACAGAGCAG
CCCTCCCCTCTCAGGTGCTCTGCCGCTGCAACCACCTCACCTACTTTGC
TGTTCTCATGCAACTCTCCCCAGCCCTGGTCCCTGCAGAGTTGCTGGCA
CCTCTTACGTACATCTCCCTCGTGGGCTGCAGCATCTCCATCGTGGCCTC
GCTGATCACAGTCCTGCTGCACTTCCATTTTCAGGAAGCAGAGTGACTCC
TTAACACGCATCCACATGAACCTGCATGCCTCCGTGCTGCTCCTGAACA
TCGCCTTCTGCTGAGCCCCGCATTGCAATGTCTCCTGTGCCCGGGTC
AGCATGCACGGCTCTGGCCGCTGCCCTGCACTACGCGCTGCTCAGCTGC
CTCACCTGGATGGCCATCGAGGGCTTCAACCTCTACCTCCTCCTCGGGC
GTGTCTACAACATCTACATCCGCAGATATGTGTTCAAGCTTGGTGTGCT
AGGCTGGGGGGCCCCAGCCCTCCTGGTGTGCTTTCCCTCTCTGTCAAG
AGCTCGGTATACGGACCCTGCACAATCCCCGTCTTCGACAGCTGGGAGA
ATGGCACAGGCTTCCAGAACATGTCCATATGCTGGGTGCGGAGCCCCGT
GGTGCACAGTGTCTGGTCATGGGCTACGGCGGCCTCACGTCCCTCTTC
AACCTGGTGGTGTGCTGGCCTGGGCGCTGTGGACCCTGCGCAGGCTGCGG
GAGCGGGCGGATGCACCAAGTGTGAGGGCCTGCCATGACACTGTCACT
GTGCTGGGCCTCACCGTGCTGCTGGGAACCACCTGGGCCTTGGCCTTCT
TTTCTTTTGGCGTCTTCCTGCTGCCCCAGCTGTTCCCTCTTCACCATCTTAA
ACTCGCTCTACGGTTTCTTCCTTTTCTGTGGTTCTGCTCCCAGCGGTGC
CGCTCAGAAGCAGAGGCCAAGGCACAGATAGAGGCCTTCAGCTCCTCC
CAAACAACACAGGGCAGCAGCGGCGTGAGCAAGGGCGAGGAGCTGTT
CACCGGGGTGGTGGCCATCCTGGTCGAGCTGGACGGCGACGTAAACGG
CCACAAGTTCAGCGTGTCCGGCGAGGGCGAGGGCGATGCCACCTACGG
CAAGCTGACCCTGAAGTTCATCTGCACCACCGGCAAGCTGCCCGTGCCC

TGGCCCACCCTCGTGACCACCCTGACCTACGGCGTGCAGTGCTTCAGCC
GCTACCCCGACCACATGAAGCAGCACGACTTCTTCAAGTCCGCCATGCC
CGAAGGCTACGTCCAGGAGCGCACCATCTTCTTCAAGGACGACGGCAA
CTACAAGACCCGCGCCGAGGTGAAGTTCGAGGGCGACACCCTGGTGAA
CCGCATCGAGCTGAAGGGCATCGACTTCAAGGAGGACGGCAACATCCT
GGGGCACAAGCTGGAGTACAACAGCCACAACGTCTATATCAT
GGCCGACAAGCAGAAGAACGGCATCAAGGTGAACTTCAAGATCCGCCA
CAACATCGAGGACGGCAGCGTGCAGCTCGCCGACCACTACCAGCAGAA
CACCCCATCGGGCAGGGCCCCGTGCTGCTGCCCGACAACCACTACCTG
AGCACCCAGTCCAAGCTTAGCAAAGATCCCAACGAGAAGCGCGATCAC
ATGGTCCTGCTGGAGTTCGTGACCGCCGCCGGGATCACTCTCGGCATGG
ACGAGCTGTACAAGTAGGAATTCTGCAGATATCCAGCACAGTGGCGGC
CGCTCGAGTCTAGAGGGCCCCGTTTAAA

ADGRG5-L-NLuc

GCTAGCCCCACCATGGATCACTGTGGTGCCCTTTTCCTGTGCCTGTGCCT
TCTGACTTTGCAGAATGCAACAACAGAGACATGGGAATACCCCTACGA
CGTCCCCGACTACGCCGAACCTCTGAGCTACATGGAGAATATGCAGGT
GTCCAGGGGCCGGAGCTCAGTTTTTTTCCTCTCGTCAACTCCACCAGCTG
GAGCAGATGCTACTGAACACCAGCTTCCCAGGCTACAACCTGACCTTGC
AGACACCCACCATCCAGTCTCTGGCCTTCAAGCTGAGCTGTGACTTCTC
TGGCCTCTCGCTGACCAGTGCCACTCTGAAGCGGGTGCCCCAGGCAGG
AGGTCAGCATGCCCCGGGGTCAGCACGCCATGCAGTCCCCGCCGAGCT
GACCCGGGACGCCTGCAAGACCCGCCCCAGGGAGCTGCGGCTCATCTG
TATCTACTTCTCCAACACCCACTTTTTTCAAGGATGAAAACAACCTCATCT
CTGCTGAATAACTACGTCCTGGGGGCCAGCTGAGTCATGGGCACGTG
AACAACCTCAGGGATCCTGTGAACATCAGCTTCTGGCACAACCAAAGC
CTGGAAGGCTACACCCTGACCTGTGTCTTCTGGAAGGAGGGAGCCAGG
AAACAGCCCTGGGGGGGCTGGAGCCCTGAGGGCTGTCGTACAGAGCAG

CCCTCCCCTCTCAGGTGCTCTGCCGCTGCAACCACCTCACCTACTTTGC
TGTTCTCATGCAACTCTCCCCAGCCCTGGTCCCTGCAGAGTTGCTGGCA
CCTCTTACGTACATCTCCCTCGTGGGCTGCAGCATCTCCATCGTGGCCTC
GCTGATCACAGTCCTGCTGCACTTCCATTTTCAGGAAGCAGAGTGA CTCC
TTAACACGCATCCACATGAACCTGCATGCCTCCGTGCTGCTCCTGAACA
TCGCCTTCCTGCTGAGCCCCGCATTTCGCAATGTCTCCTGTGCCCGGGTC
AGCATGCACGGCTCTGGCCGCTGCCCTGCACTACGCGCTGCTCAGCTGC
CTCACCTGGATGGCCATCGAGGGCTTCAACCTCTACCTCCTCCTCGGGC
GTGTCTACAACATCTACATCCGCAGATATGTGTTCAAGCTTGGTGTGCT
AGGCTGGGGGGCCCCAGCCCTCCTGGTGCTGCTTTCCCTCTCTGTCAAG
AGCTCGGTATACGGACCCTGCACAATCCCCGTCTTCGACAGCTGGGAGA
ATGGCACAGGCTTCCAGAACATGTCCATATGCTGGGTGCGGAGCCCCGT
GGTGACAGTGTCTGGTCATGGGCTACGGCGGCCTCACGTCCCTCTTC
AACCTGGTGGTGCTGGCCTGGGCGCTGTGGACCCTGCGCAGGCTGCGG
GAGCGGGCGGATGCACCAAGTGTGAGGGCCTGCCATGACACTGTCACT
GTGCTGGGCCTCACCGTGCTGCTGGGAACCACCTGGGCCTTGGCCTTCT
TTTCTTTTGGCGTCTTCCTGCTGCCCCAGCTGTTCCCTCTTACCATCTTAA
ACTCGCTCTACGGTTTCTTCCTTTTCTGTTGTTCTGCTCCCAGCGGTGC
CGCTCAGAAGCAGAGGCCAAGGCACAGATAGAGGCCTTCAGCTCCTCC
CAAACAACACAGGGCAGCAGCGGCGTCTTCACACTCGAAGATTTTCGTT
GGGACTGGCGACAGACAGCCGGCTACAACCTGGACCAAGTCCTTGAA
CAGGGAGGTGTGTCCAGTTTGTTCAGAAATCTCGGGGTGTCCGTA ACTC
CGATCCAAAGGATTGTCCTGAGCGGTGAAAATGGGCTGAAGATCGACA
TCCATGTCATCATCCCGTATGAAGGTCTGAGCGGCGACCAAATGGGCCA
GATCGAAAAAATTTTTAAGGTGGTGTACCCTGTGGATGATCATCACTTT
AAGGTGATCCTGCACTATGGCACACTGGTAATCGACGGGGTTACGCCG
AACATGATCGACTATTTTCGGACGGCCGTATGAAGGCATCGCCGTGTTCCG
ACGGCAAAAAGATCACTGTAACAGGGACCCTGTGGAACGGCAACAAAA
TTATCGACGAGCGCCTGATCAACCCCGACGGCTCCCTGCTGTTCCGAGT
AACCATCAACGGAGTGACCGGCTGGCGGCTGTGCGAACGCATTCTGGC

GTAGGAATTCTGCAGATATCCAGCACAGTGGCGGCCGCTCGAGTCTAG
AGGGCCCGTTTAAA

ADGRG5-L-mCherry

GCTAGCCCCACCATGGATCACTGTGGTGCCCTTTTCCTGTGCCTGTGCCT
TCTGACTTTGCAGAATGCAACAACAGAGACATGGGAATACCCCTACGA
CGTCCCCGACTACGCCGAACCTCTGAGCTACATGGAGAATATGCAGGT
GTCCAGGGGCCGGAGCTCAGTTTTTTTCCTCTCGTCAACTCCACCAGCTG
GAGCAGATGCTACTGAACACCAGCTTCCCAGGCTACAACCTGACCTTGC
AGACACCCACCATCCAGTCTCTGGCCTTCAAGCTGAGCTGTGACTTCTC
TGGCCTCTCGCTGACCAGTGCCACTCTGAAGCGGGTGCCCCAGGCAGG
AGGTCAGCATGCCCGGGGTCAGCACGCCATGCAGTTCCCCGCCGAGCT
GACCCGGGACGCCTGCAAGACCCGCCCCAGGGAGCTGCGGCTCATCTG
TATCTACTTCTCCAACACCCACTTTTTCAAGGATGAAAACAACCTCATCT
CTGCTGAATAACTACGTCCTGGGGGCCAGCTGAGTCATGGGCACGTG
AACAACCTCAGGGATCCTGTGAACATCAGCTTCTGGCACAACCAAAGC
CTGGAAGGCTACACCCTGACCTGTGTCTTCTGGAAGGAGGGAGCCAGG
AAACAGCCCTGGGGGGGCTGGAGCCCTGAGGGCTGTCGTACAGAGCAG
CCCTCCCCTCTCAGGTGCTCTGCCGCTGCAACCACCTCACCTACTTTGC
TGTTCTCATGCAACTCTCCCCAGCCCTGGTCCCTGCAGAGTTGCTGGCA
CCTCTTACGTACATCTCCCTCGTGGGCTGCAGCATCTCCATCGTGGCCTC
GCTGATCACAGTCCTGCTGCACTTCCATTTTCAGGAAGCAGAGTGACTCC
TTAACACGCATCCACATGAACCTGCATGCCTCCGTGCTGCTCCTGAACA
TCGCCTTCCTGCTGAGCCCCGCATTCGCAATGTCTCCTGTGCCCGGGTC
AGCATGCACGGCTCTGGCCGCTGCCCTGCACTACGCGCTGCTCAGCTGC
CTCACCTGGATGGCCATCGAGGGCTTCAACCTCTACCTCCTCCTCGGGC
GTGTCTACAACATCTACATCCGCAGATATGTGTTCAAGCTTGGTGTGCT
AGGCTGGGGGGCCCCAGCCCTCCTGGTGCTGCTTTCCCTCTCTGTCAAG
AGCTCGGTATACGGACCCTGCACAATCCCCGTCTTCGACAGCTGGGAGA

ATGGCACAGGCTTCCAGAACATGTCCATATGCTGGGTGCGGAGCCCCGT
GGTGCACAGTGTCTGGTCATGGGCTACGGCGGCCTCACGTCCCTCTTC
AACCTGGTGGTGCTGGCCTGGGCGCTGTGGACCCTGCGCAGGCTGCGG
GAGCGGGCGGATGCACCAAGTGTGAGGGCCTGCCATGACACTGTCACT
GTGCTGGGCCTCACCGTGCTGCTGGGAACCACCTGGGCCTTGGCCTTCT
TTTCTTTTGGCGTCTTCCTGCTGCCCCAGCTGTTCTCTTCACCATCTTAA
ACTCGCTCTACGGTTTCTTCCTTTTCTGTGGTTCTGCTCCCAGCGGTGC
CGCTCAGAAGCAGAGGCCAAGGCACAGATAGAGGCCTTCAGCTCCTCC
CAAACAACACAGGGCAGCAGCGGCGTGAGCAAGGGCGAGGAGGATAA
CATGGCCATCATCAAGGAGTTCATGCGCTTCAAGGTGCACATGGAGGG
CTCCGTGAACGGCCACGAGTTCGAGATCGAGGGCGAGGGCGAGGGCCG
CCCCTACGAGGGCACCCAGACCGCCAAGCTGAAGGTGACCAAGGGTGG
CCCCCTGCCCTTCGCTGGGACATCCTGTCCCCTCAGTTCATGTACGGCT
CCAAGGCCTACGTGAAGCACCCCGCCGACATCCCCGACTACTTGAAGCT
GTCCTTCCCCGAGGGCTTCAAGTGGGAGCGCGTGATGAACTTCGAGGA
CGGCGGCGTGGTGACCGTGACCCAGGACTCCTCCCTGCAGGACGGCGA
GTTTCATCTACAAGGTGAAGCTGCGCGGCACCAACTTCCCCTCCGACGGC
CCCGTAATGCAGAAGAAGACCATGGGCTGGGAGGCCTCCTCCGAGCGG
ATGTACCCCGAGGACGGCGCCCTGAAGGGCGAGATCAAGCAGAGGCTG
AAGCTGAAGGACGGCGGCCACTACGACGCTGAGGTCAAGACCACCTAC
AAGGCCAAGAAGCCCGTGCAGCTGCCCGGCGCCTACAACGTCAACATC
AAGTTGGACATCACCTCCCACAACGAGGACTACACCATCGTGGAACAG
TACGAACGCGCCGAGGGCCGCGCCACTCCACCGGCGGCATGGACGAGCTG
TACAAGTAGCGGCCGTGCAGATATCCAGCACAGTGCGCGGCCGCTCGAG
TCTAGAGGGCCCGTTTAAA

B. Bacterial medium preparation

Luria-Bertani (LB) broth

According to Table B.1 components were resolved in water. Then the solution went through autoclave sterilization at 121°C for 20 minutes

Table B.1 Luria-Bertani (LB) broth preparation.

Component	Amount
Tryptone	10 g
Yeast extract	5 g
NaCl	10 g

For Luria-Bertani (LB) broth with agar preparation, same components were used with the addition of 20 g/L of agar. The solution was sterilized by autoclave. Before pouring the broth into the plates, ampicillin was added.

Super Optimum Broth with catabolite repression (SOC)

Table B.2 Super Optimum Broth with catabolite repression (SOC) preparation.

Component	Amount
Tryptone	20 g
Yeast extract	5 g
1M NaCl	10 mL
1M KCl	2.5 mL
Autoclave and add:	
1M MgCl ₂ ·6H ₂ O, 1M MgSO ₄ ·7H ₂ O	10 mL
2M Glucose	10 mL

C. Western blot and cell culture solutions and buffers

Radioimmunoprecipitation assay (RIPA) buffer

5X RIPA buffer was prepared according to the table... The volume was completed to 20 mL with water and sterilized by using a 0.22 μm pore size filter under aseptic conditions.

Table C.3 5X radioimmunoprecipitation assay (RIPA) buffer preparation.

Component	Amount
1M Tris-HCl (pH 8.0)	
1 M NaCl	1.5 mL
NP-40	1 mL
SDS	0.1 g
Sodium deoxycholate	0.5 g

Before using the buffer, protease inhibitors were added according to the table ... by completing to 5 mL with water.

Table C.4 1X RIPA buffer with protease inhibitor preparation.

Component	Amount
5X RIPA	1 mL
1 M DTT	5 μL
100 mM PMSF	25 μL
1 M Na β -glycerophosphate	250 μL
cOmplete™ ULTRA Tablets, Mini, EDTA-free, EASYpack Protease Inhibitor Cocktail (Roche, Switzerland)	1/2

Laemmli buffer

Table C.5 Laemmli buffer preparation

Component	Amount
SDS	0.8 g
1M Tris-HCl (pH 6.8)	2.5 mL
0.1% Bromophenol Blue	0.8 mL
Glycerol	4 mL
0.5 M EDTA	0.5 mL
β -mercaptoethanol	2 mL

Running buffer

Table C.6 Running buffer amounts

Component	Amount
Tris Base	30.3 g
Glycine	144.1 g
SDS	10 g

Tris-buffered saline (TBS)

Table C.7 TBS preparation amounts.

Component	Amount
Tris-HCl	24 g
Tris Base	5.6 g
NaCl	88 g
H ₂ O	800 mL

To make TBS-T buffer 250 mL of TBS was added by mixing 250 μ l of Tween®
20.

Hanks' balanced salt solution (HBSS)

Table C.8 HBSS preparation

Component	Amount
NaCl	8 g
KCl	0.4 g
CaCl	0.14 g
MgSO ₄ · 7 H ₂ O	0.1 g
MgCl ₂ · 6 H ₂ O	0.1 g
Na ₂ HPO ₄ · 2 H ₂ O	0.06 g
KH ₂ PO ₄	0.06 g
D-Glucose	1 g
NaHCO ₃	0.35 g

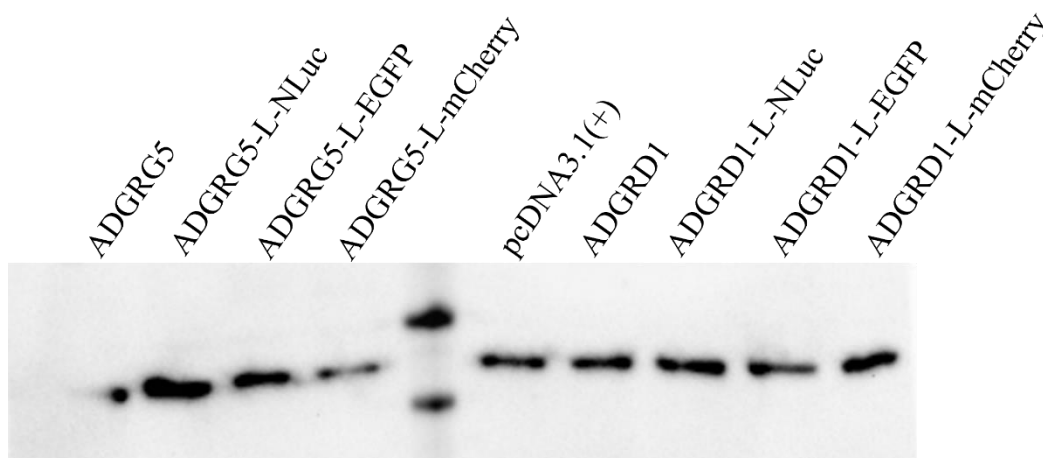


Figure C.1 The β -Actin control immunoblot image of ADGRG5 and ADGRD1 transfected cells. Bands were detected with Anti- β -Actin antibody. Protein marker is Precision Plus Protein™ All Blue Prestained Protein Standards #1610373 (Bio-Rad)